

1. Report No. FHWA/TX-05/0-1713-1		2. Government Accession No.		3. Recipient's Catalog No.	
4. Title and Subtitle EVALUATION OF THE AASHTO 18-KIP LOAD EQUIVALENCY CONCEPT				5. Report Date October 1997 / Revised May 1998	
				6. Performing Organization Code	
7. Author(s) Izydor Kawa, Zhanmin Zhang, and W. Ronald Hudson				8. Performing Organization Report No. 0-1713-1	
9. Performing Organization Name and Address Center for Transportation Research The University of Texas at Austin 3208 Red River, Suite 200 Austin, TX 78705-2650				10. Work Unit No. (TRAIS)	
				11. Contract or Grant No. 0-1713	
12. Sponsoring Agency Name and Address Texas Department of Transportation Research and Technology Implementation Division P.O. Box 5080 Austin, TX 78763-5080				13. Type of Report and Period Covered Research Report (9/96 — 8/97)	
				14. Sponsoring Agency Code	
15. Supplementary Notes Project conducted in cooperation with the Texas Department of Transportation, the U.S. Department of Transportation, and the Federal Highway Administration.					
16. Abstract  This is an interim report for Project 0-1713, which is evaluating the 18-kip equivalency concept. This report presents the information synthesis, which includes a literature review and a report of our evaluation of the AASHTO 18-kip equivalency concept accomplished so far. The results presented in this report set the stage for further evaluation of the 18-kip equivalency concept; in addition, the results can facilitate the development of mathematical models for calculating load equivalency factors, if necessary.					
17. Key Words Load equivalency concept, load equivalency factor, AASHTO 18-kip equivalency concept			18. Distribution Statement No restrictions. This document is available to the public through the National Technical Information Service, Springfield, Virginia 22161.		
19. Security Classif. (of report) Unclassified		20. Security Classif. (of this page) Unclassified		21. No. of pages 104	22. Price



**EVALUATION OF THE AASHTO 18-KIP LOAD EQUIVALENCY CONCEPT**

by

Izydor Kawa  
Zhanmin Zhang  
W. Ronald Hudson

Research Report 0-1713-1

Research Project 0-1713

Project title: *Evaluation of the AASHTO 18-Kip Equivalency Concept*

Conducted for the

**TEXAS DEPARTMENT OF TRANSPORTATION**

in cooperation with the

**U.S. DEPARTMENT OF TRANSPORTATION  
Federal Highway Administration**

by the

**CENTER FOR TRANSPORTATION RESEARCH  
Bureau of Engineering Research  
THE UNIVERSITY OF TEXAS AT AUSTIN**

October 1997

Revised May 1998



## **IMPLEMENTATION STATEMENT**

This interim report for Project 0-1713 evaluates the 18-kip equivalency concept. This report presents the information synthesis, which includes a literature review and evaluation of the AASHTO 18-kip equivalency concept accomplished so far. The results presented in this report set the stage for further evaluation of the 18-kip equivalency concept and for the development of mathematical models for calculating load equivalency factors (if necessary).

## **DISCLAIMERS**

The contents of this report reflect the views of the authors, who are responsible for the facts and the accuracy of the data presented herein. The contents do not necessarily reflect the official views or policies of the Federal Highway Administration or the Texas Department of Transportation. This report does not constitute a standard, specification, or regulation.

There was no invention or discovery conceived or first actually reduced to practice in the course of or under this contract, including any art, method, process, machine, manufacture, design or composition of matter, or any new and useful improvement thereof, or any variety of plant, which is or may be patentable under the patent laws of the United States of America or any foreign country.

NOT INTENDED FOR CONSTRUCTION, BIDDING, OR PERMIT PURPOSES

## **ACKNOWLEDGMENTS**

The researchers acknowledge the invaluable assistance provided by J. P. Leidy (DES), TxDOT project director for this study. Also appreciated is the guidance provided by K. W. Fults (DES), who also serves on the Project Monitoring Committee.

W. Ronald Hudson, P.E. (Texas No. 16821)

*Research Supervisor*

## **SUMMARY**

This interim report for Project 0-1713 describes the work carried out during the first year of this 4-year research project. In particular, this report summarizes the evaluation of the 18-kip equivalency concept accomplished so far. We have thus far determined that the 18-kip equivalency concept has merit; however, in the AASHO Road Test (where these factors were developed), super-single tires and tridem axles were not considered. Also, tire pressure was not considered as a design factor. These omissions are somewhat serious: The results of our literature review, for example, indicate that the super-single tires can impose more damage to the pavements than the dual tires used for the standard 18-kip load equivalence. Moreover, increased tire pressure can potentially further damage pavements. There is, therefore, an urgent need to investigate the validity of the AASHTO load equivalency factors.

## TABLE OF CONTENTS

### CHAPTER 1. INTRODUCTION

INTRODUCTION .....	1
WHY ARE LOAD EQUIVALENCY FACTORS NEEDED?.....	1
DEFINITION OF LEF.....	1
LEFS AND TRAFFIC FORECASTING .....	2
PURPOSE AND SCOPE OF THE REPORT.....	2
REPORT ORGANIZATION.....	2

### CHAPTER 2. THE LOAD EQUIVALENCY CONCEPTS

CONCEPT OF THE 18-KIP LOAD EQUIVALENCE .....	3
DERIVATION OF AASHTO LEFs.....	4
LIMITATIONS OF AASHTO 18-KIP LEFs.....	6
EQUIVALENT SINGLE-WHEEL LOAD .....	9
CHAPTER SUMMARY.....	9

### CHAPTER 3. A DETAILED REVIEW OF LEF STUDIES

INTRODUCTION .....	11
METHODS FOR DETERMINING LOAD EQUIVALENCE .....	11
<i>Mechanistic (Primary Pavement Responses)</i> .....	11
<i>Statistical (Survival Analysis)</i> .....	27
<i>TTI Method</i> .....	28
IMPACT OF CHANGING TRUCK CHARACTERISTICS .....	29
<i>Single, Dual, and Super-Single Tires</i> .....	29
<i>Tridem Axles</i> .....	33
<i>Variation of Tire/Pavement Interface Contact Pressure</i> .....	34
<i>Effect of Increased Tire Pressure</i> .....	36
OTHER METHODS USED TO CONSIDER TRAFFIC DATA.....	39
<i>Calibrated Mechanistic Design Procedure</i> .....	39
<i>Asphalt Institute Method for Flexible Pavements</i> .....	40
COMPUTER MODELING OF PAVEMENT STRUCTURE .....	41
CHAPTER SUMMARY.....	45

<b>CHAPTER 4. IRICK REANALYSIS OF AASHO ROAD TEST DATA</b>	
AASHO ROAD TEST DATA .....	47
IRICK'S ANALYSIS .....	47
RECOMMENDATIONS FOR FURTHER STUDIES OF LOAD EQUIVALENCE	75
<b>CHAPTER 5. EVALUATION OF AASHO AND IRICK MODELS USING RESIDUAL ANALYSIS</b>	
BACKGROUND .....	77
MEASURES OF MODEL ADEQUACY.....	77
RESIDUALS FOR LOG APPLICATIONS .....	78
RESIDUALS FOR LOG LER .....	82
CONCLUSIONS ON RESIDUAL ANALYSIS FOR LOG APPLICATIONS.....	85
CONCLUSIONS ON RESIDUAL ANALYSIS FOR LOG LER.....	86
CHAPTER SUMMARY.....	87
<b>CHAPTER 6. SUMMARY, CONCLUSIONS, AND RECOMMENDATIONS</b>	
REPORT SUMMARY .....	89
RECOMMENDATIONS.....	90
MOVE TO SECOND PROJECT PHASE.....	90
<b>REFERENCES.....</b>	<b>93</b>

## CHAPTER 1. INTRODUCTION

### INTRODUCTION

There are increasing demands for the almost 500,000 kilometers of public roads in Texas that are experiencing significant congestion. According to the Federal Highway Administration (FHWA), 25 percent of the Texas urban interstate highways have exceeded 95 percent of their capacity, and 43 percent are operating at over 80 percent of their carrying capacity. The resulting congestion not only costs Texas motorists an estimated \$3.9 billion in delays and fuel costs each year, but also contributes to higher deterioration of pavement structures. At the same time, the Texas Department of Transportation (TxDOT), given its limited resources, is constrained in its efforts to maintain and improve these congested roadways.

Determining load equivalency factors (LEFs) is critical in pavement design and rehabilitation. Incorrect evaluation of the damage from axle loads on pavements can lead to costly early failure. Overestimating equivalent single axle loads (ESALs) will cause unnecessary expenditures in over-designed pavements that can divert funding from other projects.

### WHY ARE LEFS NEEDED?

LEFs are needed to represent mixed-axle loads in terms of a single-design axle load. LEFs multiplied by the number of axle loads within a given weight category and axle configuration (single, dual, tridem) give the number of 18-kip single-axle load applications that will have an equivalent effect on the performance of the pavement structures. The obtained number of 18-kip single-axle load applications for all weight categories and axle types is used in the design procedure.

Current LEFs are listed in Appendix D of the *AASHTO Guide for Design of Pavement Structures*. To use the current LEFs, the user has to assume a structural number (SN) for flexible pavements or slab thickness (D) for rigid pavements.

### DEFINITION OF LEF

The LEF represents the ratio of the number of repetitions of any axle load and axle configuration (single, tandem, tridem) necessary to cause the same reduction in the present serviceability index (PSI) as one application of an 18-kip single-axle load. The LEF can be defined as:

$$\text{LEF}_{\text{wc}} = \frac{N_{18s}}{N_{\text{wc}}} \quad (1.1)$$

where:

$LEF_{wc}$  = the LEF for an axle of weight “w” and configuration “c,”

$N_{18s}$  = the number of repetitions of an 18,000 single-axle load required to cause a specific reduction in PSI, and

$N_{wc}$  = the number of repetitions of an axle of weight “w” and configuration “c” required to cause the equivalent reduction in PSI.

## **LEFs AND TRAFFIC FORECASTING**

The LEF for a given axle is a complex function of many variables, including axle weight, axle configuration (single, tandem, tridem), pavement type (structural number for flexible pavements, thickness of the concrete slab for rigid pavements), and terminal serviceability.

The goal in traffic load forecasting is to develop the best possible estimate of traffic expected at the project site over the design period. Given the expected number of axles of each configuration in each weight category, the LEF for each configuration and weight category is used to convert the mixed axle loads to ESALs. The ESALs contributed by axles of each axle configuration in each weight category are then summed to obtain a cumulative ESAL forecast for use in pavement design.

## **PURPOSE AND SCOPE OF THE REPORT**

The purpose of this report is to summarize the research accomplished so far in the evaluation of the current 18-kip load equivalency concept, including:

1. Literature review
2. A history and evolution of the load equivalency concept
3. Evaluation of impact of changing vehicle characteristics on LEFs
4. Reanalysis of the AASHO road test data
5. Residual analysis of the AASHO model to determine the model adequacy

## **REPORT ORGANIZATION**

This report consists of six chapters. Chapter 1 has introduced the issues to be discussed, while Chapter 2 presents the 18-kip load equivalence concept. Chapter 3 summarizes the results of the literature review, and describes mechanistic and statistical methods used to calculate LEFs; state-of-the-art methods used to determine LEFs are also discussed. Chapter 4 then describes some further analysis of the AASHO road test data conducted by Irick. Chapter 5 evaluates the current AASHO equation model and alternative Irick models using residual analysis. The validity of current LEFs are also discussed. Chapter 6 summarizes and concludes the report. Recommendations leading to the second phase of the research are also presented.

## CHAPTER 2. THE LOAD EQUIVALENCE CONCEPTS

### CONCEPT OF THE 18-KIP LOAD EQUIVALENCE

Traffic loads applied to a pavement system, in combination with the effects of climate, determine the service life of a pavement. The AASHO road test demonstrated that a highway structure deteriorates with increasing levels of load and the number of load repetitions. Thus, the estimated traffic loads expected to be applied to the pavement system are critical in determining the life expectancy of a given pavement system/structure. Traffic loads applied to the pavement system are usually in various combinations of axle loads and configurations, each having a specific damage effect. These mixed axles can be equated to an arbitrary chosen reference single-axle load, generally 18 kip, for pavement design purposes. The ratio of the reference axle load/configuration damage to the damage caused by any given axle load/configuration is the LEF (LEF). In terms of the number of applications, a LEF can be defined as shown in Equation 2.1.

$$\text{LEF}_{w/c} = \frac{N_r}{N_{w/c}} \quad (2.1)$$

where:

$\text{LEF}_{w/c}$  = LEF for a given axle load/configuration,

$N_r$  = number of applications of the reference axle load/configuration, and

$N_{w/c}$  = number of applications of the given axle load/configuration.

The American Association of State Highway Officials (AASHO) and the Bureau of Public Roads introduced the 18-kip equivalency concept soon after the AASHO road test was completed in 1961. The 18-kip single-axle load was chosen mainly because it was the legal maximum load in most states at the time of the AASHO road test (Van Til 72). LEFs were based on empirical data obtained during the AASHO road test; they were published in the American Association of State Highway and Transportation Officials (AASHTO) Interim Guide for Design of Pavement Structures (AASHTO 72) and in all subsequent editions of the AASHTO Design Guide (AASHTO 93).

AASHTO LEFs are used to convert mixed-design traffic streams on a pavement system to 18-kip equivalent single axle loads (ESALs). There are four independent variables affecting the AASHTO 18-kip LEFs: (1) L1 — load on single, tandem, or tridem axle; (2) L2 — axle type code (1 for single axle, 2 for tandem axle, 3 for tridem axle); (3) Pt — serviceability at the end of time  $t$ , equal to 2, 2.5, 3; and (4) the structural number (SN) for

flexible pavements from 1 to 6 or the slab thickness (D) for rigid pavements from 15 to 36 cm (6 to 14 in.).

The AASHTO 18-kip LEFs represent the ratio of the number of repetitions of any axle load and axle configuration (single, tandem, tridem) necessary to cause the same reduction in present serviceability index (PSI) as one application of an 18-kip single-axle load. Equation 2.2 is used to determine AASHTO 18-kip LEFs.

$$LEF_{L1} = \frac{N_{18}}{N_{L1}} \quad (2.2)$$

where:

$N_{18}$  = number of axle load applications at the end of time  $t$  for  $L1=18$  kip,  
and

$N_{L1}$  = number of axle load applications at the end of time  $t$  for any load  $L1$ .

### DERIVATION OF AASHTO LEFs

The following equations (AASHTO 72) were used to calculate LEFs for flexible and rigid pavements, respectively.

**Flexible pavements.**  $N_{L1}$  is given by Equation 2.3:

$$\log(N_{L1}) = 5.93 + 9.39 * \log_{10}(SN + 1) - 4.79 * \log_{10}(L1 + L2) + 4.331 * \log_{10}(L2) + \frac{G_t}{\beta} \quad (2.3)$$

where:

$G_t$  = a function (the logarithm) of the ratio of loss in serviceability at time  $t$  to the potential loss taken to a point where  $pt=1.5$ .

$$G_t = \log_{10} \left( \frac{4.2 - p_t}{4.2 - 1.5} \right) \quad (2.4)$$

$\beta$  = a function of design and load variables that influence the shape of the p-versus-W serviceability curve.

$$\beta = 0.40 + \frac{0.081 * (L1 + L2)^{3.23}}{(SN + 1)^{5.19} * L2^{3.23}} \quad (2.5)$$

For  $L1=18$  kip and single axle, Equation 2.4 can be simplified:

$$\log(N_{18}) = 5.93 + 9.39 * \log_{10}(SN + 1) - 4.79 * \log_{10}(18 + 1) + \frac{G_t}{\beta_{18}} \quad (2.6)$$

Substituting Equations 2.3 and 2.6 into Equation 2.2, the following equation can be obtained for flexible pavements:

$$LEF_{L1} = \left[ \frac{(L1 + L2)^{4.79}}{(18 + 1)^{4.79}} \right] * \left[ \frac{10^{G_t / \beta_{18}}}{(10^{G_t / \beta_{L1}}) * L2^{4.331}} \right] \quad (2.7)$$

**Rigid pavements.**  $N_{L1}$  is given by Equation 2.8:

$$\log N_t = 5.85 + 7.35 * \log(D + 1) - 4.62 * \log(L_1 + L_2) + 3.28 * \log L_2 + \frac{G_t}{\beta} \quad (2.8)$$

where:

$G_t$  = a function (the logarithm) of the ratio of loss in serviceability at time t to the potential loss taken to a point where  $p_t=1.5$

$$G_t = \log_{10} \left( \frac{4.5 - p_t}{4.5 - 1.5} \right) \quad (2.9)$$

$\beta$  = a function of design and load variables that influence the shape of the p-versus-W serviceability curve.

$$\beta = 1.00 + \frac{3.63 * (L_1 + L_2)^{5.2}}{(D + 1)^{8.46} * L_2^{3.52}} \quad (2.10)$$

For  $L1=18$  and single axle, Equation 2.8 can be simplified:

$$\log N_{t18} = 5.85 + 7.35 * \log(D + 1) - 4.62 * \log(18 + 1) + \frac{G_t}{\beta_{18}} \quad (2.11)$$

Substituting Equations 2.8 and 2.11 into Equation 2.2, the following equation can be obtained for rigid pavements:

$$LEF_{L1} = \left[ \frac{(L1 + L2)^{4.62}}{(18 + 1)^{4.62}} \right] * \left[ \frac{10^{G_t / \beta_{18}}}{(10^{G_t / \beta_{L1}}) * L2^{3.82}} \right] \quad (2.12)$$

**AASHO model.** AASHO model (AASHTO 72) can be expressed as:

$$\left(\frac{N}{\rho}\right)^{\beta} = \frac{p_o - p}{p_o - p_t} \quad (2.13)$$

where:

$W$  = number of 18-kip axle repetitions that will reduce the serviceability from  $p_o - p$ ,

$\rho$  = number of axle repetitions at terminal serviceability ( $p_t$ ), and

$\beta$  = shape factor.

By mathematical rearrangement of Equation 2.13, the relationship is obtained:

$$\log_{10}(N) = \log_{10}(\rho) + \frac{\log_{10}\left(\frac{p_o - p}{p_o - p_t}\right)}{\beta} = \log_{10}(\rho) + \frac{G}{\beta} \quad (2.14)$$

On each section of the AASHO road test, the present serviceability ( $p$ ) and traffic ( $N$ ) were determined at intervals of two weeks throughout the life of the section. The unknown parameters ( $\beta$  and  $\rho$ ) were obtained by regression analysis. Logarithms of traffic for serviceability of 3.5, 3.0, 2.5, 2.0, and 1.5 were used for the regression to obtain estimates of  $\beta$  and  $\rho$ . Having obtained the two parameters ( $\beta$  and  $\rho$ ) for each section, it was assumed that these parameters were functions of the section design (i.e., thickness) and traffic type. On this basis, the following functional relationships for flexible pavement were assigned to  $\beta$  and  $\rho$ :

$$\rho = A0 * (D + 1)^{A1} * (L1 + L2)^{A2} * L2^{A3} \quad (2.15)$$

$$\beta = B0 * (D + 1)^{B1} * (L1 + L2)^{B2} * L2^{B3} \quad (2.16)$$

In these equations  $L1$ ,  $L2$ , and  $D$  were known for each section. The eight unknown constants  $A0-3$  and  $B0-3$  were obtained by regression analysis (Corre 90).

## LIMITATIONS OF AASHTO 18-KIP LEFs

The current LEFs are developed with the consideration of only four variables:

1. Axle type load
2. Axle configuration (single, tandem, tridem)
3. Structural number for flexible pavements and slab thickness for rigid pavement
4. Terminal serviceability level

However, there are more variables that could affect LEFs. The full list of such variables is presented in Table 2.1. The first three classes (symbolized by R, D, and CD) represent pavement response and distress variables. The next three classes represent single-application loading variables (Class L) and structural variables (Class P); their different combinations will generally lead to different states of structural stress (Class S). Classes N, E, and W represent applications variables. Class N is for repeated loadings at a fixed stress level. Class E is for equivalence ratios between applications that have been repeated at different stress levels. Class W is for equivalent load applications relative to standard loading conditions.

The fact that the current LEFs are based on the AASHO road test prompts the following questions and concerns:

1. *Extrapolation of AASHO models outside the test parameters.* Because empirical models are usually valid only within the range of the data used to develop them, the AASHO model is theoretically valid only within the scope of the environmental conditions, materials, and vehicle characteristics that prevailed during the test.
2. *New axle configurations, tire widths, and suspension systems.* There are concerns about the validity of using AASHO equivalencies for super single tires, suspension systems, and tridem axles not present in the AASHO road test.
3. *Effects of higher tire pressures.* As axle load increases, higher tire pressures become more popular for long-haul trucks. Several studies have been conducted on the effect of tire pressures on LEFs. It was reported that increased tire pressure increases the values of primary responses and can affect the fatigue life of pavements (Hudson 88, Bonaquist 88).
4. *Composite pavements.* Most highway agencies approximate the behavior of composite pavements to that of asphalt or concrete pavements. In fact, the 1993 AASHTO design guide suggests that concrete pavement LEFs be used to assess the effects of traffic on composite pavements. This approximation still needs further validation through field measurements and analytical procedures.
5. *Statistical techniques used to analyze the data.* Subsequent analyses of the original AASHO data have yielded different equivalency ratios by using more accurate statistical methods that were not available for the computers used in the early 60s.

Table 2.1 Classification of variables relevant to load equivalences (from Irick 89)

SYMBOL CLASS SUBCLASS	CLASS AND SUBCLASS NAMES	ILLUSTRATIVE VARIABLES AND COMMENTS	
R	PAVEMENT RESPONSE	Deflection parameters ( $\delta$ ), critical strains ( $\epsilon$ ), critical stresses ( $\sigma$ )	
D	DISTRESS (SINGULAR)	AC cracking and rutting, PCC cracking, faulting, and pumping	
	D*	TERMINAL DISTRESS	Allowable rut depth, maximum percentage of Class 2 cracking
	D/D*	SINGULAR DAMAGE	Ranges from 0 to 1
CD	PAVEMENT DISTRESS (COMPOSITE)	Surface roughness, serviceability ( $p$ ) loss ( $q=p_0-p$ )	
	CD*	TERMINAL DISTRESS	Terminal serviceability level ( $p^*$ ) ( $q^* = p_0 - p$ )
	CD/CD*	COMPOSITE DAMAGE	Ranges from 0 to 1
L	LOADING FACTORS	Axle load ( $L_1$ ), axle configuration ( $L_2$ ), speed, tire pressure	
	SAL	STANDARD AXLE LOAD	$L_1 = 80 \text{ kN (18 kip)}$ , $L_2 = \text{single axles}$
P	PAVEMENT STRUCTURE AND ROADBED FACTORS	Composition, thickness, stiffness, and strength of structural components	
S	STRESS STATE OF STRUCTURE	Stress states are not quantified but are related to response variables	
	$S_i$	STRESS LEVEL	Used to distinguish between two stress levels, $i$ and $j$
N	FIXED-STRESS Applications	AASHO road test load applications	
	$N_i$	Appl. to distress D or CD	
	$N_i^*$	Appl. to distress D* or CD*	Road Test applications when $p^* = 2.5$
E	FIXED-STRESS EQUIVALENCE	Respective numbers of applications at different fixed-stress levels that produce equal degrees of pavement distress	
	$SER_{ij}$	STRESS EQUIVALENCY RATIOS	Ratio of $N_i$ and $N_j$ when $S_i$ and $S_j$ produce equal values for D ( $D^*$ )
	$SER_{ij}^*$		
	$LER_{ij}$	LOAD EQUIVALENCY RATIOS	Value of SER when factors (P) equal for $S_i$ and $S_j$
	$LER_{ij}^*$		
$LEF_j$	LOAD EQUIVALENCY FACTOR	Value of $LER_{ij}$ when $S_i$ is produced by standard axle loadings, SAL	
W	EQUIVALENT STANDARD AXLE LOADINGS	Calculated number of standard axle loadings that produce D or CD equal to that produced by a given set of applications at mixed stress levels	
	$W_j$	ESAL FOR LEVEL $S_j$	$W_j = (N_i^*/N_j^*)N_j$ where $N_i^*$ is for SAL
	W	TOTAL ESAL to D or CD	Summation of $W_j$ for all ( $S_j, N_j$ ) mixed stressed applications
	$W^*$	TOTAL ESAL to D* or CD*	Value of W when equal to $N_i^*$ for standard applications

## **EQUIVALENT SINGLE WHEEL LOAD (ESWL)**

Yoder defined an ESWL as the load on a single tire that will cause an equal magnitude of a preselected parameter (stress, strain, deflection, or distress) at a given location within a specific pavement system to that resulting from a multiple-wheel load at the same location within the pavement structure (Yoder 75). Depending on the procedure selected, either the tire pressure or contact area of the ESWL may be equal to that of one tire on the multiple-gear assembly. Several parameters have been used in pavement analysis to define the method of evaluating ESWL. In general, these parameters fall into two categories: (1) theoretically calculated or experimentally derived stress, strains, or deflections; or (2) pavement distress parameters, such as cracking, serviceability level, or equal failure conditions. An equivalent wheel load factor defines the damage per pass caused to a specific pavement system by the vehicle in question relative to the damage per pass of an arbitrarily selected standard vehicle moving on the same pavement system.

## **CHAPTER SUMMARY**

The 18-kip equivalency concept is a useful concept; however, the original AASHTO LEFs were based on AASHO road test data that are now more than 30 years old. Because the AASHO LEF results were empirical, it should be understood that empirical models are valid only within the range of the data used to calibrate them. In the AASHO road test, tire inflation pressures ranged from 520 to 550 kPa (75 to 80 psi). Trucks today are normally operated at tire inflation pressures in the range from 600 to 800 kPa (85 to 115 psi). In some cases, tire pressures can go as high as 900 to 1000 kPa (130 to 145 psi). In addition, today's applied axle load (80 kN in AASHO), suspension systems (steel springs in AASHO), and tire construction (bias ply in AASHO) differ from those of the AASHO road test. Overall, these differences call into question the continued use of the AASHO road test relationships.



## CHAPTER 3. A DETAILED REVIEW OF LOAD EQUIVALENCY FACTOR STUDIES

### INTRODUCTION

A literature search was conducted using the library facilities at the Center for Transportation Research (CTR) of The University of Texas at Austin and at The University of Texas at San Antonio. CTR's dial-up facilities were also used to access all major research information database services, particularly the following:

- Transportation Research and Information System (TRIS)
- National Technical Information Service (NTIS)
- Compendex Plus (on-line form of Engineering Index)

The current state of the art with respect to load equivalencies and determination of current design practices was the primary focus of the research. In the initial keyword search, approximately 300 articles related to load equivalencies and pavement damage were retrieved.

This chapter first reviews the background and historical development of the load equivalency concept. It then focuses on available methods to evaluate design traffic loads, including the state of the art versus the state of the practice in the determination of load equivalencies. Also examined are the pavement loading conditions that influence the type and severity of induced pavement damage. These conditions include: (1) the stationary load on each tire or axle; (2) the number and location of tires on each axle; (3) the number and location of axles; and (4) the tire-pavement contact conditions.

### METHODS FOR DETERMINING LOAD EQUIVALENCE

#### *Mechanistic (Primary Pavement Responses)*

In general, mechanistic methods are used to estimate the LEFs for different axle loads as the ratio of the calculated or measured pavement response under some axle load or group to the calculated or measured response under the standard axle load. Various methods have been developed on the basis of mechanistic estimates of pavement life. The pavement life,  $N$ , can be related to a pavement response parameter, such as  $\beta$ , as follows:

$$N = k_1 * \left( \frac{1}{\beta} \right)^{k_2} \quad (3.1)$$

where  $k_1$  and  $k_2$  are material constants determined through regression on fatigue test data.

The pavement response parameter  $\beta$  can be chosen as one of the following response parameters:

- Maximum vertical strain on top of the subgrade
- Maximum tensile strain at the bottom of the pavement layer
- Maximum surface vertical deflection
- Maximum tensile stress in a concrete pavement

These pavement response parameters can be analytically calculated or experimentally measured utilizing instrumented pavement sections.

Substituting Equation 3.1 for Equation 2.2 yields:

$$LEF_{L1} = \left( \frac{\beta_{L1}}{\beta_{18}} \right)^{k1} \quad (3.2)$$

The most widely used mechanistic LEF methods are either deflection-based or strain-based methods. The deflection-based methods use the maximum surface vertical deflection as the pavement response parameter, whereas the strain-based methods may utilize the maximum vertical strain on top of the subgrade or the maximum tensile strain at the bottom of the pavement layer as the pavement response parameter. The following sections summarize the methods used to determine mechanistic or primary pavement response-based LEFs.

**The Christison Method (Christison 86).** Christison developed load equivalency using field data collected at fourteen sites across Canada during the summer of 1985. Equivalency factors for different axle loads for the Christison method are evaluated using the following expressions:

Single axles:

$$LEF = \left( \frac{D}{D_b} \right)^{3.8} \quad (3.3)$$

Tandem and tridem axles:

$$F = \left( \frac{D_1}{D_b} \right)^{3.8} + \sum_{i=1}^{n-1} \left( \frac{\Delta_i}{D_b} \right)^{3.8} \quad (3.4)$$

where:

$D/D_b$  = the ratio of pavement surface deflections caused by a single-axle load to those recorded under the standard 18,000-lb single ( $D_b$ ) axle-dual tire load of the Benkelman Beam vehicle,

$\Delta/D_b$  = the ratio of the difference in magnitude between the maximum deflection recorded under each succeeding axle and the minimum residual deflection preceding the axle to deflections caused by the standard load,

$n$  = the number of axles in the axle group, and

3.8 = the slope of the deflection versus anticipated traffic loading curve.

The Christison method also uses strain as the primary response parameter to evaluate LEFs. In this method, strain-based equivalency factors are evaluated using the expression:

$$F = \sum_{i=1}^n \left( \frac{S_i}{S_b} \right)^{3.8} \quad (3.5)$$

where:

$S_i/S_b$  = the ratio of longitudinal interfacial tensile strains recorded under each axle to those recorded under the standard load,

$n$  = the number of axles in the axle group, and

3.8 = the slope of the fatigue life versus tensile strain curve.

**Christison and Shields (Christison 80).** Christison and Shields documented the results of an experiment performed by the Alberta Research Council in which responses on asphaltic concrete pavements were obtained for different tire types, tire sizes, and axle configurations. The results were used to obtain LEFs, which give the relative potential damaging effects of the different tire and axle configurations compared to those of a standard load. LEFs were defined as the ratio of the number of applications of a standard load to one application of a given load, equivalent in destructive effect.

Pavement life, expressed in terms of the number of equivalent standard load applications, can be approximated as:

$$N = \left( \frac{1}{\varepsilon_i} \right)^c \quad (3.6)$$

and

$$N = \left( \frac{1}{\delta_i} \right)^c \quad (3.7)$$

where:

$N$  = the number of standard load applications,

$\varepsilon_i$  = the induced tensile strain, and

$\delta_i$  = the induced deflection.

Using the definition of LEFs and the expressions given above, the following equations can be written for single-axle loads:

$$F_i = \left( \frac{\varepsilon_i}{\varepsilon_b} \right)^c \quad (3.8)$$

and

$$F_i = \left( \frac{\delta_i}{\delta_b} \right)^c \quad (3.9)$$

where:

$F$  = the LEF,

$\varepsilon_b$  = the tensile strain caused by the standard load (80 kN), and

$\delta_b$  = the deflection caused by the standard load.

The exponent  $c$  is assumed equal to 3.0.

The loads, both moving and static, were applied on two pavement sections of 28 cm and 20 cm in thickness. For moving loads, the maximum recorded data with asphalt concrete (deflection, horizontal strain, and vertical stress) were plotted versus time and the recorded vehicle speed.

**Results.** The results obtained from this experiment made it possible for them to predict LEFs and the assessment of the potential damaging effect of wide-base radial and bias-ply tire wheel loadings. These results may be summarized as follows:

**Tire Type.** For comparable single-axle loads on single tires, it was found that the difference in tensile strains yielded by 18:00 x 22.5<sup>1</sup> radial tires and 18:00 x 22.5 bias-ply tires was very small, which suggests that the damaging effect of these tires may be considered equal. However, for single-axle loads on dual tires, the tensile strains and deflections induced by dual radial tires were approximately 8 percent lower than the tensile strains and deflections induced by dual bias-ply tires. When an exponential factor  $c$  of 3.0 is applied, this difference results in a 25 percent difference in the predicted equivalency factors.

**Tire Pressure.** The small difference found in the tensile strains yielded by 18:00 x 22.5 radial tires and 18:00 x 22.5 bias-ply tires suggests that the effect of the variation in normally encountered tire pressure and contact area is small.

---

<sup>1</sup> An 18:00 x 22.5 tire has a nominal footprint width of 18 inches with an inside diameter of 22.5 inches. In other words, the wheel that fits this tire is 22.5 inches in diameter. An 18:00 x 22.5 tire may have a metric designation similar to the following: 445/65R22.5, where 445 is the width of the tire in millimeters, 65 is the aspect ratio (tire height/width x 100), and 22.5 is the diameter of the wheel.

**Tire Size.** For single-axle loads on single tires, the following expressions relate axle load to the average tensile strain and deflection ratios:

$$\text{For 18:00 tires: } R_T = 0.0145 (L) - 0.149 \quad (3.10)$$

$$\text{For 16:50 tires: } R_T = 0.126 (L) + 0.108 \quad (3.11)$$

where:

$R_T$  = the average tensile strain and deflection ratios (response ratios), and

$L$  = axle load in kN.

The relative difference between these two tire sizes is better appreciated where LEFs have been obtained applying the exponential factor  $c$  equal to 3.0. For single-axle loads on single tires, the 16:50 tire has 1.4 times the potential damaging effect of the 18:00 tire.

**Axle and Tire Configuration.** Tandem axle loads on single tires and single-axle loads on dual tires were also tested. It was found that a load on tandem axles had an equivalent damaging effect of 60 percent of the same load on a single axle. This is consistent with a value of 57 percent used by the Asphalt Institute. The LEFs for a single tire are 1.2 to 1.8 times larger than those for the dual-tire loads.

**Gerrard and Harrison (Gerrard 70).** Gerrard and Harrison presented a comparison of various loading configurations and their different effects on two-layer pavements consisting of isotropic homogeneous elastic materials. The purpose of the research was to apply layered elastic theory to predict the equivalent loads of dual-tandem and dual-wheel assemblies under Australian highway conditions. Gerrard and Harrison acknowledged that there was a unified criterion for pavement distress. The following criteria were included in their study:

- Vertical displacement at the surface
- Vertical displacement at the interface
- Vertical stress at the interface
- Vertical strain in the lower layer at the interface
- Maximum stress difference (shear stress) in the lower layer at the interface
- Principal tensile strain in the upper layer.

The conditions under which the analyses were conducted are summarized as follows:

**Axle Configuration.** The wheel loads were applied by dual-tandem, dual, and single-wheel assemblies. Dual-tandem and dual assemblies had three different tire spacings and the dual-tandem had three different axle spacings. All contact areas were assumed constant and equal, with a 22.86 cm (9 in.) diameter. The tire considered was the 9 x 20 (12 ply).

**Pavement Material.** The pavement was considered to be a two-layer system. The top layer had a finite depth,  $h$ , and the bottom layer was of infinite depth. The material in each layer was linearly elastic, isotropic, and homogenous, and the interface between layers

was assumed fully continuous. Layer modulus ratios ( $E_1/E_2$ ) of the top layer to the bottom layer were chosen so as to represent the following range of climatic conditions:

- 1)  $E_1/E_2 = 1$  for hot and dry conditions
- 2)  $E_1/E_2 = 5$  for average conditions
- 3)  $E_1/E_2 = 50$  for cold and wet conditions

Two different values of Poisson's ratio were considered:

- 1) 0.2 to represent the lower end of the range of pavement materials
- 2) 0.5 corresponding to the upper end of the range

**Pavement Thickness.** Various pavement thicknesses were considered. The value of the ratio of the thickness  $h$  of the top layer to the radius of the load  $a$  (with a constant value of 11.43 cm or 4.5 in.) was taken from the range from 1 to 4.

**Results.** For each of the six criterion studied, all the combinations of modulus ratios ( $E_1/E_2$ ) and Poisson's ratios were considered. The following wheel assemblies were also compared:

- Dual-tandem assembly versus dual assembly
- Dual assembly versus single wheel
- Dual-tandem assembly versus single wheel

The results of the analyses were shown as curves representing the ratios of these assembly loads. These ratios gave equivalent destructive effects as defined by the criteria involved. The ratios of the loads were also plotted against the relative pavement thickness  $h/a$ . The authors put the different criteria into the following categories.

The results for vertical displacement at the surface and vertical displacement at the interface were similar for high modulus ratios, but significantly different for a modulus ratio of 1. The surface criterion produced ratios higher than the one for the interface. Poisson's effect had little impact.

The results for vertical stress at the interface, vertical strain in the lower layer at the interface, and maximum stress difference in the lower layer at the interface are almost identical, though significantly different from those of the displacement criteria. The ratios for the maximum stress difference and vertical strain criteria are slightly higher than that of the vertical stress.

**Principal tensile strain in upper layer.** The results for this criterion are complex and vary from those of the previous criteria. This criterion is influenced by the location of the maximum value, which may occur at the surface or at the interface, depending on the assembly geometry and pavement properties and geometry.

Because of the variation of the assembly loads ratios with pavement thickness and modulus ratio, the authors acknowledged the difficulty in determining a single value of load ratio. However, considering the principal tensile strain as the *pavement distress* and the maximum stress difference in the lower layer at the interface as the *subgrade distress*,

permissible ratios are presented in Table 3.1. These ratios considered the “average” wheel spacing.

*Table 3.1 Equivalency factors*

	Dual Versus Single		Dual Tandem Versus Single		Dual Tandem Versus Dual
	Shallow Pavement	Deep Pavement	Shallow Pavement	Deep Pavement	Shallow or Deep Pavement
Low Modular Ratio	1.8	1.5	3.6	3.0	1.8 to 1.9
High Modular Ratio	1.5	1.0	3.1	2.0	1.8 to 1.9

**Ramsamooj, Majidzadeh, and Kauffmann (Ramsamooj 72).** Ramsamooj et al. described the experiments conducted to verify the use of fracture mechanics in the analysis of fatigue cracking and failure of flexible pavements. The criterion for fatigue failure of pavements was defined as the time for the stress-intensity-factor,  $K$ , at the tip of the largest crack, to reach its critical value. When this value is reached, rapid crack propagation occurs. Failure may also be considered to have occurred at the time when the total area of cracking exceeds 10 percent of the area of the pavement surface. The rate of crack propagation ( $dc/dN$ ) was expressed as:

$$\frac{dc}{dN} = A * K^4 \quad (3.12)$$

where:

- $K$  = stress-intensity-factor, and
- $A$  = constant of the material.

The stress-intensity factor is a measure of the magnitude of the stress field in the vicinity of the crack; it is a function of the load, size of crack, and of the geometrical and boundary conditions.  $K$  is also proportional to the force tending to cause crack extension. The value of  $K$  may be determined by applying the theory of elasticity or, for very complicated systems, by applying the finite element method.

**Results.** Because crack propagation is proportional to the fourth power of  $K$ , which is proportional to the applied load, LEFs for single-axle loads are also proportional to the fourth power of the load. For tandem axles, LEFs depend on the spacing of the axles and the shape of the influence line as the load moves across the crack. However, this theory applies only to plain strain conditions, when the thickness of the asphalt layer exceeds  $1.25 (K_{Ic} / \sigma_y)^2$ , where:

$K_{Ic}$  = critical value of  $K_I$  (component of  $K$  produced by the symmetrical component of the stresses on the crack surface), and

$\sigma_y$  = yield strength.

For thin slabs at high temperatures, failure was considered to have taken place when about 10 percent of the total area was cracked.

**Jung and Phang (Jung 74).** Jung and Phang presented LEFs based on calculated subgrade deflection. This criterion was found to be the best indicator of performance of a pavement. Successful Ontario thickness designs were examined to find a more rational method of pavement design. “Chevron,” a computer program that employs elastic layer analysis, was used to obtain stresses, strains, and deflections for different sets of moduli assigned to the pavements and subgrades. The deflection on top of the subgrade gave the most consistent results. Accordingly, subgrade deflection was selected as the design criteria, although tensile stress or strain in the asphaltic layer must also be considered. However, while tensile strain, under repeated loads and varying temperature, could be used to determine the thickness of the asphaltic layer, subgrade deflection determines the total thickness.

**Hutchinson, Haas, Meyer, Hadipour, and Papagiannakis (Hutchinson 87).** Hutchinson et al. presented LEFs for different axle groups, using a mechanistic approach and field data from fourteen sites across Canada. The three approaches used in the development of LEFs (empirical, theoretical, and mechanistic) were reviewed. The steps involved in the mechanistic development of equivalency factors were outlined as follows:

- Selection of a pavement response parameter.
- Measurement of the variation in the response parameter under the passage of different axle groups.
- Isolation and counting of the damage-related response cycles from the observed pavement response under an axle group.
- Assessment of the accumulated damage created by cyclic loading, expressed as LEFs.

Following the outlined procedure, the LEFs for single, tandem, and tridem loads were obtained as follows:

**Pavement damage-related response parameters.** Two principal load-associated damage mechanisms and the response parameters related to them are shown in Table 3.2. For this study, surface deflections and pavement-base interfacial strains were measured. The LEF calculations were based on surface deflections, although the maximum measured deflection had never been well correlated with pavement deterioration.

Table 3.2 Damage mechanisms and response parameters

Damage mechanism	Response parameter
Fatigue-induced deterioration of the bituminous surface (cracking)	Tensile strain at the bottom of the layer
Permanent deformation in subgrade and pavement	Vertical subgrade strains

**Variation in the response parameter.** There is variation of pavement surface deflection under the passage of a tridem load. It is clear that the maximum deflection is induced under the third axle, although, in some cases, the maximum deflection is induced under the central axle of the tridem.

**Isolating and counting damage-related response cycles.** Two-cycle counting techniques were considered:

1. The ASTM standard technique constructs the largest possible cycle by using the highest peak and the lowest valley (distance  $D_1$ ), followed by the second largest cycle (distance  $D_2$ ), until all peaks are counted.
2. The Christison method uses the peak-trough difference of each passing axle.

**Damage accumulation and LEF calculation.** The accumulated damage from different axle groups is usually expressed as:

$$LEF(x) = \left[ \frac{D_1(x)}{D(s)} \right]^c + \left[ \frac{D_2(x)}{D(s)} \right]^c + \left[ \frac{D_3(x)}{D(s)} \right]^c \quad (3.13)$$

where:

$LEF(x)$  = LEF for axle group  $x$ ,

$D_1(x), D_2(x)$ ,

and  $D_3(x)$  = deflections observed under axle group  $x$ , which can vary according to the cycle count technique,

$D(s)$  = deflection observed under the standard axle loads, and

$c$  = damage exponent for a particular pavement type.

**Results.** Hutchinson et al. used the ASTM load-deformation cycle counting method and a value of 3.8 for the exponent  $c$  to calculate LEFs for the different axle groups and axle spacings. When compared with the LEFs calculated by Christison from the same data, Hutchinson's results are higher by as much as 12 percent for tandem axles and by 24 percent for tridems. The following regression equation was obtained from load data of a 1.5 meter tandem axle and the corresponding LEFs, calculated from Equation 3.13:

$$LEF(TA) = A * L^B \quad (3.14)$$

where:

LEF(TA) = LEF for a tandem axle group,

L = load in tons, and

A and B = parameters estimated from the regression analysis for each site.

The difference in LEFs between sites may be a reflection of the method used to calculate the LEF function and not of the difference in pavement structure between the sites.

**Other Factors.** The LEF equations presented above were developed for all pavement temperatures and test speeds. An analysis of variance was performed on the tandems and the tridems at one of the sites. The following nonlinear regression equations were estimated for tandems and for tridems:

$$LEF(TA) = 0.0002703 L^{2.3909} T^{0.6867} V^{-0.04979} \quad (3.15)$$

$$LEF(TR) = 0.0003278 L^{2.1291} T^{0.6700} V^{-0.06135} \quad (3.16)$$

from which the following observations were made:

- Axle spread was not significant.
- Temperature had the following significant effect: LEFs increase with temperature, but at a decreasing rate.
- Speed also had a significant effect: higher speeds result in lower LEFs.

The last observation is related to the fact that vehicle speed influences the load-deflection cycle. Increasing speeds decrease the magnitude of the deflection observed in the primary load-deflection cycle. Also, at higher speeds, there is less time for the pavement to recover between the passing axles, reducing the incremental deflections of the minor cycles.

**Papagiannakis, Oancea, Ali, Chan, and Bergman (Papagiannakis 91).** Papagiannakis et al. gave an overview of different cycle counting methods used to determine the life of the pavement for which LEFs are being calculated. Particular attention is given to the rainflow/range-pair counting method of ASTM E1049-85, and to the use of this method in comparing the LEFs of an entire vehicle with the sum of the LEFs of its individual axles and axle groups, calculated from the interfacial asphaltic concrete strains induced by such axles.

The following is the definition of LEF as the ratio of pavement lives, calculated with the expression:

$$LEF_{L1} = \frac{N_{18}}{N_{L1}} \quad (3.17)$$

where:

$LEF_{L1}$  = LEF of load L1, and

$N$  = life of a pavement, expressed as the number of repetitions needed for terminal serviceability.

The suffix 18 or L1 represents the standard load or load L1, respectively, and the mechanistic estimation of pavement life as:

$$N = k_1 * \left(\frac{1}{\varepsilon}\right)^{k_2} \quad (3.18)$$

where:

$\varepsilon$  = selected pavement response parameter (usually interfacial asphalt concrete strain or surface deflection), and

$k_1$  and  $k_2$  = material constants.

LEFs may be expressed as:

$$LEF_{L1} = \left(\frac{\varepsilon_{L1}}{\varepsilon_{18}}\right)^{k_2} \quad (3.19)$$

The response parameters  $\varepsilon_{L1}$  and  $\varepsilon_{18}$  correspond to load L1 and to the standard load, respectively, and may be calculated analytically or measured from the field. The use of the latter type of response values constitutes the *mechanistic* determination of LEFs.

Several methods of determining damage cycles, with discrete or integral values from the measured response curves, are currently employed. Four methods were documented in the ASTM standard for counting cycles E1049-85:

1. Level crossing method
2. Peak counting method
3. Simple-range counting method
4. Rainflow/range-pair counting and related methods

The rainflow/range-pair counting method is the one best suited for counting pavement strain cycles under multiple-axle loads. This method provides a direct relationship between the strain history and the stress-strain behavior of the asphalt concrete.

This method defines *range* as the sum of the absolute values of its peak and valley strains, and a range can be counted as a cycle if it can be paired with a subsequent loading in the opposite direction. The sign of the range (+ or -) is not differentiated by the method, and the type of cycle counted should be determined by the mode of fatigue; that is, valley-peak-valley cycles should only be counted for tensile failure, and peak-valley-peak cycles for compressive failure. Full ranges (peak-to-peak) are taken into account by this method,

though this is not necessarily as appropriate for asphalt concrete pavements as it is for metals.

A pavement was tested at the instrumented pavement site on HW-16 north of Saskatoon, Canada. The pavement cross section consisted of 175 mm of asphalt concrete, 100 mm of base, and 100 mm of subbase on a glacial till subgrade. Three types of vehicles were used: a Benkelman Beam truck for the reference load; a three-axle, single-unit truck; and a five-axle, semitrailer truck. Three different speeds were considered in the 54 runs: 20, 40, and 50 km/hr. Temperature was not considered a variable because of the narrow temperature range prevailing during the experiment.

**Results.** Using the Equation 3.19,  $LEF_{L1} = (\epsilon_{L1} / \epsilon_{18})^{k_2}$ , with the strain counting method and a value of  $k_2$  equal to 3.8, LEFs were calculated for three-axle trucks and for five-axle trucks.

The following observations were made:

1. LEFs decreased with vehicle speed. This is a result of the viscous properties of the asphalt concrete. Strain ratios and, consequently, LEFs decrease with increasing speed.
2. LEFs calculated for entire vehicles can be significantly higher than the sum of the LEFs of their individual axle groups.

These observations suggest that the damaging effect of a vehicle may be underestimated by adding the LEFs of its individual axle groups, a practice that ignores the strain cycles between axle groups. This trend increases with larger numbers of axle groups and vehicle speeds.

Finally, the results obtained from the 50 km/hr runs were compared with two sets of values: (1) LEFs obtained with the mechanistic method used by the Roads and Transportation Association of Canada, and (2) AASHTO LEFs based on the static axle loads measured, a terminal serviceability of 2.5, and a structural number of 3. The LEFs obtained by the mechanistic methods differed significantly but exhibited no definite patterns. However, there was a better agreement between two sets of mechanistic LEFs than between any one of them and the AASHTO LEFs.

**Scala (Scala 70).** Scala used the total vertical elastic deflection at the surface of a pavement to establish LEFs. These LEFs were used to compare the effect of repeated loading. From the results of the AASHTO test, he found that the LEFs are approximately equal to the fourth power of the ratio of the actual loads. Furthermore, if the deflections caused by a load are proportional to such loads, the corresponding LEFs are proportional to the fourth power of the ratio of the deflections caused by the loads.

The following equations were suggested, based on deflections caused by single-axle single tires, single-axle dual tires, tandem-axle groups with dual tires, and tridem axles:

$$\text{For single-axle single tires:} \quad F_i = (W_S / 12)^4 \quad (3.20)$$

$$\text{For tandem-axle groups with dual tires: } F_i = (W_T / 30)^4 \quad (3.21)$$

$$\text{For triple axle with normal tires: } F_i = (W_{TR} / 40.7)^4 \quad (3.22)$$

where:

$F_i$  = the LEFs,

$W_S$  = the load on the single-axle single tire,

$W_T$  = the load on the tandem axle system, and

$W_{TR}$  = the load on the triple axle.

An important finding in this study was that surface deflections are significantly sensitive to vehicle speed. Hence, a power rule may apply to speed ratios. For example, a vehicle traveling at 10 mph is approximately 8 times as damaging as one, with the same loading, traveling at 45 mph.

**Von Quintus (Von Quintus 78).** Von Quintus established a relationship between a pavement structural response (e.g., strain, stress, deflection) and AASHO equivalency factors. LEFs were obtained using the surface deflection, the tensile stress or the strain at the bottom of the surface layer, and the vertical compressive strain at the top of the subgrade as response parameters. ELSYM5 and SLAB-49 were used to obtain the magnitudes of these parameters for both flexible and rigid pavements, respectively.

The relationship between performance equivalencies and the response variables was established by the following methods:

$$\text{Ratio Method: } F_T(2x) = [RV_T(2x) / RV_S(x)] F_S(x) \quad (3.23)$$

$$\text{Exponential Method: } F_i(x) = [RV_i(x) / RV_S(18)]^B \quad (3.24)$$

where:

$F_T(2x)$  = the predicted equivalency factor for a tandem-axle load of  $2x$ ,

$F_S(x)$  = the AASHO equivalency factor for a single-axle load of  $x$ ,

$RV_T(2x)$  = the maximum response variable under a tandem-axle load of  $2x$ ,

$RV_S(x)$  = the maximum response variable under a single-axle load of  $x$ ,

$F_i(x)$  = the equivalency factor for an axle configuration  $i$  of load  $x$ ,

$RV_S(18)$  = the maximum response variable for an 18-kip single-axle load,

$RV_i(x)$  = the difference in magnitude between response variables under and between axle loads, and

$B$  = an experimentally determined constant.

The equations presented above were calibrated with the AASHO single-axle equivalency factor.

For rigid pavements, the LEFs were dependent on the model and loading configuration used to simulate in-field conditions, and could not be predicted within reasonable accuracy from the AASHO conditions.

**Terrel and Rimstrong (Terrel 76).** Terrel et al. used the CHEV 5L computer program to calculate the radial tensile strain on the bottom of asphalt concrete layers, and the vertical compressive strain on the subgrade. Graphs that relate the number of repetitions for failure to axle load, tire width, and asphalt concrete thickness, were prepared for dual and single tires. LEFs were found using the following equation:

$$F_i = \frac{N_b}{N_i} \quad (3.25)$$

where:

- $N_b$  = the number of load repetitions of the standard load, and
- $N_i$  = the number of load repetitions of the applied load.

The reference load was applied by a truck with an 80 kN (18-kip) axle load on 25.4 cm (10 in.) dual tires, running at 16 km/h (10 mph) on a 15.24 cm (6 in.) thick asphalt pavement, and at 20.3° C (68.5° F).

The authors concluded that single wide flotation tires are generally more destructive than dual tires with equivalent contact area.

**Nordic Cooperative Research Project (NCRP 77).** The purpose of this project was to determine the applicability of the AASHO road test results in the Nordic countries. LEFs were determined from axle loads with the expression:

$$F_i = \left( \frac{P_i}{P_s} \right)^n \quad (3.26)$$

where:

- $F_i$  = the LEF,
- $P_i$  = the applied axle load,
- $P_s$  = the standard load, and
- $N$  = an exponent that varies with the type of subgrade and the structural pavement response considered.

Different values of the exponent  $n$  were computed with finite element analysis for the conditions shown in Table 3.3.

Table 3.3 Mean and standard deviation of n

Criterion	Vertical strain at the top of the subgrade		Horizontal strain at the bottom of AC	
	n	Std. Dev.	n	Std. Dev.
Clay	3.98	0.31	3.77	0.25
Sand	3.05	0.51	3.28	0.31

**Southgate and Deen (Southgate 84).** Southgate et al. used a strain energy formulation to obtain LEFs. The work strain,  $e_w$ , of a body was expressed in terms of the strain energy  $W$ , and Young's modulus  $E$  as:

$$e_w = (2W / E)^{0.5} \quad (3.27)$$

which was related to the tensile strain at the bottom of the asphalt concrete  $e_a$  in the regression equation:

$$\log(e_a) = 1.1483 \log(e_w) - 0.1638 \quad (3.28)$$

The LEFs considered fatigue of the pavement. The number of repetitions of the loads, standard and applied, was related to work strain by the following equation:

$$\log(N) = -6.4636 (e_w) + 17.3081 \quad (3.29)$$

This expression was the basis for the equation used for the calculation of the LEFs:

$$F_i = N_{18} / N_L \quad (3.30)$$

where:

$N_{18}$  = the number of repetitions calculated from the work strain owing to an 18-kip, four-tire, single-axle load, and

$N_L$  = the number of repetitions of the candidate axle or group of axles, calculated from their work strain.

Furthermore, the LEFs were also expressed in terms of the axle loads, with the following regression equation:

$$\log F_i = a + b \log A_i + c (\log A_i)^2 \quad (3.31)$$

where:

$F_i$  = the LEF,

$A_i$  = the axle load in kip, and

$a$ ,  $b$ , and  $c$  = regression coefficients.

Because of uneven load distributions, the LEFs had to be adjusted by a multiplication factor MF, given by:

$$\log(\text{MF}) = 0.0018635439 + 0.0242188935 R - 0.0000906996 R^2 \quad (3.32)$$

for tandem-axle groups, where:

$$R = |(\text{axle load No. 1} - \text{axle load No. 2})| / (\text{axle load No. 1} + \text{axle load No. 2}) \quad (3.33)$$

and for tridem-axle groups:

$$\log(\text{MF}) = a + b (\text{Ratio}) + c (\text{Ratio})^2 \quad (3.34)$$

where:

$$\text{Ratio} = (M - L) / I,$$

M = the maximum axle load in kip,

I = the intermediate axle load in kip,

L = the least axle load in kip, and

a, b, and c = regression coefficients.

**Southgate and Deen (Southgate 85).** Southgate et al. developed equations to adjust the equivalency factor equations from their previous work (Southgate and Deen 1984) on the strain energy approach. These adjustment equations account for the spacing between two axles of a tandem group and for the varying tire contact pressure. The following equations are the result of this work:

$$\log(\text{adj}) = -1.589745844 + 1.505262618 \log x - 0.3373568476 (\log x)^2 \quad (3.35)$$

for the spacing between two axles, and

$$\log(\text{adj}) = A + B \log p + C (\log p)^2 \quad (3.36)$$

for varying tire contact pressure, where:

adj = the adjustment factor to modify the load equivalency from the previous work,

x = the spacing in inches between two axles of a tandem group,

p = the tire contact pressure in psi, and

A, B, and C = regression coefficients.

**Federal Highway Administration Study (Hudson 1992).** The Federal Highway Administration (FHWA) conducted a field study at the pavement testing facility at the Turner-Fairbank Highway Research Center to investigate the effects of axle type, axle load, tire pressure, and speed on the response of two asphalt-concrete pavement sections. The

pavement type of the first section was described as “weak;” whereas the pavement type of the second section was described as “strong.” The weak pavement consisted of 8.89 cm (3.5 in.) of hot-mix asphalt concrete over 30.48 cm (12 in.) of crushed aggregate base on a select subgrade soil. The strong pavement had 17.78 cm (7 in.) of hot-mix asphalt concrete over the same 30.48 cm (12 in.) crushed aggregate base and selected subgrade soil. The length of each pavement section was approximately 30.48 m (100 ft).

In the FHWA study, three axle types were used, namely, single-axle dual tire, tandem-axle group, and tridem-axle group. Three levels of axle loads were used for each axle type with two inflation pressures. Also, two speeds were used: 8 km/h and 72.4 km/h (5 mph and 45 mph).

The general objective of the field experiments was to obtain pavement response data to validate and to compare with selected load equivalency methods. The experiments were conducted to collect field test data that could verify the use of primary responses of strain and deflection for predicting LEFs for various axle configurations and weights.

The research indicated that LEFs based on primary pavement responses represent a reasonable method for estimating the equivalent damaging effects of various load parameters, as compared with a standard loading condition. The research also indicated that the deflection method proposed by Hutchinson et al. (1987), which is a modification of the method originally proposed by Christison (1986), appears to be the most viable method currently available.

It was also concluded that the axle load was by far the most significant factor. Small additional contributions from increased (or decreased) tire pressure and from increased (or decreased) speed were not nearly as evident as axle load. The fact that axle load appears to be so significant emphasizes the general validity of the concept of primary pavement response LEFs.

Pavement type did not appear to be highly significant in this study, indicating that the structural number (SN) or pavement thickness may not be a necessary factor in a response-based equivalency factor method for flexible pavements. This finding agrees with the AASHTO LEFs, given that their variation with SN is actually quite small and may not necessarily be considered statistically significant at a high level of confidence.

### ***Statistical (Survival Analysis)***

Statistical procedures have been used to calibrate models from empirical data. Small and Winston reviewed the original AASHTO data using survival analysis techniques (also called Tobit analysis) with an underlying normal distribution (Small 89). In their book, *Road Work*, Small and Winston proposed that the original AASHTO analysis overestimates the life of thick rigid pavements, and that a right-censored survival regression analysis would be more correct. They used only serviceability data collected during the two years of the Road Test. It should be noted that most of the thicker rigid test sections of the AASHTO Road Test were incorporated into Interstate 80 and received twelve additional years of heavy traffic. In a report published by the Illinois Department of Transportation (Little 77), Little and

McKenzie re-analyzed the AASHO data, including the additional traffic, using the least-squares method of regression analysis.

Hudson et al. (Hudson 91) reviewed three different computer analyses of the AASHTO Road Test for rigid pavements. They also present their own analysis of the AASHTO Road Test for rigid pavements. Their study concluded that:

1. The AASHTO performance equation overestimates the prediction of traffic a rigid pavement can carry for thicknesses greater than 24.13 cm (9.5 in.).
2. The Small/Winston analysis of the AASHO road test data provides a poor prediction of the serviceability of thick rigid pavements and severely underestimates the life of rigid pavements greater than 20.32 cm (8.0 in.) in thickness.
3. The load power factor is approximately 4.3 for the AASHTO model, 3.01 for the Small/Winston model, and 4.05 for the revised Small/Winston model.

These results can be interpreted in the following way. In the Small and Winston analysis, the power law coefficient is lower than that in the Hudson et al. analysis. This indicates that, for the Small/Winston model, the damage effect of loads heavier than 80 kN (18 kip) is lower. On the other hand, the Small/Winston model estimates a rigid pavement design life that is shorter than that given in the Hudson et al. model.

### ***TTI Method***

A Texas Transportation Institute (TTI) report (Roberts 87) presents a new method for predicting LEFs for flexible pavement design within the state of Texas. The TTI method considers the following factors in calculating LEFs:

- Load level
- Axle type (single, tandem, tridem)
- Structural number
- Asphalt thickness
- Elastic modulus of the subgrade
- The environmental zone (wet freeze, dry freeze, wet no-freeze, dry no-freeze)
- Three types of distress (loss of serviceability index, rutting, cracking)

The TTI report used the data output from the FHWA's VESYS-IVB computer program from the Cost Allocation Study (Rauhut 82). Based on the field data collected in Texas, TTI adopted the use of the S-shaped performance curve.

$$g = \frac{P_i - P_f}{P_i - P_t} * e^{\left(\frac{\rho_2}{N}\right)^{\beta_2}} \quad (3.37)$$

where:

$$g = \frac{P_i - P_f}{P_i - P_t} = \text{the damage function defined in terms of PSI,}$$

$P_i$  = the initial serviceability index,

$P$  = the present serviceability index,

$P_t$  = the terminal serviceability index,

$P_f$  = the final serviceability index,

$\rho_2$  = a curve fit parameter coefficient which gives the scale of the curve, and

$\beta_2$  = a curve fit parameter that indicates the degrees of curvature.

Table 3.4 compares the AASHTO LEFs and TTI LEFs. Both methods use some of the same variables in calculating LEFs. AASHTO LEFs are calculated for changing terminal serviceability index, while TTI LEFs are calculated for changing subgrade modulus. TTI LEFs increase significantly with decreasing subgrade modulus. Overall, Table 3.4 shows that the AASHTO LEFs differ significantly from the TTI LEFs.

### **IMPACT OF CHANGING TRUCK CHARACTERISTICS**

Heavy-axle LEFs developed from the AASHO road test data may need to be modified in light of the fact that heavy-truck characteristics are changing. For example, new axle configurations, new suspensions, new tire types, and inflation pressures are changing the values of stresses, strains, and deflections that are imposed on the pavement.

#### ***Single, Dual, and Super-Single Tires***

The tires used on modern trucks are configured in single or dual tire arrangements. The front steering axle on cars, trucks, and most tractors use single tires. However, tractor drive axles and trailer axles generally use dual tires. There are exceptions to these rules: When the load on a steering axle exceeds 62.3 kN (14 kip), a super-single or wide-based tire may be used. On the drive axles and trailer axles, super-single tires may be used in place of dual tires (Mahoney 95).

Table 3.4 Comparison of AASHTO and TTI LEFs for single axle, SN=5, surface thickness 15 cm (6 in.) in dry freeze zone

Axle Load		LEFs					
		AASHTO LEF			TTI LEF		
		Terminal serviceability pt			Subgrade modulus		
[kN]	[kip]	2.0	2.5	3.0	34500 kPa (5000 psi)	103500 kPa (15000 psi)	172500 kPa (25000 psi)
8.9	2	0.000	0.000	0.000	0.000	0.000	0.000
17.8	4	0.002	0.002	0.002	0.003	0.000	0.000
26.7	6	0.009	0.009	0.010	0.074	0.000	0.000
35.6	8	0.029	0.031	0.034	0.858	0.000	0.000
44.5	10	0.076	0.080	0.086	5.845	0.000	0.000
53.4	12	0.168	0.176	0.187	28.090	0.003	0.000
62.3	14	0.331	0.342	0.358	105.661	0.027	0.002
71.2	16	0.596	0.606	0.622	331.699	0.187	0.017
<b>80.1</b>	<b>18</b>	<b>1.000</b>	<b>1.000</b>	<b>1.000</b>	<b>906.345</b>	<b>1.000</b>	<b>0.131</b>
89.0	20	1.588	1.554	1.509	2219.089	4.331	0.781
97.9	22	2.408	2.299	2.161	4971.238	15.876	3.736
106.8	24	3.513	3.266	2.959	10348.210	50.805	14.992
115.7	26	4.964	4.484	3.907	20256.170	145.278	52.055
124.6	28	6.825	5.982	5.005	37626.470	377.935	160.185
133.5	30	9.169	7.793	6.256	66814.310	907.231	445.145
142.4	32	12.073	9.953	7.667	114087.400	2032.460	1133.809
151.3	34	15.628	12.504	9.251	188241.100	4288.367	2679.101
160.2	36	19.933	15.496	11.027	301295.100	8585.824	5929.996
169.1	38	25.099	18.984	13.019	469427.800	16414.630	12397.420
178.0	40	31.248	23.036	15.258	713891.400	30121.610	24643.750

Truck tire contact patch or contact area is an important consideration in studying damage caused by vehicles. The truck tire width, length, and area varies with tire sizes. Tires also differ in vertical stiffness (ply rating). Tire size, ply rating, and inflation pressure determine the load capacity of a tire. Standard dimensions and load ratings for tires used in the U.S. are set by the Tire and Rim Association (TRA). Tread widths are also an important property of tires, with their maximum value set as a percentage of section width — 80 percent for rib tires and 90 percent for traction tires. Truck operators generally prefer to use the 11R22.5 tire in dual tire applications, for example, on 89 kN (20 kip) single axles and 151.3 kN (34 kip) tandem axles. It is the convenience of having the same tire size on both the steering and drive axles that makes it the tire of choice on many heavy trucks. 11R22.5 and wide base 15R22.5 and 18R22.5 represent the nominal size necessary to carry front axle loads of 53.4, 71.2, and 89 kN (12, 16, and 20 kip, respectively) on single tires.

**Bonaquist study.** (Bonaquist 92) In 1989, the FHWA initiated a research program to assess the impact of super-single tires on flexible pavement response and distress. This study was conducted at the FHWA Pavement Testing Facility. Using the Accelerated Loading Facility pavement testing machine to simulate traffic loading, researchers collected pavement

response and distress data for comparable dual and super-single tires. Bonaquist (Bonaquist 92) provides comparisons of the response and distress data for these two tire types, which he uses to assess the relative damage potential of the super singles.

This research involved both pavement response and pavement distress experiments. The purpose of the response experiment was to assess the relative damage potential of super-single tires through a comparative analysis of measured pavement responses. The responses considered in this experiment were tensile strain at the bottom of the asphalt concrete layer, and average vertical strains in the asphalt concrete, crushed aggregate base, and upper 152 mm of the subgrade. The tensile strains were considered indicators of the tire's fatigue damage potential, while the compressive strains were considered indicators of the rutting potential. The purpose of the pavement distress experiment was to assess the relative damage potential of super-single tires through a comparative analysis of pavement distress (rutting and cracking). Additionally, the distress tests provided validation of the damage estimates from the experiments.

The study was limited to one set of comparable dual and super-single tires. The basis for selecting comparable tires was the load rating established by the U.S. TRA. During an FHWA workshop in September 1988, the 11R22.5 radial tire was identified as one of the most common tires used in the United States. This tire carries a dual tire load rating of 23.58 kN (5.3 kip) per tire or a total load of 47.16 kN (10.6 kip) for the pair. Based on the load rating, a comparable single tire is the 425/65R22.5, which has a load rating of 46.71 kN (10.5 kip). Thus, the tires used in this research were dual 11R22.5 and a single 425/65R22.5.

The experiment showed that the single tire produced higher vertical strains in all pavement layers, and higher tensile strains at the bottom of the asphalt layer. The relative magnitude of the increased damage for these conditions can be estimated using mechanistic damage models. Equations 3.38 and 3.39 express the forms of currently accepted damage models for fatigue cracking and rutting. Table 3.5 presents factors used in the experiment.

*Table 3.5 Response experiment factors and factor levels*

<b>Factor</b>	<b>Levels</b>
Season	Summer, winter, spring
Pavement temperature	Low, moderate, high
Load	41, 54, 64, 74 kN
Tire pressure	520, 712, 959 kPa
Design asphalt thickness	89 and 178 mm

Fatigue Damage

$$\frac{1}{N_f} = a * (\epsilon_t)^b \quad (3.38)$$

Layer Rutting

$$\Delta_p = \Delta_r * c * N^d \quad (3.39)$$

where:

- $N_f$  = fatigue life,
- $N$  = number of load applications to reach  $\Delta_p$ ,
- $\varepsilon_t$  = tensile strain at the bottom of the asphalt concrete layer,
- $\Delta_p$  = layer permanent deformation,
- $\Delta_r$  = resilient layer compression, and
- $a, b, c, d$  = material coefficients.

Equation 3.38 shows the fatigue damage to be an exponential function of the tensile strain at the bottom of the asphalt layer. Typical recorded values for the exponent range from approximately 3 to 5. Equation 3.39 shows the layer permanent deformation to be linear functions of the resilient layer compressions. Thus, assuming the material coefficients to be independent of the tire configuration, the relative damaging effects for rutting of the single tire can be estimated directly from the ratio of the measured pavement responses.

Table 3.6 presents damage estimates for the loading and temperature conditions prevailing during the pavement distress tests. For these conditions, the single tire is expected to cause 3.5 to 4.3 times greater fatigue damage and 1.1 to 1.5 times greater rutting than the dual tire.

*Table 3.6 Relative damage estimates for super-single tire*

	Relative Damage Estimates			
	54.4 kN Load, 703 kPa Tire Pressure			
	89 mm Asphalt, 14°C		178 mm Asphalt, 23°C	
	Type	Ratio	Damage	Ratio
Asphalt Rutting	1.23	1.23	1.31	1.31
Base Course Rutting	1.40	1.40	1.31	1.31
Subgrade Rutting	1.53	1.53	1.09	1.09
Fatigue Damage	1.44	4.30 <sup>a</sup>	1.37	3.52 <sup>a</sup>

<sup>a</sup> Assuming fatigue exponent of 4.0.

The pavement distress experiment showed the super-single tire to be significantly more damaging. For an equal number of load repetitions, the rutting under the single tire loading was approximately twice that for the dual tires. Table 3.7 summarizes the distribution of the rutting in the dual and single tire sections just before failure of the super-single tire section. The majority of the permanent deformation for both tires occurred in the crushed aggregate base layer. The single tire produced greater permanent deformation in both the asphalt and the base course layers. The amount of rutting in the subgrade was small for all test conditions.

The fatigue life of the single tire section was only one-quarter that of the dual tire section. The measure of the fatigue life used in the study was the sum of the length of the cracks in the test section. For all distress tests except the single tire on the 178 mm asphalt section, the fatigue cracking began as transverse cracks. For the single tire on the 178 mm asphalt section, the cracks began as longitudinal cracks. This may be the result of the deeper rutting under the single tire loading, particularly under hot-pavement conditions.

Table 3.7 Layer pavement deformation

Layer	Layer Pavement Deformation							
	89 mm Asphalt Section 75,000 Passes				178 mm Asphalt Section 150,000 Passes			
	Dual		Single		Dual		Single	
	Rutting mm	%	Rutting mm	%	Rutting mm	%	Rutting mm	%
Asphalt	1.5	33	2.8	32	3.6	28	8.6	46
Base	2.3	50	5.1	57	8.9	68	9.7	51
Subgrade	0.8	17	1.0	11	0.5	4	0.5	3
Total	4.6	100	8.9	100	13.0	100	18.8	100

*Conclusions:* The Bonaquist results showed the 425/65R22.5 super-single tire to be significantly more damaging to conventional flexible pavements than traditional 11R22.5 dual tires. For the same load and tire pressure, the super-single tire produced higher vertical compressive strains in all layers of the pavement and higher tensile strains at the bottom of the asphalt concrete layer. These increased strains translate into greater rutting and shorter fatigue life for pavements trafficked with the super-single tire. For the pavements included in the experiment, the super-single tire produced ruts that were approximately twice as deep as those produced by the dual tires, and the fatigue life of pavements trafficked with the super-single tire was approximately one-quarter that obtained under the dual tire loading.

### ***Tridem Axles***

It must be emphasized that there were no tridem axles used in the AASHO Road Test. Initially, after the AASHO Road Test, the axle code variable had only two values: 1 for single axle and 2 for tandem axles. To accommodate the tridem axles, the value 3 was assigned to the axle code variable. Therefore, there is no certainty with respect to the tridem LEFs.

There is disagreement among researchers about what is the equivalent tridem load for 80 kN (18 kip) single-axle load. A similar situation exists for tandem axles.

In his 1988 study, Rilett (Rilett 88) reports LEFs versus axle load regression equations for single-, tandem-, and tridem-axle groups. These functions have been developed

from truck loading test data collected from nine sites across Canada in 1985. Regression analysis of the pooled single-axle data showed that load was statistically significant. Regression analysis of the pooled tandem data showed that load and axle spacing were statistically significant. Analysis of the pooled tridem-axle group data showed that load, axle spacing, structural number, and vehicle speed were statistically significant. The following regression equation was estimated for tridem axles:

$$LEF = 0.0008276 * LOAD^{2.669} * AXLE - SPACING^{-0.168} * SN^{-0.251} * SPEED^{0.074} \quad (3.40)$$

Table 3.8 (Hudson 94) summarizes the results of various studies. The AASHTO Guide suggests that a 48-kip tridem axle is equivalent to one 18-kip single. Christison shows that a tridem axle of 42 kip has an ESAL of 18 kip. Hutchinson suggests that a tridem axle of 38 kip causes the same damage as a single axle. Hajek, in his analysis of the Christison data points out that the AASHTO Guide underestimates tandem and tridem damage by 15 percent to 20 percent.

*Table 3.8 Predicted equivalent axle loads*

		Single Axle	Tandem Axle	Tridem Axle
Flexible Pavement	Christison	80 kN (18 kip)	133.5 kN (30 kip)	186.9 kN (42 kip)
	Hutchinson	80 kN (18 kip)	142.4 kN (32 kip)	169.0 kN (38 kip)
	AASHTO	80 kN (18 kip)	146.8 kN (33 kip)	231.6 kN (48 kip)
Rigid Pavement	Tayabji	80 kN (18 kip)	129.0 kN (29 kip)	160.2 kN (36 kip)
	AASHTO	80 kN (18 kip)	129.0 kN (29 kip)	173.5 (39 kip)

For rigid pavements, Tayabji (Tayabji 83, 84) used both measured and calculated edge and corner deflections calculated for each of the axle types — single, tandem, and tridem. Tayabji used the results of the field measurements primarily for corner loads and his calculated deflection for edge load. He compared his results with deflections taken at the AASHO Road Test. He then used observed deflections from the AASHO Road Test for single- and tandem-axle loads to extrapolate findings to estimate tridem-axle deflections.

#### ***Variation of Tire/Pavement Interface Contact Pressure***

In pavement design, two assumptions are generally made:

1. The tire contact pressure is equal to the tire inflation pressure.
2. The tire contact pressure is distributed uniformly over a circular area.

Hanson et al. in their 1989 study tested a bias Goodyear 18-22.5 LR-H super-single truck tire at 35.6, 44.5, and 53.4 kN (8, 10, and 12 kip) loads at inflation pressures of 586 and 690 kPa (85 and 100 psi) (Hanson 89). Pezo et al. tested the same tire at a load of 66.7 kN (15 kip) (Pezo 89). They noted that, generally, the mean contact pressures were higher than

the tire inflation pressures, as shown in Figure 3.1. Figure 3.2 shows the variation of tire contact area with load. Details about print width, print length, and testing systems are provided in their reports.

Hanson et al. and Pezo et al. concluded that if the inflation pressure is kept constant, the contact area tended to increase with an increase in wheel load. Also, at constant wheel loads, an increase in inflation pressure resulted in a decrease in contact area. The walls of the tested super-single tire initially established contact and had a circular contact patch that became more rectangular as the load increased beyond 44.5 kN (10 kip).

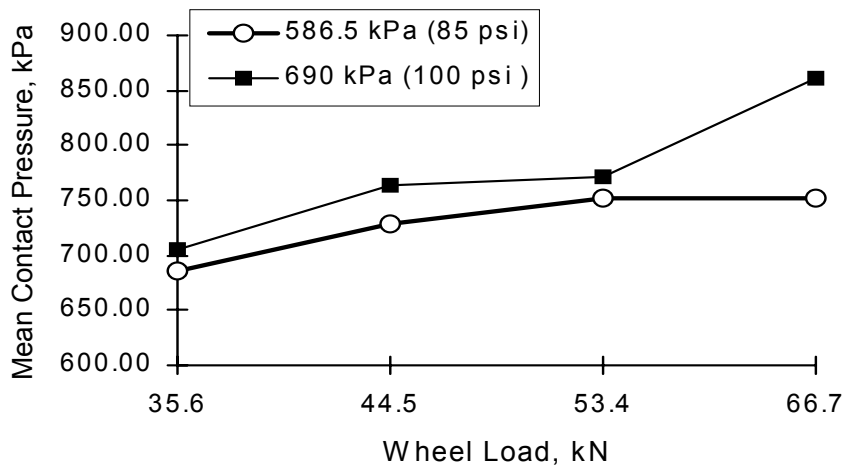
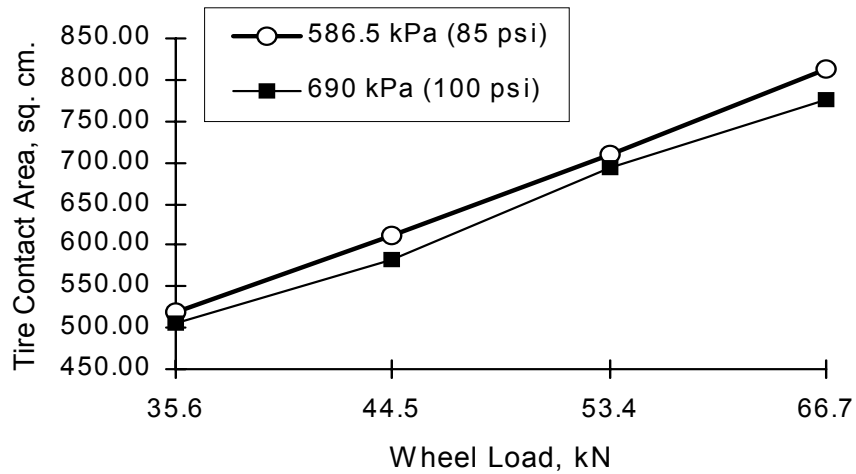


Figure 3.1 Variation of mean contact pressure at 586 and 690 kPa (85 and 100 psi) inflation pressure for various wheel loads (Bias Goodyear 18-22.5 LR-H Super-single tire)

A South African study (De Beer 97) used the Vehicle-Road Surface Pressure Transducer Array (VRSPTA), a device that consists of an array of triaxial strain gauged steel pins fixed to a steel base plate, together with additional uninstrumented supporting pins, fixed flush with the road surface.

Data were collected simultaneously on sixty-four channels or strain gauges. The data collection system, activated by a moving wheel, is capable of measuring at wheel speeds from 1 to 120 km/h (0.3 to 33 m/s), vertical loads up to 200 kN, and horizontal loads up to 20 kN. This system is installed flush with the surface of the pavement to a relatively high precision to minimize load variation as a result of dynamic impact on the system.



*Figure 3.2 Variation of tire contact area at 586 and 690 kPa (85 and 100 psi) inflation pressure for various wheel loads (Bias Goodyear 18-22.5 LR-H Super-single tire)*

Using the VRSPAT system De Beer et al. tested seven tires in June and July of 1996. Three among these were super-single tires — Michelin 425/65 R 22.5, Bridgestone 425/65 R 22.5-R160AZ and R164BZ. The Michelin was tested using the HVS in South Africa and the Bridgestones were tested in The Netherlands at the Lintrack facility. It was clearly demonstrated during their study that the maximum vertical contact stresses are indeed, most of the time, higher than the tire inflation pressure. Even under the rated load and inflation pressures these stresses can be up to twice the tire inflation pressure (De Beer 97).

The device used by Himeno et al. to measure tire contact pressure was developed by the Komatsu Corporation and has piezo electric ceramic sensors that are 14 mm wide and 18 mm long. The measuring device consists of sixty-four sensors placed at intervals of 15 mm laterally on a board. Contact pressure was obtained by dividing the measured weight by the area of the sensor. While they did not test any super-single tires, their results for standard truck tires were consistent with those obtained in other studies (Himeno 97).

### ***Effect of Increased Tire Pressure***

Gillespie et al. in their 1993 NCHRP document reported the effects of heavy vehicle characteristics on pavement performance (NCHRP 93). They determined that there was a strong interaction between pavement fatigue and tire type and between wheel load and inflation pressure, among other factors. As reported by Gillespie et al., the effect of tire type on rigid pavement fatigue derives from its influence on peak stress at the bottom of the concrete slab (NCHRP 93). For the same load, the dual-tire configuration produced the least peak tensile stress. Wide base or super-single tires produced a peak tensile stress that was 2 to 9 percent higher than that produced by dual tires under similar load conditions. The conventional single tire had the highest peak tensile stress, 15 to 20 percent greater than that

for the dual tires (a result of its small contact patch). For flexible pavements the same trend continued. Peak tensile strains at the bottom of a 16.51 cm (6.5 in.) asphalt surface layer were determined. The conventional single tire had the highest tensile strain, again a result of its small contact patch. The wide base or super-single tire, followed by the dual tires, had lower peaks (NCHRP 93).

Tire inflation pressure is a parameter that can be readily set and varied by the truck operator. Gillespie et al. studied the effects of a super-single tire loaded to 71.2 kN (16 kip) and a dual tire loaded to 88.9 kN (20 kip) on a rigid pavement using the finite element method; their results are shown in Figure 3.3. Expected fatigue damage from the super-single tire increased by 53 percent over the range of inflation pressure from 518 to 828 kPa (75 to 120 psi). This finding was a result of the contact length of the tire changing significantly with inflation pressure at constant load. On the other hand, the duals were not as sensitive to change in inflation pressure, changing by 15 percent over the range of pressure from 518 to 828 kPa (75 to 120 psi).

For a 12.7 cm (5 in.) wearing course thickness flexible pavement, under the same conditions, damage for the 15R22.5 tire increased by a factor of more than 9 over the range of inflation pressures from 518 to 828 kPa (75 to 120 psi). For 11R22.5 duals the damage varies by a factor of 2.8 over the same inflation range. This variation in damage is owing to the significant change in the contact length of the super-single (15R22.5) tire with changing inflation pressure under the same load, whereas 11R22.5 tires are not as sensitive to changes in inflation pressure.

Hudson et al. (Hudson 88) used a mechanistic approach to evaluate the impact of increased tire pressures. In their study, the elastic layer theory program ELSYM5 was used to model an average pavement structure. Computer runs were made for axle loads of 80 and 125 kN (18 and 28 kip), and tire pressures ranging from 483 to 1104 kPa (70 to 160 psi), varying at 69-kPa (10-psi) increments. The results indicate that horizontal tensile strain and shear strain increase as tire pressure increases, whereas vertical strain on the roadbed soil remains fairly constant.

From the data collected in the field at three Arizona port-of-entry weigh stations, it was established that the mean radial tire pressure (front axle) was equal to 730.71 kPa (105.9 psi) and an interval containing 90 percent of all observations ranged from 622.38 to 839.04 kPa (90.2 to 121.6 psi). The tire pressure range corresponded to a strain range from  $1.30 \cdot 10^{-3}$  cm/cm to  $1.50 \cdot 10^{-3}$  cm/cm ( $0.51 \cdot 10^{-3}$  in./in. to  $0.59 \cdot 10^{-3}$  in./in.).

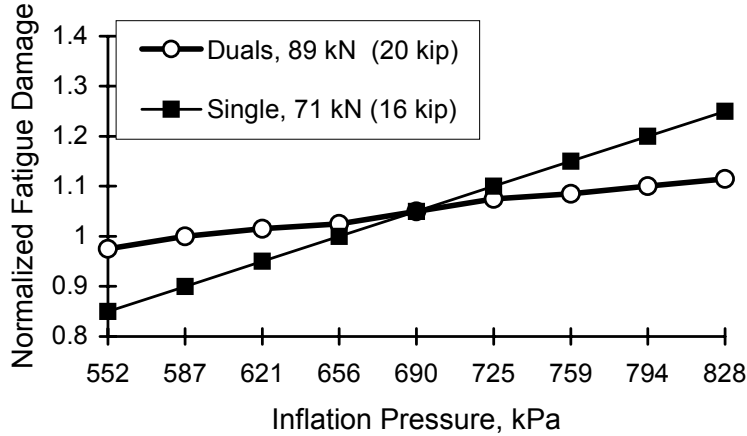


Figure 3.3 Rigid pavement fatigue damage versus inflation pressure or duals (11R22.5) and wide based (15R22.5) tires (NCHRP 93)

The fatigue equation for less than 10 percent cracking developed by Finn (Finn 77) produced the following results:

$$\log N_f (\leq 10\%) = 15.947 - 3.291 * \log(\text{strain} / 10^{-6}) - 0.854 * \log\left(\frac{E}{103}\right) \quad (3.41)$$

This equation produced  $N_f = 83350$  applications for a strain of  $1.30 * 10^{-3}$  cm/cm ( $0.51 * 10^{-3}$  in./in.) and  $N_f = 51601$  applications for a strain of  $1.50 * 10^{-3}$  cm/cm ( $0.59 * 10^{-3}$  in./in.). A 35 percent increase in tire pressure increased strain by only 15.7 percent, but reduced pavement life by 38 percent, according to the Finn equation.

Hudson et al. developed a program to predict 80 kN (18 kip) ESALs for Arizona highways. Table 3.9 compares AASHTO and ARE load equivalency for selected loads. Table 3.9 shows that the tire pressure has significant effect on the relative damage of different loads on pavement with SN=4.

Table 3.9 Comparison of AASHTO and ARE Inc. equivalence factors for single axles (Hudson 88)

Axle Load (kip)	AASHTO Equiv. Factor 517.5 kPa (75 psi)	ARE Equiv. Factor 517.5 kPa (75 psi)	ARE Equiv. Factor 759 kPa (110 psi)	ARE Equiv. Factor 1000.5 kPa (145 psi)
4	0.003	0.0026	0.0060	0.0096
10	0.102	0.1446	0.5555	1.2790
<b>18</b>	<b>1.0</b>	<b>1.0</b>	<b>5.295</b>	<b>15.517</b>
30	6.8	6.97	25.3	90.1
50	60	60.5	236.9	427.7

Pt = 2.5, and SN = 4

## **OTHER METHODS USED TO CONSIDER TRAFFIC DATA FOR PAVEMENT DESIGN**

### ***Calibrated Mechanistic Design Procedure***

In calibrated mechanistic design, there is no need for LEFs. Traffic is divided into a number of load groups, each group having different load magnitudes and configurations and different numbers of load repetitions.

When the design is based on each type of distress, it is unreasonable to use an ESAL because the equivalent factor for one type of distress differs from that of the other. The load magnitude and configuration, such as wheel spacing, contact radius, and contact pressure, are used in the structural models, while the number of repetitions is used in the distress models.

*Calibrated mechanistic procedure* is a more specific name for the mechanistic-empirical procedure. It contains a number of mechanistic distress models that require careful calibration and verification to ensure that satisfactory agreement between predicted and actual distress can be obtained. The purpose of calibration is to establish transfer functions relating mechanistically determined responses to specific forms of physical distress. Verification involves the evaluation of the proposed models by comparing results to observations in other areas not included in the calibration exercise. This procedure has been used in several design methods (e.g., the Asphalt Institute method). However, these existing methods are based on many simplifying assumptions and are not as rigorous as desired.

The general methodology for flexible and rigid pavement design is presented in Figure 3.4. In this figure, it is assumed that the materials to be used for the pavement structure are known *a priori* and that only the pavement configuration is subjected to design iterations. If changing the pavement configuration does not satisfy the design requirements, it may be necessary to change the types and properties of the materials to be used. If so, the iteration should also go through Steps 2 and 3, instead of directly from Step 1 to 5.

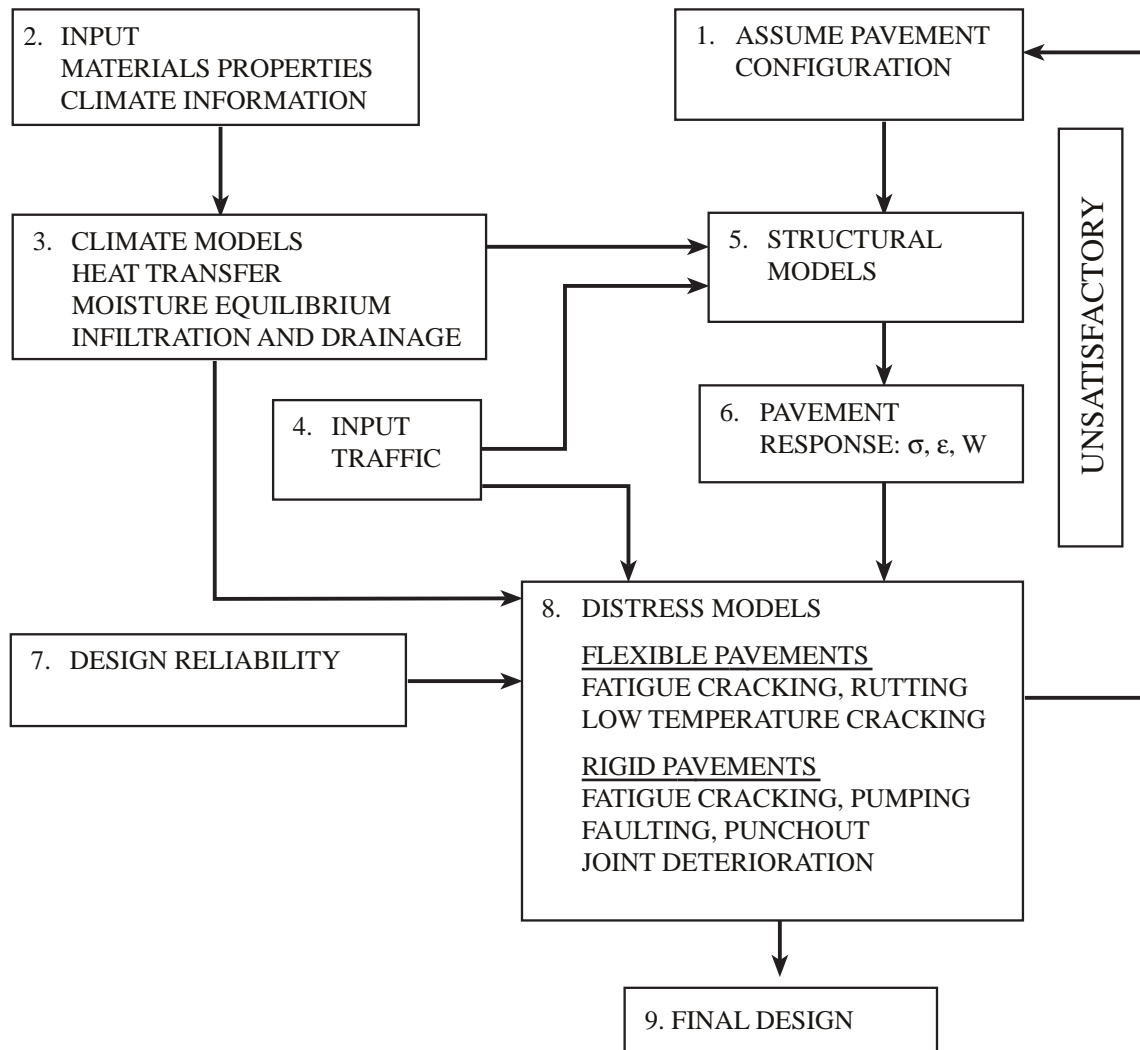


Figure 3.4 Methodology of calibrated mechanistic procedure for flexible and rigid pavement design (Huang 93)

The pavement configuration in Figure 3.4 includes the number of layers, the thicknesses of each layer, and the type of materials.

The basic material properties for the structural models are the resilient modulus of HMA, base, subbase, and subgrade, while those for the distress models involve the various failure criteria, one for each distress. If temperature and moisture at different times of the year vary significantly, it is unreasonable to use the same modulus for each layer throughout the entire year. Each year should be divided into a number of periods, each having a different set of moduli based on the climatic data specified.

#### ***Asphalt Institute Method for Flexible Pavements***

The ninth edition of *Manual Series No. 1* (MS-1), published by the Asphalt Institute, is based on mechanistic-empirical methodology, using the mechanistic multilayer theory in

conjunction with empirical failure criteria to determine pavement thicknesses. Based on the results obtained from the DAMA computer program, a series of design charts covering three different temperature regimes were developed. The Asphalt Institute uses the two following design criteria:

*Fatigue criterion:* For a standard mix with asphalt volume of 11 percent and air void volume of 5 percent, the fatigue equation is

$$N_f = 0.0796 * (\varepsilon_t)^{-3.291} |E^*|^{-0.854} \quad (3.42)$$

where:

$N_f$  = the allowable number of load repetitions to control fatigue cracking,

$|E^*|$  = the dynamic modulus of the asphalt mixture, and

$\varepsilon_t$  = horizontal strain at the bottom of the asphalt layer.

It was reported that the use of Equation 3.42 would result in fatigue cracking of 20 percent of the total area, as observed on selected sections of the AASHO road test.

*Permanent deformation criterion:* The allowable number of load repetitions to control permanent deformation can be expressed as

$$N_d = 1.365 * 10^{-9} * (\varepsilon_c)^{-4.477} \quad (3.43)$$

where:

$\varepsilon_c$  = the vertical compressive strain on the surface of the subgrade, which causes permanent deformation of rutting.

The use of Equation 3.43 should not result in rutting greater than 1.27 cm (0.5 in.) for the design traffic.

## COMPUTER MODELING OF PAVEMENT STRUCTURES

Researchers at The University of Texas at Austin and at The University of Texas at San Antonio performed computer modeling using finite element methods. Because factors such as increased tire pressures are not reflected in the current LEFs, the pilot computer modeling was used to evaluate how the change on tire pressure affects the primary pavement responses. If the primary responses are affected by a change in vehicle characteristics, LEFs based on primary responses would reflect the changing vehicle characteristics.

Preliminary computer modeling was performed at The University of Texas at Austin using the finite element program ABAQUS. In the first set of runs, linear elastic models were used. The results were compared with those generated from the elastic program ELSYM5 to check if the results from ABAQUS were in agreement with general elastic theory. The primary responses (surface deflection, tensile strain at the bottom of the AC

layer, compressive strain at the top of subgrade) from ABAQUS were slightly lower than those from ELSYM5. In the first set of runs, four cases were considered.

*Table 3.10 Pilot experiment*

	<b>Wheel</b>	<b>Tire</b>
	<b>Load</b>	<b>Pressure</b>
<b>Case 1</b>	44.5 kN (10 kip)	552 kPa (80 psi)
<b>Case 2</b>	44.5 kN (10 kip)	828 kPa (120 psi)
<b>Case 3</b>	89 kN (20 kip)	552 kPa (80 psi)
<b>Case 4</b>	89 kN (20 kip)	828 kPa (120 psi)

The results for radial strain throughout the pavement structure of the four cases are shown in Figures 3.5 through 3.8. Since the load was applied to the pavement structure symmetrically, only half of the pavement structure is shown. Node 1 is located under the center of the wheel load; node 5, at the interface of AC layer and base layer; and node 10, at the interface of base layer and subgrade.

It can be seen from the figures that with the same wheel load, increased tire pressure has an impact on radial stresses in the flexible pavement structure. Figures 3.5 through 3.6 show the results for a wheel load of 44.5 kN (10 kip) and tire pressure of 552 and 828 kPa (80 and 120 psi), respectively. Figures 3.5 and 3.6 indicate that, for the same wheel load but with different tire pressure, there are changes in radial strains in the pavement structure. The compressive strain is increased at the top of the AC layer; the tensile strain is increased at the bottom of the AC layer and the base layer. A similar situation is observed for the 88.9 kN (20 kip) load with tire pressures of 552 and 828 kPa (80 and 120 psi), as shown in Figures 3.7 and 3.8, respectively.

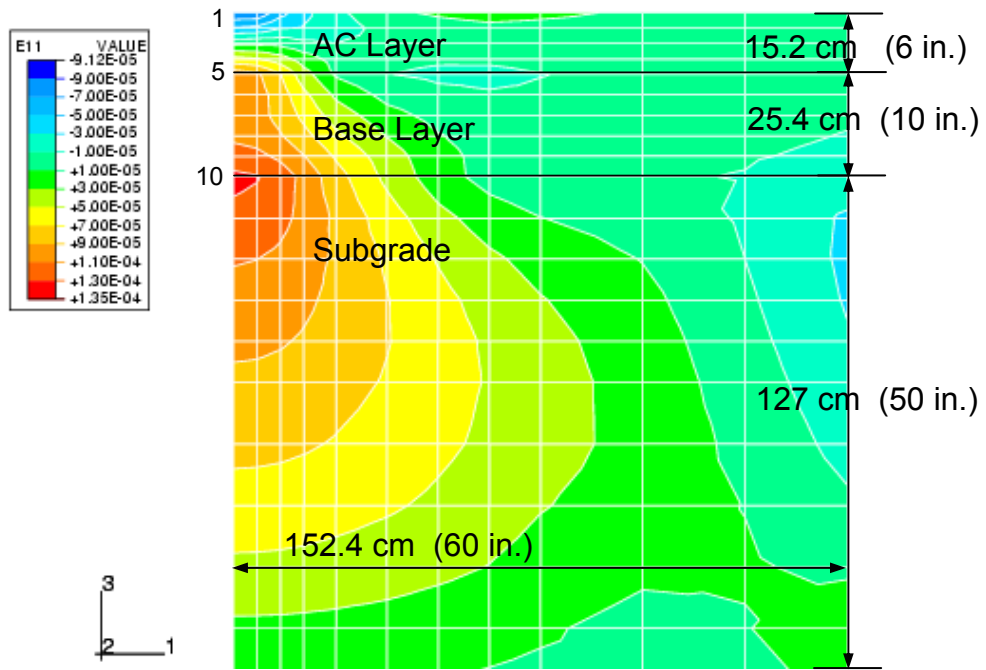


Figure 3.5 Radial strains in flexible pavement: 44.5 kN (10 kip) wheel load, 552 kPa (80 psi) tire pressure

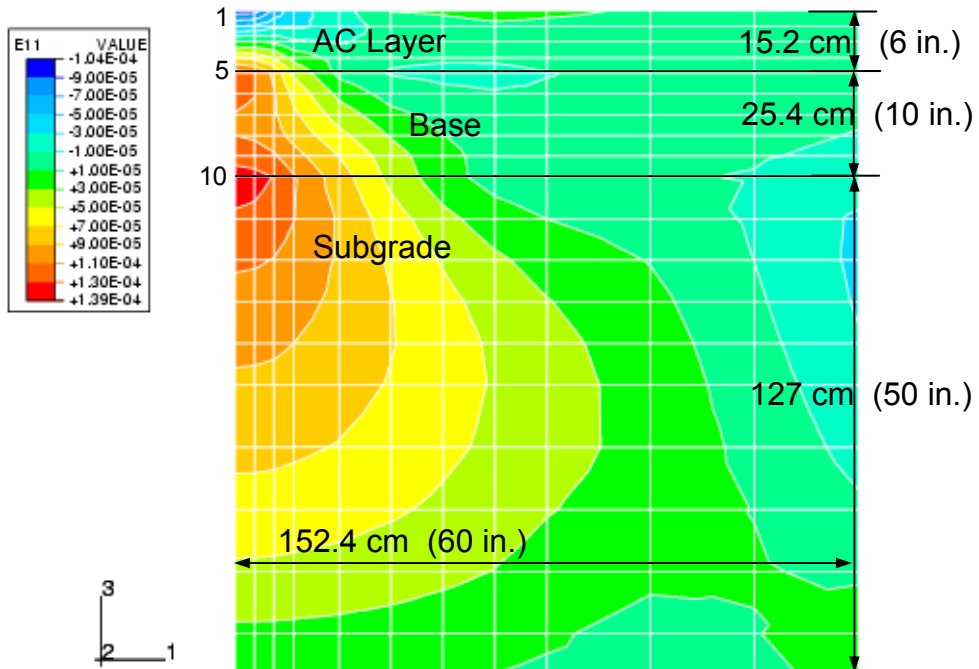


Figure 3.6 Radial strains in flexible pavement: 44.5 kN (10 kip) wheel load, 828 kPa (120 psi) tire pressure

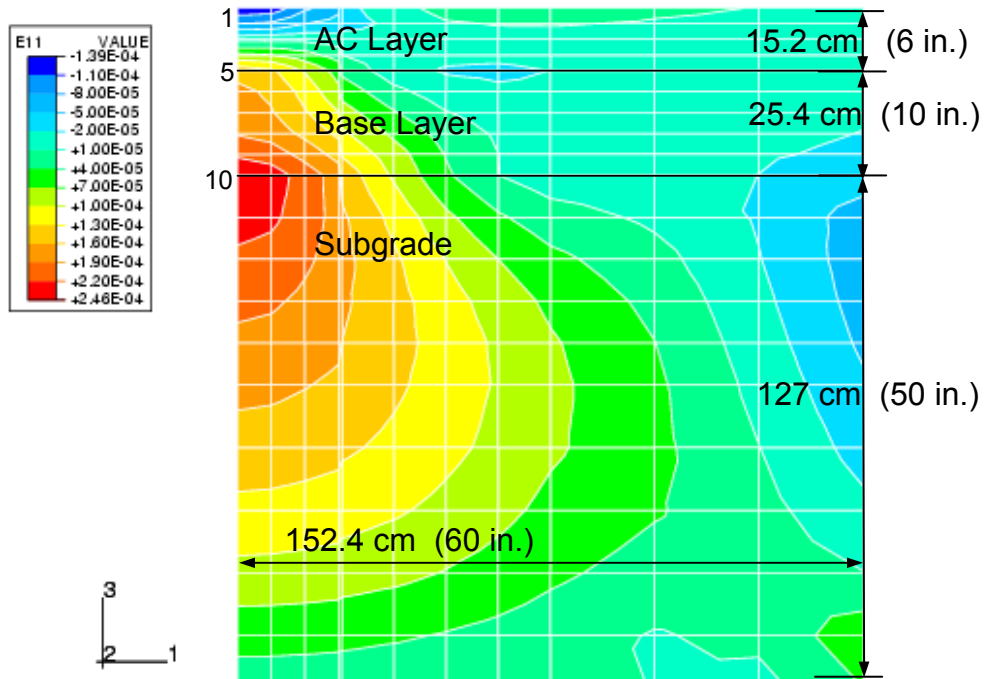


Figure 3.7 Radial strains in flexible pavement: 89 kN (20 kip) wheel load, 552 kPa(80 psi) tire pressure

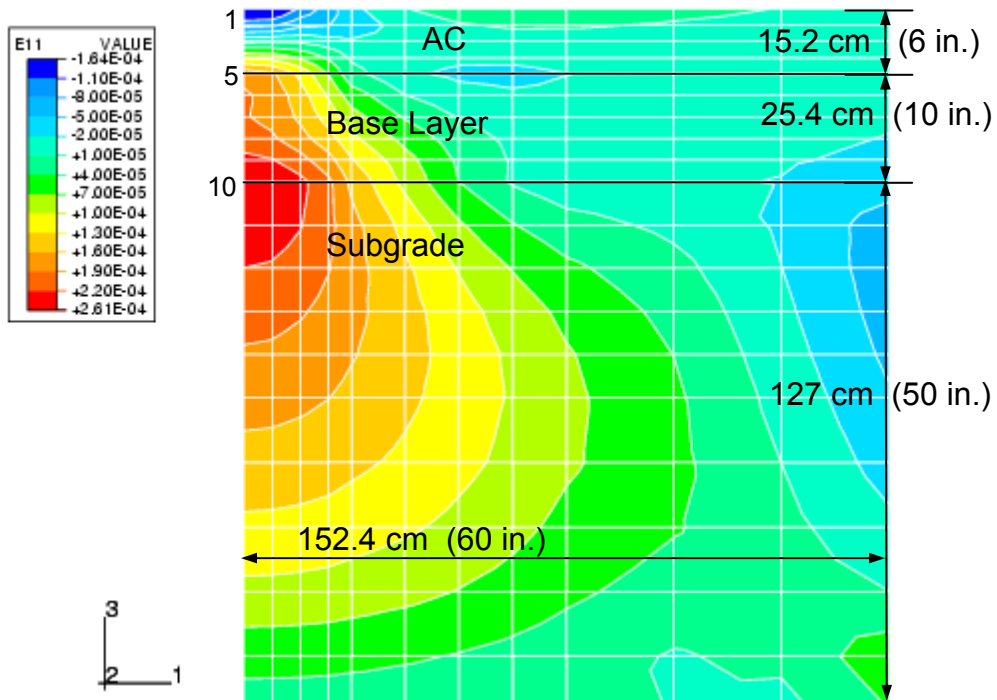


Figure 3.8 Radial strains in flexible pavement: 89 kN (20 kip) wheel load, 828 kPa (120 psi) tire pressure

## CHAPTER SUMMARY

This chapter presented a comprehensive literature review of mechanistic and statistical methods for determining LEFs. It was concluded from the review that the calculation of LEFs can be based on such primary responses as deflections, strains, or stresses in the pavement structure. Hudson et al. (Hudson 92) concluded that the Hutchinson deflection method appears to be the most viable method currently available.

Important findings that have potential impact on LEFs are summarized as follows:

1. Super-single tires can cause more damage to the pavement structure. Bonaquist observed that for the same load and tire pressure, fatigue damage of the super-single tire 425/65R22.5 is 4 times greater and layer rutting 1.0 to 2.4 times deeper than those of the dual tire (Bonaquist 92).
2. There is a general consensus among researchers that an increase in tire pressure accelerates pavement deterioration. Most researchers came to this conclusion based on the structural analysis of pavements. The Bonaquist study (Bonaquist 88) showed that doubling the tire pressure from 524.4 to 966 kPa (76 to 140 psi) could increase predicted damage by 20 percent, which is equivalent to an axle load increase of approximately 8.9 kN (2,000 lb).
3. The TTI study indicates that the subgrade modulus, the AC layer thickness for flexible pavements, and the environmental zone can be important factors in calculating LEFs.
4. According to some researchers, the speed of vehicles could be another factor to consider in calculating LEFs (Hutchinson 87, Papagiannakis 92).



## CHAPTER 4. IRICK REANALYSIS OF AASHO ROAD TEST DATA

### AASHO ROAD TEST DATA

A portion of the test data collected at the AASHO Road Test is documented in Appendix A of Special Report 61E (AASHO 62E). The following data are available for each section:

1. Log applications for serviceability levels of 3.5, 3.0, 2.5, 2.0, 1.5.
2. Serviceability index for AASHO index day 11, 22, 33, 44, and 55 (one AASHO index day lasted for two weeks and the complete test lasted for fifty-five index days).

Since not all sections at the AASHO Road Test reached a serviceability level of 1.5, the data for some sections are not complete. Most of the flexible pavement sections failed before the end of the test. However, most of the *rigid* pavement sections did *not* fail by the end of the test. The selection of the slab thicknesses for rigid pavements was based on the judgment of a large number of experts, with the objective that approximately two-thirds of the sections would fail in the experiment under chosen loading conditions. In fact, approximately one-third of the rigid pavements did fail before the end of the AASHO Road Test.

Tables 4.1 through 4.5 present the AASHO Road Test data for rigid pavements and test sections with single-axle loadings. The final serviceability index for each section is also included. The tables also contain information on which data items were used in the AASHO and Irick analyses. Lane 1 of Loop 2 was completely excluded from the analyses, since the test sections deteriorated only slightly. For the same reason, the sections having the thickest slab in each loop were excluded from the AASHO and Irick analyses. Irick did use data from sections that reached a final serviceability index of at least 3.5.

### IRICK'S ANALYSIS

Irick (Irick 89) conducted a new study of the AASHO Road Test data to develop a set of LEFs characteristics that are (1) consistent with current knowledge about pavement distress and performance and (2) in general agreement with load equivalency ratios calculated directly from AASHO test data.

For the purpose of his study, Irick created four databases. He selected those sections with only single-axle loadings for his study. The first database contains traffic data and environmental data that relate to all AASHO road test sections, including flexible pavement deflection data from Loop 1 to show how the structural condition of these sections changed during various seasons of the year. In the second database, Irick presented only the full serviceability histories for the selected twelve flexible and the selected twelve rigid sections. In the third database, flexible test sections that have similar SN values are grouped into "structural classes" whose values are the SN median values for all SNs within a class. The

value of “structural class” was selected as the median for all structures within the “structural class.”

Table 4.1 AASHO Road Test data for loop 2, lane 2, and single-axle loading of 26.7 kN (6.0 kip)

Slab Type	Thickness		Lane 2			PSI level Reached	Sect. No.
	Slab	Subbase	AASHO	Irick Indirect	Irick Direct		
Non Reinforced	2.5	0				<1.5	806
		3				2.2	792
		6				3.1	786
	3.5	0				3.7	814
		3				4.0	812
		6				4.0	788
	5.0	0				4.1	802
		3				4.1	798
		3				3.6	778
	2.5	6				4.0	804
		0				<1.5	782
		3				<1.5	800
6					3.8	790	
0					4.1	794	
3					4.1	816	
Reinforced	3.5	3				4.2	780
		6				4.6	784
		0				4.5	808
	5.0	3				4.6	810
		6				4.3	796
		0				4.3	796

-  log W given for PSI = 3.5, 3.0, 2.5, 2.0, and 1.5 (AASHO model).  
log W given for PSI = 3.0, 2.5, 2.0, and 1.5 (Irick model).
-  log W and PSI given for index day = 11, 22, 33, 44, and 55.  
(only AASHO analysis)
-  log W estimated on partial data (only Irick analysis)
-  Section included in the estimation of the mean log applications  
(only Irick analysis)
-  Section eliminated from the analysis

Table 4.2 AASHO Road Test data for loop 3, lane 1, and single-axle loading of 53.4 kN (12.0 kip)

Slab Type	Thickness		Lane 1					
	Slab	Subbase	AASHO	Irick Indirect	Irick Direct	PSI level Reached	Sect. No.	
Non Reinforced	3.5	3				<1.5	195	
		6				<1.5	239	
		9				<1.5	213	
	5.0	3					3.7	225
		6					3.5	245
		6					3.1	221
		9					3.7	219
	6.5	3					4.4	217
		3					3.9	193
		6					4.1	249
	8.0	9					4.2	207
		3					4.4	201
		6					4.3	235
		9					4.0	185
	Reinforced	3.5	3				<1.5	209
6						<1.5	205	
9						<1.5	231	
5.0		3					2.8	251
		3					4.0	203
		6					<1.5	191
		9					3.3	233
6.5		3					4.2	199
		6					4.3	247
		6					4.5	237
		9					4.4	241
8.0		3					4.3	211
		6					4.2	215
		9					4.1	197

-  log W given for PSI = 3.5, 3.0, 2.5, 2.0, and 1.5 (AASHO model).  
log W given for PSI = 3.0, 2.5, 2.0, and 1.5 (Irick model).
-  log W and PSI given for index day = 11, 22, 33, 44, and 55.  
(only AASHO analysis)
-  log W estimated on partial data (only Irick analysis)
-  Section included in the estimation of the mean log applications  
(only Irick analysis)
-  Section eliminated from the analysis

Table 4.3 AASHO Road Test data for loop 4, lane 1, and single-axle loading of 80 kN (18.0 kip)

Slab Type	Thickness		Lane 1				
	Slab	Subbase	AASHO	Irick Indirect	Irick Direct	PSI level Reached	Sect. No.
Non Reinforced	5.0	3	■	■	■	<1.5	643
		6				<1.5	647
		9				<1.5	677
	6.5	3	■	■	■	3.8	649
		6	■	■	■	4.4	697
		6	■	■	■	4.3	655
	9	6	■	■	■	3.0	703
		3	■	■	■	4.4	671
		3	■	■	■	4.5	687
	8.0	6	■	■	■	4.4	683
		9	■	■	■	4.3	651
		3	■	■	■	4.2	675
	9.5	6	■	■	■	4.5	701
		9	■	■	■	4.1	689
		3	■	■	■	4.2	675
Reinforced	5.0	3	■	■	■	<1.5	681
		6				<1.5	661
		9				<1.5	673
	6.5	3	■	■	■	3.8	641
		3	■	■	■	3.6	705
		6	■	■	■	3.4	685
	9	9	■	■	■	1.8	653
		3	■	■	■	3.9	691
		6	■	■	■	4.4	669
	8.0	6	■	■	■	3.9	707
		9	■	■	■	4.3	695
		3	■	■	■	4.0	645
	9.5	6	■	■	■	4.5	665
		9	■	■	■	4.8	667
		3	■	■	■	4.8	667

■ log W given for PSI = 3.5, 3.0, 2.5, 2.0, and 1.5 (AASHO model).  
 ■ log W given for PSI = 3.0, 2.5, 2.0, and 1.5 (Irick model).

■ log W and PSI given for index day = 11, 22, 33, 44, and 55.  
 (only AASHO analysis)

■ log W estimated on partial data (only Irick analysis)

■ Section included in the estimation of the mean log applications  
 (only Irick analysis)

■ Section eliminated from the analysis

Table 4.4 AASHO Road Test data for loop 5, lane 1, and single-axle loading of 99.7 kN (22.4 kip)

Slab Type	Thickness		Lane 1			PSI level Reached	Sect. No.
	Slab	Subbase	AASHO	Irick Indirect	Irick Direct		
Non Reinforced	6.5	3				failed	513
		6				failed	517
		9				failed	505
	8.0	3				4.2	547
		6				4.2	539
		6				4.1	533
	9.5	9				failed	507
		3				4.4	511
		3				4.3	541
		6				3.7	525
		9				4.5	535
		3				4.1	529
11.0	6				4.5	497	
	9				4.5	509	
	9				4.5	509	
Reinforced	6.5	3				failed	523
		6				failed	491
		9				failed	549
	8.0	3				failed	519
		3				4.3	521
		6				4.0	501
	9.5	9				4.6	531
		3				4.3	553
		6				4.5	543
	11.0	6				4.3	503
		9				4.4	499
		3				4.1	515
11.0	6				4.4	545	
	9				4.4	495	
	9				4.4	495	

-  log W given for PSI = 3.5, 3.0, 2.5, 2.0, and 1.5 (AASHO model).  
log W given for PSI = 3.0, 2.5, 2.0, and 1.5 (Irick model).
-  log W and PSI given for index day = 11, 22, 33, 44, and 55.  
(only AASHO analysis)
-  log W estimated on partial data (only Irick analysis)
-  Section included in the estimation of the mean log applications  
(only Irick analysis)
-  Section eliminated from the analysis

Table 4.5 AASHO Road Test data for loop 6, lane 1, and single-axle loading of 133.5 kN (30.0 kip)

Slab Type	Thickness		Lane 1					
	Slab	Subbase	AASHO	Irick Indirect	Irick Direct	PSI level Reached	Sect. No.	
Non Reinforced	8.0	3				failed	353	
		6				3.9	393	
		9				3.4	369	
	9.5	3				3.6	351	
		6				4.3	367	
		6				4.3	389	
	11.0	9				4.2	375	
		3				4.2	377	
		3				4.4	363	
	12.5	6				4.2	397	
		9				4.3	365	
		3				4.2	395	
	Reinforced	8.0	6				4.0	349
			9				4.2	379
			3				failed	341
9.5		6				failed	385	
		9				failed	347	
		3				4.5	381	
11.0		3				1.6	371	
		6				4.0	403	
		9				2.2	339	
12.5		3				4.4	391	
		6				4.0	337	
		6				4.3	345	
12.5		9				4.2	343	
		3				4.4	359	
		6				4.2	355	
		9			4.5	357		

-  log W given for PSI = 3.5, 3.0, 2.5, 2.0, and 1.5 (AASHO model).  
log W given for PSI = 3.0, 2.5, 2.0, and 1.5 (Irick model).
-  log W and PSI given for index day = 11, 22, 33, 44, and 55.  
(only AASHO analysis)
-  log W estimated on partial data (only Irick analysis)
-  Section included in the estimation of the mean log applications  
(only Irick analysis)
-  Section eliminated from the analysis

SN was defined at the AASHO Road Test to be a linear combination of layer thicknesses adjusted by coefficients representing the relative strength/stiffness of the respective layers:

$$\text{SNU} = 0.37 \cdot D1 + 0.14 \cdot D2 + 0.10 \cdot D3 \quad \text{for unweighted applications} \quad (4.1)$$

$$\text{SNW} = 0.44 \cdot D1 + 0.14 \cdot D2 + 0.11 \cdot D3 \quad \text{for weighted applications} \quad (4.2)$$

For rigid pavement sections the structural class was defined to be equal to the PCC surfacing thickness (D1).

Missing data occur whenever a test section did not reach the specified distress or serviceability level during the road test. For any particular test section, database 3 contains eight application entries: four for two levels of two types of distress and four for serviceability levels. Database 3 for flexible pavements thus contains  $8 \times 164 = 1312$  cells, of which 355 have missing data and 957 contain numbers of axle load applications. Database 3 for rigid pavements contains  $8 \times 152 = 1216$  data cells, of which 875 have missing data and only 341 contain numbers of axle load applications.

Database 4 is for the logarithms of applications for each selected level of distress or serviceability for flexible and rigid pavements. The sets of sections whose structural numbers vary less than 0.10 have been grouped into the same structural classes. The rigid pavement test sections are grouped by PCC thickness for each axle load. Six different pavement designs were used for each thickness-load combination, each containing either 0, 1, or 2 replicate sections.

For sections that had not reached the given distress or serviceability level by the end of the road test, log applications are shown to be greater than 6.05 (the logarithm of 1,113,800 applications). In some cases, the PSI for a section reached 1.5 before the given levels of cracking or rutting depth had been reached. In these instances, log applications for the given distress level are indefinite and greater than the log applications for  $PSI = 1.5$ .

**Statistical distribution of log applications among sections experiencing similar stress levels.** In Irick's study, it was assumed that the statistical frequency distributions of 'the number of applications to failure is log-normal, or alternatively, that the distribution of log applications to failure is normal. Irick's report is based on the assumption that the log applications for a given distress or serviceability level are normally distributed among test sections that experience similar stress levels.

Irick grouped the test sections according to SN. If, in such a group, not all test sections have reached the desired distress level, then the mean log application can be estimated only if at least one or more test sections reached the desired distress level.

There are  $M$  test sections, such that only a partial set  $m$  reached desired distress level.  $LN^p$  is the mean value for the  $m$  observed log applications, and  $LN''$  is the (unobserved) mean value for the complete set of  $M$  sections (Figure 4.1).

Irick stated that through integral calculus, it could be shown that the mean value ( $LN^p$ ) of  $LN$  within the partial distribution is given by:

$$LN^p = LN'' - SD * f(LN^p)/p \quad (4.3)$$

Rearranging the terms the following equation can be obtained:

$$LN'' = LN^p + SD * f(LN^p)/p \quad (4.4)$$

where  $p=m/M$ . The distribution mean  $LN''$  can be calculated knowing  $p$ ,  $SD$ , and  $f(LNp)$ .

Table 4.6 gives tabulated values for combinations of  $m$  and  $M$ , corresponding values for  $p$  and  $f(LNp)$ , and final adjustments to be added to the partial means  $LNp'$  that have been observed for  $m$  sections.

The values of  $Sdfu$  for unweighted flexible pavement application and  $Sdfw$  for weighted flexible pavement application were estimated from AASHO Road Test data. Values of  $f(LNp)$  are for the standard normal distribution.

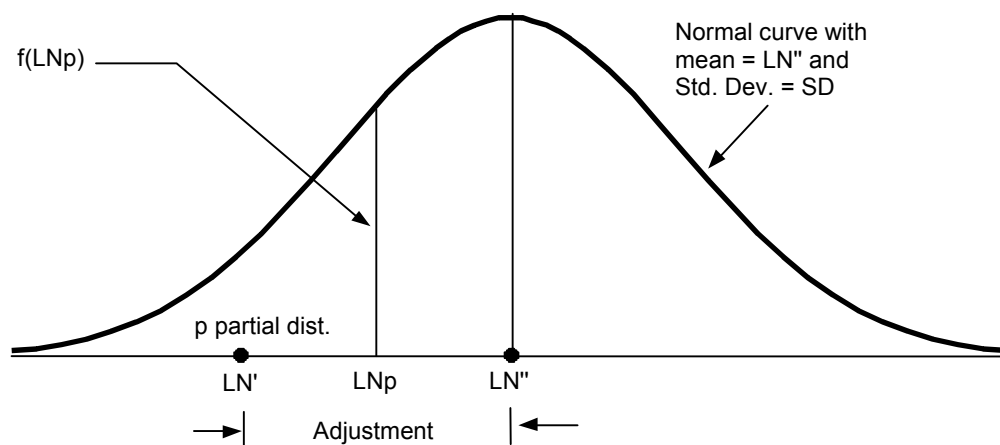


Figure 4.1 Theoretical relationship between the mean of a partial distribution and the mean of the complete distribution

**Regression Analyses for Log Application Data.** Irick conducted regression analyses for the log application data and log equivalence data (Irick 89). He provided graphs to show how the log applications appear to be related to axle load, structural characteristics, and distress levels, respectively. From graphs with log scale provided by Irick, log applications decrease linearly with increase log axle loads for flexible pavements. There are, however, some data points that are outliers. For rigid pavements such linearity cannot be demonstrated, because very few cases have three or more points for a given combination of structure and distress level. Other graphs in Irick's study show log applications plotted against log SN or log PCC thickness. These graphs show nonlinearities with opposite curvatures for rigid and flexible pavements. This indicates that load equivalence ratios for any two axle loads will change with pavement structure.

Table 4.6 Adjustments added to partial data mean to estimate complete data mean (Irick 89)

M	m	p	f(LNp)	Sdfu	FP-UA Adj.	Sdfw	FP-WA Adj.
					f*Sduf/p		f*Sdwf/p
7	6	0.857	0.226	0.294	0.078	0.307	0.081
	5	0.714	0.340	0.294	0.140	0.307	0.146
	4	0.571	0.393	0.294	0.202	0.307	0.211
	3	0.429	0.393	0.294	0.270	0.307	0.282
	2	0.286	0.340	0.294	0.350	0.307	0.365
	1	0.143	0.226	0.294	0.465	0.307	0.486
6	5	0.833	0.250	0.294	0.088	0.307	0.092
	4	0.667	0.364	0.294	0.161	0.307	0.168
	3	0.500	0.399	0.294	0.235	0.307	0.245
	2	0.333	0.364	0.294	0.321	0.307	0.335
	1	0.167	0.250	0.294	0.441	0.307	0.461
5	4	0.800	0.280	0.294	0.103	0.307	0.107
	3	0.600	0.386	0.294	0.189	0.307	0.198
	2	0.400	0.386	0.294	0.284	0.307	0.296
	1	0.200	0.280	0.294	0.412	0.307	0.430

Equation 4.5 gives the linear mathematical model used for the initial regression analyses of log applications data.

$$LAP = A + B*(LLOAD) + C*(LSTRU) + D*(LDIST) + E*(LLOAD)*(LSTRU) + F*(LLOAD)*(LDIST) + G*(LSTRU)*(LDIST) + Residual \quad (4.5)$$

where:

- LAP = log applications; LUAP if unweighted, LWAP if weighted,
- LLOAD = log axle load (kip),
- LSTRU = log structural number (LUSN or LWSN) for flexible pavements,
- LSTRU = log PCC thickness (LTHK) for rigid pavements, and
- LDIST = log distress
  - = LCRA for flexible pavement area cracking
  - = LCRI for rigid pavement cracking index
  - = LRUT for flexible pavement rut depth
  - = LPMP for rigid pavement pumping index
  - = LSIL for flexible and rigid pavement serviceability loss.

Rearranging the terms of Equation 4.5 produces:

$$\text{LAP} = [A + C*(\text{LSTRU}) + D*(\text{LDIST}) + G*(\text{LSTRU})*(\text{LDIST})] + [B + E*(\text{LSTRU}) + F*(\text{LDIST})]*(\text{LLOAD}) + \text{Residual} \quad (4.6)$$

The first bracket represents the intercepts and the second bracket represents the slopes of lines for the graphs of LAP versus LLOAD.

The residual term in the model has three components. The first two represent error variance from within-lane and between-lane variability of the data points. The third component represents the lack-of-fit of the model to the observed points.

The shortcoming of this model is that it does not account for nonlinearities that were observed to various degrees in some graphs.

**Summary results for log applications regressions.** Irick conducted six different regression analyses for the log applications data: one analysis for each of the three flexible pavement distress types and one for each of three rigid pavement distress types.

The three-run equations for flexible pavement log weighted applications resulted in:

Cracking: CRA = 10 percent and 45 percent  $(R^2 = 0.89, \text{SEE} = 0.23)$   

$$\text{LWAP} = 3.651 + 2.311*\text{LWSN} + 2.553*\text{LCRA} - 2.521*\text{LLOAD}*\text{LCRA} + 2.267*\text{LWSN}*\text{LCRA} \quad (4.7)$$

Rut Depth: RUT = 0.2" or 0.4"  $(R^2 = 0.82, \text{SEE} = 0.25)$   

$$\text{LWAP} = 7.037 - 2.604*\text{LLOAD} + 3.823*\text{LWSN} + 1.255*\text{LRUT} \quad (4.8)$$

PSI Loss: SIL = 1.2, 1.7, 2.2, or 2.7  $(R^2 = 0.91 \text{SEE} = 0.23)$   

$$\text{LWAP} = 6.300 - 2.627*\text{LLOAD} + 4.432*\text{LWSN} + 0.690*\text{LSIL} \quad (4.9)$$

For the rigid pavement, the following three regression equations were obtained:

Cracking: Index = 50 or 100  $(R^2 = 0.91, \text{SEE} = 0.10)$   

$$\text{LUAP} = 6.549 - 3.369*\text{LLOAD} + 2.143*\text{LTHK} + 0.308*\text{LCRI} + 1.349*\text{LLOAD}*\text{LTHK} \quad (4.10)$$

Pumping Index: PMP = 1000 or 9000  $(R^2 = 0.92, \text{SEE} = 0.09)$   

$$\text{LUAP} = 8.298 - 4.126*\text{LLOAD} - 2.002*\text{LTHK} + 2.745*\text{LLOAD}*\text{LTHK} + 0.508*\text{LTHK}*\text{LPMP} \quad (4.11)$$

PSI Loss: SIL = 1.5, 2.0, 2.5, or 3.0  $(R^2 = 0.92 \text{SEE} = 0.07)$   

$$\text{LUAP} = 6.997 - 3.318*\text{LLOAD} + 2.733*\text{LTHK} + 0.082*\text{LSIL} + 0.997*\text{LLOAD}*\text{LTHK} \quad (4.12)$$

It should be noticed that none of the flexible pavement equations contains a term for LLOAD\*LWSN but all of the rigid pavement equations contain a term for LLOAD\*LTHK. This means that the flexible pavement load equivalence ratios (LERs) derived from these equations will not depend on a structural number, but the corresponding rigid pavement LERs will depend on PCC thickness.

**Regression analysis for log LER data.** The LER for two-axle loads (L1 and L2), on the same pavement structure and for a given distress level, is the ratio of the number of applications of L1 to the number of applications of L2 when both structures reach the same given distress level. The logarithm of LER is therefore the difference between the logs of the two numbers of applications.

Irick provided in Appendix C of his report tables with all possible log of load equivalency ratios (LLER) for the study variables and test sections.

The indirect way of obtaining load equivalency ratio is to use the model given in Equation 4.13 for axle load L1 and L2:

$$\begin{aligned} [LAP(L1) - LAP(L2)] = & B * [LLOAD(L1) - LLOAD(L2)] + E * [LLOAD(L1) \\ & - LLOAD(L2)]*(LSTRU) + F * [LLOAD(L1) \\ & - LLOAD(L2)]*(LDIST) + Residual \end{aligned} \quad (4.13)$$

$$\begin{aligned} LLER(L1,L2) = & B*[LLR(L1,L2)] + E*[LLR(L1,L2)]*(LSTRU) \\ & + F*[LLR(L1,L2)]*(LDIST) + Residual \end{aligned} \quad (4.14)$$

or

$$LLER(L1,L2) = [LLR(L1,L2)]*[B + E*(LSTRU) + F*(LDIST)] + Residual \quad (4.15)$$

where:

$$LLR(L1,L2) = [LLOAD(L1) - LLOAD(L2)] = \log [LOAD(L1)/LOAD(L2)]$$

For fixed structure and distress levels, the graph of Equation 4.15 is a straight line that passes through the origin (LLER=0, LLR=0) and has a slope given by

$$[B + E*(LSTRU) + F*(LDIST)].$$

Irick also used the direct way to obtain LER by the following regression analysis model:

$$LLER = (LLR)*[B + E*(LSTRU) + F*(LDIST) ] + Residual \quad (4.16)$$

where:

- LLER = log of load equivalency ratio,
- LLR = log load ratio =  $\log(L1/L2) = (\log L1 - \log L2)$ ,
- LSTRU = log structural number (LUSN or LWSN) for flexible pavements,
- LSTRU = log PCC thickness (LTHK) for rigid pavements,
- LDIST = log cracking (LCRA), log rut depth (LRUT), or log PSI loss (LSIL) for flexible pavement, and
- LDIST = log crack index (LCRI), log pumping index (LPMP), or log SIL for rigid pavements.

In Power Law formulas, an 18-kip load is usually assigned to the denominator. Irick expressed the regression results in terms of log LEF by assigning 18k to the numerator in Equation 4.16. By assigning 18 kip to the numerator, the regression results give a negative B power in Equation 4.17.

$$LLER = [\log(18k/LOAD)] * [B + E * (LSTRU) + F * (LDIST)] + Residual \quad (4.17)$$

The antilog form of Equation 4.17 gives:

$$LEF = \left( \frac{18k}{LOAD} \right)^{[B + E * (LSTRU) + F * (LDIST)]} * 10^{Residual} \quad (4.18)$$

The antilog form shows that the LER for this model is a power function of the axle load ratio of L1 to L2. If LER does not depend on levels for STRU and DIST, the LER is simply of L1/L2 with a B power.

Irick obtained the following regression equations for LER for flexible pavements:

Cracking: CRA = 10 percent or 45 percent

$$LWLER = LLR * (-3.460 * LWSN - 1.621 * LCRA) + 0.27 * SEE \quad (4.19)$$

Rut Depth: RUT = 0.2" or 0.4"

$$LWLER = LLR * (-1.595 - 3.227 * LWSN) + 0.35 * SEE \quad (4.20)$$

PSI Loss: SIL = 1.2, 1.7, 2.2, or 2.7

$$LWLER = LLR * (-2.057 - 2.273 * LWSN - 1.224 * LSIL) + 0.25 * SEE \quad (4.21)$$

Equations 4.19 through 4.21 show that LER increases as the structural number and/or distress level increases.

Irick obtained the following regression equations for LER for rigid pavements:

Crack Index: CRI = 50 or 100

$$LULER = LLR*(-5.736 + 3.121*LTHK) + 0.14*SEE \quad (4.22)$$

Pumping Index: PMP = 1000 or 9000

$$LULER = LLR*(-5.439 + 5.104*LTHK) + 0.13*SEE \quad (4.23)$$

PSI Loss: SIL = 1.5, 2.0, 2.5, or 3.0

$$LULER = LLR*(-6.948 + 5.283*LTHK) + 0.12*SEE \quad (4.24)$$

Equations 4.22 through 4.24 show LLER decreases with the increase of PCC thickness, but do not show dependence on distress levels.

**LEFs for the study data.** The LEF for a given axle load (LOAD) is the LER of 18-kip single-axle applications to LOAD applications when a prescribed pavement distress level (D\*) has been reached for both sets of applications. Then

$$\begin{aligned} \text{Log LEF(LOAD)} &= \text{Log LER(18K, LOAD)} \\ &= \text{Log(18K App. to D*)} - \text{Log(LOAD App. to D*)} \end{aligned} \quad (4.25)$$

Values for LEF can be derived indirectly from the regression equations for log applications or directly from the regression equations for log LER. For the indirect derivation of LEF from a log applications equation, the general equation for LOAD is subtracted from the same equation with LOAD = 18k. All regression equations for calculation of LEF derived from the study data are summarized in Table 4.7.

It can be seen from Table 4.7 that the flexible pavement equations for weighted applications generally fit the observed data points better than the corresponding equations for unweighted applications. For weighted applications, all indirectly derived equations show LEF dependency only on the load ratio, except for an additional dependence on cracking level. The direct derivations all show dependence of LEF on load ratio, structural number, and distress levels (except for RUT).

Irick assumed for his study that the direct derivations provided a better indicator of LEF characteristics. The following equations for flexible pavements are:

Cracking: CRA = 10 percent or 45 percent (44 Data Points)

$$\begin{aligned} LLEF(\text{LOAD}) &= L(\text{LOAD}/18)*[3.460*LWSN + 1.621*LCRA] \\ &+ 0.27*SEE \end{aligned} \quad (4.26)$$

Rut Depth: RUT = 0.2" or 0.4" (49 Data Points)

$$LLEF(\text{LOAD}) = L(\text{LOAD}/18)*[1.595 + 3.227*LWSN] + 0.35*SEE \quad (4.27)$$

PSI Loss: SIL = 1.2, 1.7, 2.2, or 2.7 (104 Data Points)

$$\text{LEF (LOAD)} = L(\text{LOAD}/18) * [2.057 + 2.273 * \text{LWSN} - 1.224 * \text{LSIL}] + 0.25 * \text{SEE} \quad (4.28)$$

For rigid pavements the following equations for log LEF were obtained:

Crack Index: CRI = 50 or 100 (10 Data Points)

$$\text{LLEF(LOAD)} = L(\text{LOAD}/18) * [5.736 - 3.121 * \text{LTHK}] + 0.14 * \text{SEE} \quad (4.29)$$

Pumping Index: PMP = 1000 or 9000 (18 Data Points)

$$\text{LLEF(LOAD)} = L(\text{LOAD}/18) * [5.439 - 5.104 * \text{LTHK}] + 0.13 * \text{SEE} \quad (4.30)$$

PSI Loss: SIL = 1.5, 2.0, 2.5, or 3.0 (11 Data Points)

$$\text{LLEF(LOAD)} = L(\text{LOAD}/18) * [6.948 - 5.283 * \text{LTHK}] + 0.12 * \text{SEE} \quad (4.31)$$

In contrast to the flexible pavement equations, the coefficients for LTHK are negative for all distress types. Thus, the quantities in square brackets decrease, as does LEF, for increasing thicknesses.

Irick tabulated the derived LEF with observed LEF. The differences between observed and derived LEF values were presented graphically. Irick concluded that many residuals are systematic rather than random. This suggests that alternative models should be investigated.

**Comparison among Irick's LEFs and previously derived LEFs.** Irick made comparisons of LEFs as log LEFs. Table 4.8 shows the comparisons of flexible pavement AASHTO log LEFs with log LEFs derived from the Irick study and with LEF equations from the FHWA cost allocation study. A similar comparison was also made for rigid pavements, as shown in Table 4.9.

Both the flexible pavement LEF equations derived in Irick's study and the LEF equations derived in the cost allocation study produce increasing LEFs with increasing structure for loads over 18k. For loads less than 18k, the same equations produce larger LEF as the structure number decreases. Generally, AASHTO LEFs are slightly higher than Irick LEFs, especially for the low structural number.

Table 4.7 Summary of LEF Equations derived from the study data (Irick 89)

			EQUATIONS COEFFICIENTS & (Sig. Lev.)				FIT TO DATA		
APP WTS	DERIV METH.	NO. PTS.	FOR LLR =LOAD/18	FOR LLR * Log Struct.	FOR LLR * Log Dist.		R Sq.	SEE	EVR
FLEXIBLE PAVEMENT CRACKING: CRA = 10 percent & 45 percent									
UNW	IND	53	- (62)	- (00)	2.166 (00)	0.82	0.36	2.1	
	DIR	44	- (84)	2.904 (00)	1.683 (00)	0.85	0.31	1.3	
WTD	IND	53	- (92)	- (00)	2.521 (00)	0.89	0.33	1.7	
	DIR	44	- (76)	3.464 (00)	1.621 (00)	0.92	0.27	0.9	
FLEXIBLE PAVEMENT RUT DEPTH:RUT = 0.5 cm & 1.0 cm (0.2" & 0.4")									
UNW	IND	58	2.103 (00)	- (40)	- (40)	0.78	0.31	2.4	
	DIR	49	1.516 (00)	2.311 (20)	- (20)	0.79	0.33	2.1	
WTD	IND	58	2.604 (00)	- (48)	- (48)	0.82	0.35	1.7	
	DIR	49	1.595 (00)	3.226 (35)	- (35)	0.84	0.35	1.3	
FLEXIBLE PAVEMENT PSI LOSS: SIL = 1.2, 1.7, 2.2, & 2.7 from PSI=4.2									
UNW	IND	123	2.466 (00)	0.476 (21)	- (21)	0.90	0.30	2.0	
	DIR	104	1.879 (00)	0.812 (01)	2.373 (01)	0.83	0.36	1.9	
WTD	IND	123	2.627 (00)	- (38)	- (38)	0.91	0.33	2.5	
	DIR	104	2.057 (00)	2.273 (03)	1.224 (03)	0.93	0.25	1.0	
RIGID PAVEMENT CRACKING INDEX: CRI=50 & 100									
UNW	IND	21	3.369 (00)	-1.349 (81)	- (81)	0.91	0.14	1.5	
	DIR	10	5.736 (19)	-3.121 (85)	- (85)	0.94	0.14	1.0	
RIGID PAVEMENT PUMPING INDEX: PMP=1000 & 9000									
UNW	IND	25	4.126 (00)	-2.745 (23)	- (23)	0.92	0.13	2.0	
	DIR	18	5.439 (03)	-5.104 (76)	- (76)	0.90	0.13	2.2	
RIGID PAVEMENT PSI LOSS: SIL=1.5, 2.0, 2.5, & 3.0 FROM PSI=4.5									
UNW	IND	34	3.318 (00)	-0.997 (10)	0.092 (10)	0.92	0.10	1.3	
	DIR	11	6.948 (10)	-5.283 (59)	- (59)	0.92	0.12	1.0	

For rigid pavements, Irick's study gave smaller LEFs for loads above 18k, and larger LEFs for loads below 18k, compared to those given by the AASHTO design guide tables for rigid pavement LEFs. Unlike the flexible pavement derivations, the rigid pavement results give decreasing LEFs with increasing PCC thicknesses for loads above 18k, and vice versa for loads below 18k. The AASHTO LEFs are practically insensitive to PCC thickness.

**Conclusions on determinants of pavement performance.** Based on the log application graphs, Irick concluded that, in spite of evident irregularities, the relationships between log applications and log load, or log structure, are generally linear. The model in Equation 4.5 would be adequate for estimating the main effects and two-factor interaction effects of the three determinant factors. For flexible pavements, the only significant interactions are for cracking levels with both load and structural number. For rigid pavements, there are load-thickness interactions for all three types and an additional interaction between thickness and pumping levels.

Irick states that, except for pumping, the effects of load on log applications are about the same (Power Law coefficients around 2.5 for Equations 4.7-4.12) for flexible pavement and rigid pavement distress types. It is noted, however, that the AASHO Road Test equation for serviceability loss contains Power Law coefficients that are in the neighborhood of 4.0 (Irick 89). The regression analyses for log applications show that the equations account for about 90 percent of the data variations, since the R-square is between 0.89 and 0.92 for all except the rutting depth equation, which has an R-square of 0.82. The standard error of estimate (SEE) is between 0.23 and 0.25 for flexible pavement equations and ranges from 0.07 to 0.10 for rigid pavements. Irick concludes that the log applications for regression equations provide reasonable fits with the observed data. The SEEs of approximately 0.2 for flexible and 0.09 and rigid pavement log applications are similar in size to those reported by the AASHO Road Test.

Table 4.8 Comparison of study of log LEF for flexible pavements with previously derived LEF (Irick 89)

DIST TYPE LEVS	SING AXLE LOAD	STRU NUMB (WTD)	STUDY LOG LEF				AASHTO <sup>a)</sup>		COST STUDY <sup>b)</sup>	
			DIST LEV 1		DIST LEV 2		DIST LEV 1	DIST LEV 2	DIST LEV 1	DIST LEV 2
			OBS	DER	OBS	DER				
CRA  @ 10%  & 45%	6	2.18		-1.29		-1.79			(Wet - Freeze)	
		3.06		-1.53		-2.04			-0.73	(AC=3")
		3.92		-1.71		-2.15			-1.09	(AC=6")
	12	2.18	-0.32	-0.45	-0.18	-0.63			(Es = 10 kpsi)	
		3.06	-0.65	-0.54	-0.46	-0.72			-0.28	
		3.92		-0.60		-0.79			-0.41	
	22.4	2.18		0.31	1.02	0.41				
		3.06	0.30	0.36	0.71	0.46			0.15	
		3.92	0.17	0.39	0.40	0.49			0.23	
	30	2.18		0.66		0.90				
		3.06	0.79	0.78	1.14	1.01			0.36	
		3.92	0.81	0.86	1.14	1.09			0.53	
RUT  @ 0.2"  & 0.4"	6	2.18	-1.51	-1.28		-1.28				
		3.06		-1.51		-1.51				-2.65
		3.92		-1.67		-1.67				-3.22
	12	2.18	-0.99	-0.47		-0.47				
		3.06	-0.59	-0.56	-0.59	-0.56				-1.00
		3.92		-0.62		-0.62				-1.25
	22.4	2.18		0.23		0.23				
		3.06	0.76	0.28	0.48	0.28				0.55
		3.92	0.40	0.32	0.29	0.32				0.67
	30	2.18		0.60		0.60				
		3.06	0.73	0.70		0.70				1.30
		3.92	0.85	0.78	0.58	0.78				1.58
PSI LOSS  to 2.5  & 2.0	6	2.18		-1.48		-1.55	-1.77	-1.92		
		3.06		-1.64		-1.71	-1.77	-1.96	-2.29	
		3.92		-1.76		-1.83	-1.89	-2.00	-2.69	
	12	2.18	-0.29	-0.55	-0.29	-0.57	-0.70	-0.75		
		3.06	-0.63	-0.61	-0.75	-0.63	-0.64	-0.72	-0.87	
		3.92		-0.65		-0.67	-0.67	-0.74	-1.02	
	22.4	2.18	0.32	0.29	0.24	0.31	0.41	0.42		
		3.06	0.39	0.33	0.42	0.34	0.37	0.40	0.48	
		3.92	0.24	0.35	0.16	0.36	0.35	0.40	0.56	
	30	2.18		0.69		0.67	0.98	1.00		
		3.06	0.71	0.76	0.74	0.79	0.90	0.96	1.13	
		3.92	0.95	0.82	0.94	0.85	0.83	0.93	1.32	

a) (AASHTO 86), Appendix D. b) (FHWA 84), Table A-2.

Table 4.9 Comparison of study of log LEF for rigid pavements with previously derived LEF (Irick 89)

DIST TYPE LEVS	SING AXLE LOAD	PCC THK (in.)	STUDY LOG LEF				AASHTO <sup>b)</sup>		COST STUDY <sup>c)</sup>	
			DIST LEV 1		DIST LEV 2		DIST LEV 1	DIST LEV 2	DIST LEV 1	DIST LEV 2
			OBS	DER	OBS	DER				
CRA  @ 50 & 100	6	5.0		-1.32		-1.32	-1.17	-1.17 <sup>a)</sup>	(Wet - Freeze) (THK = 23. cm or 9")	
		8.0		-1.02		-1.02	-1.17	-1.17		
	12	9.5		-0.91		-0.91	-1.17	-1.17		-1.39
		5.0	-0.54	-0.49	-0.46	-0.49	0.46	0.46		
	22.4	8.0		-0.38		-0.38	0.46	0.46		
		9.5		-0.34		-0.34	0.46	0.46		-0.53
	30	5.0		0.24		0.24	0.23	0.23		
		8.0	0.10	0.20		0.20	0.23	0.23		
		9.5		0.18		0.18	0.23	0.23		0.28
		5.0		0.62		0.62	0.55	0.55		
PMP  @ 1000 & 9000	6	5.0		-1.20		-1.20				
		8.0		-0.70		-0.70				
	12	9.5		-0.52		-0.52			-3.19	
		5.0	-0.33	-0.44		-0.44				
	22.4	8.0	-0.07	-0.26		-0.26			-1.21	
		9.5		-0.19		-0.19				
	30	5.0		0.24		0.24				
		8.0	0.12	0.14		0.14				
		9.5	0.14	0.11		0.11			0.64	
		5.0		0.56		0.56				
PSI LOSS  to 2.5 & 2.0	6	5.0		-1.34		-1.34	-1.90	-1.93 <sup>b)</sup>		
		8.0		-0.83		-0.83	-2.00	-2.00		
	12	9.5		-0.64		-0.64	-2.00	-2.00		-1.99
		5.0	-0.46	-0.50	-0.44	-0.50	-0.68	-0.71		
	22.4	8.0		-0.31		-0.31	-0.74	-0.76		
		9.5		-0.24		-0.24	-0.76	-0.76		-0.75
	30	5.0		0.27		0.27	0.36	0.38		
		8.0		0.17		0.17	0.39	0.40		
		9.5		0.13		0.13	0.41	0.41		0.4
		5.0		0.62		0.62	0.91	0.95		
30	8.0		0.39		0.39	0.89	0.94			
	9.5		0.30		0.30	0.93	0.96	0.92		

<sup>a)</sup> (AASHTO 62), page 167.

<sup>b)</sup> (AASHTO 86), Vol. 1 Appendix D.

<sup>c)</sup> (FHWA 84), Vol. 1, Table 9.3.

**Conclusions on determinants of LERs.** Regression equations for observed LLER were derived from Equation 4.16. Approximate coefficients for LLR and LLR\*LSTRU (Equations 4.19-4.24) are shown in Table 4.8 and Table 4.9. Except for cracking at 45 percent, the flexible pavement results show consistent effects of load and structure and give higher equivalence ratios for the heavier structures (at WSN=4) than for the lighter structures (at WSN=3). Table 4.7 shows that R-squares for the cracking, rutting depth, and PSI loss are 0.85, 0.79, and 0.83, respectively. Corresponding SEEs are 0.31, 0.33, and 0.36, respectively, which agree closely with the estimated 0.34.

For rigid pavements, the respective R-squares for cracking index, pumping index, and PSI loss are 0.94, 0.91, and 0.92. SEEs are 0.14, 0.13, and 0.12, respectively, and are quite close to the estimate of 0.13. Contrary to the flexible pavement equations, the rigid pavement equations show decreasing load effects as PCC thickness increases from 12.7 cm to 22.86 cm (5 in. to 9 in.).

*Table 4.10 Flexible pavement coefficients (Irick 89)*

	LLR	LLR*LWSN	LLR at WSN=3	LLR at WSN=4
Cracking at 10 percent	1.6	3.5	<b>3.3</b>	<b>3.7</b>
At 45 percent	2.7	3.5	<b>4.3</b>	<b>4.8</b>
Rut Depth at 5 and 10 mm (0.2" and 0.4")	1.6	3.2	<b>3.1</b>	<b>3.5</b>
PSI loss at PSI =3.0	2.2	2.3	<b>3.2</b>	<b>3.5</b>
At PSI = 2.5	2.3	2.3	<b>3.4</b>	<b>3.7</b>
At PSI = 2.0	2.5	2.3	<b>3.6</b>	<b>3.8</b>

*Table 4.11 Rigid pavement coefficients (Irick 89)*

	LLR	LLR*LTHK	LLR at THK=12.7 cm (5 in.)	LLR at THK=22.9 cm (9 in.)
Cracking index at 50 and 100	5.7	3.1	<b>3.6</b>	<b>2.8</b>
Pumping Index at 1000 and 9000	5.4	5.1	<b>1.9</b>	<b>0.6</b>
PSI Loss at all levels	6.9	5.3	<b>3.3</b>	<b>1.9</b>

**Conclusions on characteristics of LEFs.** The standard errors of estimate for the derived log LEFs are 0.3 for flexible pavements and 0.1 for rigid pavements. This means that a maximum of two significant digits should be used to express LEFs.

The “Power Law” coefficients were calculated from AASHTO LEFs to compare results with Irick’s results. The Power Law relates to the following equation:

$$LEF = \left(\frac{L1}{18}\right)^a \quad (4.32)$$

By taking the logarithm of both sides of the Equation 4.32, Equation 4.33 is obtained:

$$\log_{10}(LEF) = a * \log_{10}\left(\frac{L1}{18}\right) \quad (4.33)$$

Mathematical rearrangement gives the Power Law coefficient as:

$$a = \frac{\log_{10}(LEF)}{\log_{10}(L1) - \log_{10}(18)} \quad (4.34)$$

Using Equation 4.34, Power Law coefficients were calculated from AASHTO LEFs and then averaged for the same structural number for flexible pavements or thickness of PCC for rigid pavements. Table 4.12 and Table 4.13 show the results of calculations, together with Irick's results for flexible and rigid pavements, correspondingly. Irick stated that the comparison between his study and the AASHTO LEFs for flexible pavements show general agreement (Irick 89). In Table 4.12, the Irick LEFs are slightly lower than AASHTO LEFs, especially for low structural numbers. The difference between LEFs increases with lower terminal serviceability and lower structural numbers.

*Table 4.12 Power Law coefficient for flexible pavement*

Terminal Serviceability		Structure Number					
		1	2	3	4	5	6
2.0	AASHTO	4.49	4.40	4.28	4.22	4.26	4.32
	IRICK	2.48	3.16	3.56	3.84	4.06	4.24
	Difference in Power Law Between AASHTO and IRICK	2.01	1.24	0.72	0.38	0.19	0.08
2.5	AASHTO	4.44	4.24	3.96	3.84	3.92	4.07
	IRICK	2.34	3.02	3.42	3.71	3.93	4.11
	Difference in Power Law Between AASHTO and IRICK	2.11	1.22	0.54	0.13	-0.01	-0.04
3.0	AASHTO	4.39	4.02	3.54	3.33	3.46	3.73
	IRICK	2.15	2.84	3.24	3.52	3.74	3.92
	Difference in Power Law Between AASHTO and IRICK	2.23	1.19	0.30	-0.20	-0.28	-0.19

For rigid pavements, the differences are greater (Irick 89, page 186). LEFs significantly decrease with increasing PPC thickness, as is shown in Table 4.11 and Table 4.13.

It can be concluded that Irick's re-analysis showed a significant difference between AASHTO LEFs and Irick LEFs. Additional efforts are needed to further study these differences.

*Table 4.13 Power law coefficient for rigid pavement*

Terminal		Slab Thickness, D								
		15 cm (6 in.)	18 cm (7 in.)	20 cm (8 in.)	23 cm (9 in.)	25 cm (10 in.)	28 cm (11 in.)	31 cm (12 in.)	33 cm (13 in.)	36 cm (14 in.)
2.0	AASHTO	4.23	4.22	4.24	4.27	4.30	4.32	4.33	4.35	4.35
	IRICK	2.84	2.48	2.18	1.91	1.67	1.45	1.25	1.06	0.89
	Difference in Power Law Between AASHTO and IRICK	1.39	1.74	2.06	2.36	2.63	2.87	3.09	3.28	3.46
2.5	AASHTO	4.07	4.05	4.09	4.16	4.22	4.26	4.30	4.32	4.34
	IRICK	2.84	2.48	2.18	1.91	1.67	1.45	1.25	1.06	0.89
	Difference in Power Law Between AASHTO and IRICK	1.23	1.57	1.92	2.25	2.55	2.82	3.05	3.26	3.45
3.0	AASHTO	3.86	3.83	3.90	4.01	4.11	4.19	4.25	4.30	4.32
	IRICK	2.84	2.48	2.18	1.91	1.67	1.45	1.25	1.06	0.89
	Difference in Power Law Between AASHTO and IRICK	1.03	1.34	1.72	2.10	2.45	2.75	3.01	3.23	3.43

A closer look at the observed LER explains big differences between Irick's results and AASHTO's results for rigid pavements. Table 4.14 shows all observed LERs from the AASHTO Road Test.

*Table 4.14 Observed LER from AASHTO Road Test data*

PVT VAR	STAT	Pavement Thickness		
		12.7 cm (5 in.)	16.5 cm (6.5 in.)	20.3 cm (8 in.)
		Load Ratio		
		12/18	18/22.4	22.4/30
PSI = 3.0	MEAN	0.526	0.355	0.148
	##	2/6	2/6	2/4
PSI = 2.5	MEAN	0.456	0.398	0.148
	##	1/6	2/6	2/4
PSI = 2.0	MEAN	0.442	0.408	0.180
	##	1/6	1/6	2/4
PSI = 1.5	MEAN	0.443		0.190
	##	1/6		2/4

As shown in Table 4.14, only 11 points were available for estimating LER for rigid pavements. In this table, the number of sections used to estimate LER is also shown. For example, for a PCC thickness of 12.7 cm (5 in.) and a PSI of 3.0, two sections were included for estimating log applications for 53.4 kN (12 kip) loading, and six sections were included for estimating log applications for 80 kN (18 kip) loading.

Power Law coefficients were calculated for the actual AASHO data points and for the AASHTO and Irick models. They are shown in Table 4.15 and the Figure 4.2. The average Power Law coefficient for AASHTO model is about 4.

Table 4.15 Power law coefficients for actual AASHO data points and different models

	AASHO Data Points			AASHTO LEFs		
	Pavement Thickness			Pavement Thickness		
	12.7 cm (5 in.)	16.5 cm (6.5 in.)	20.3 cm (8 in.)	12.7 cm (5 in.)	16.5 cm (6.5 in.)	20.3 cm (8 in.)
PVT	Load Ratio			Load Ratio		
VAR	12/18	18/22.4	22.4/30	12/18	18/22.4	22.4/30
PSI =3.0	2.987	3.738	1.167	3.570	3.560	3.620
PSI =2.5	2.590	4.191	1.167	3.890	3.910	3.970
PSI =2.0	2.510	4.296	1.419	4.130	4.180	4.230
PSI =1.5	2.516		1.498	4.320		4.450

	Irick LEFs (indirect)			Irick LEFs (direct)		
	Pavement Thickness			Pavement Thickness		
	12.7 cm (5 in.)	16.5 cm (6.5 in.)	20.3 cm (8 in.)	12.7 cm (5 in.)	16.5 cm (6.5 in.)	20.3 cm (8 in.)
PVT	Load Ratio			Load Ratio		
VAR	12/18	18/22.4	22.4/30	12/18	18/22.4	22.4/30
PSI =3.0	2.621	2.507	2.418	3.255	2.653	2.177
PSI =2.5	2.621	2.507	2.418	3.255	2.653	2.177
PSI =2.0	2.621	2.507	2.418	3.255	2.653	2.177
PSI =1.5	2.621		2.418	3.255		2.177

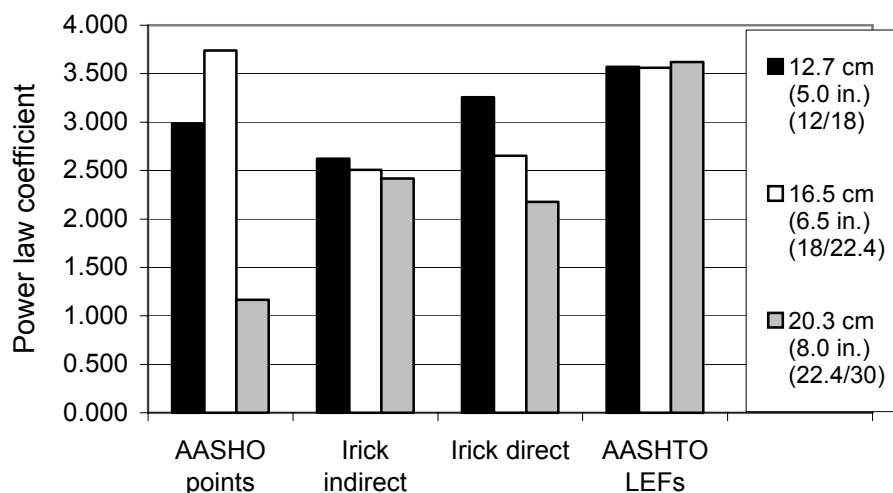


Figure 4.2 Power law coefficients for actual AASHO data points and different models

This value is supported by only one AASHTO Road Test data point. Two other data points give the average Power Law coefficient of 2.65 and 1.31. The Power Law coefficient of 1.31 for the load ratio of 99.7 kN to 133.5 kN (22.4 kip to 30 kip) is decisive in Irick models. This is the reason why Irick's Power Law coefficients are below the fourth Power Law for rigid pavements.

An additional comparison was made to evaluate the relative difference between AASHTO LEFs and Irick LEFs. The calculations were made using Equation 4.35.

$$\Delta = \frac{Irick\_LEF - AASHTO\_LEF}{AASHTO\_LEF} * 100\% \quad (4.35)$$

The results are presented in Tables 4.16-4.18 and Tables 4.18-4.21 for flexible pavements and for rigid pavements, respectively.

*Table 4.16 Relative change in LEFs between AASHTO LEFs and Irick LEFs for flexible pavements, terminal serviceability of 2.0, and single axles*

Axle Load		Structural Number, SN					
Kip	kN	1	2	3	4	5	6
2	8.9	1865.7%	325.4%	96.7%	21.4%	-17.5%	-41.5%
4	17.8	1026.4%	244.0%	103.1%	51.6%	19.7%	-4.0%
6	26.7	596.3%	168.0%	76.1%	45.0%	24.6%	7.3%
8	35.6	353.3%	119.3%	53.3%	33.5%	21.1%	9.4%
10	44.5	210.2%	84.2%	36.9%	23.2%	15.9%	8.4%
12	53.4	122.2%	56.5%	24.9%	15.0%	10.8%	6.3%
14	62.3	65.3%	33.8%	15.4%	8.7%	6.4%	4.0%
16	71.2	26.9%	15.2%	7.3%	3.9%	2.8%	1.8%
<b>18</b>	<b>80.1</b>	<b>0.0%</b>	<b>0.0%</b>	<b>0.0%</b>	<b>0.0%</b>	<b>0.0%</b>	<b>0.0%</b>
20	89.0	-19.5%	-12.5%	-6.8%	-3.3%	-2.2%	-1.5%
22	97.9	-34.0%	-22.8%	-13.0%	-6.4%	-3.9%	-2.6%
24	106.8	-45.0%	-31.4%	-18.8%	-9.2%	-5.3%	-3.5%
26	115.7	-53.6%	-38.6%	-24.1%	-12.1%	-6.5%	-4.0%
28	124.6	-60.4%	-44.7%	-28.9%	-14.8%	-7.5%	-4.4%
30	133.5	-65.9%	-49.9%	-33.3%	-17.6%	-8.6%	-4.6%
32	142.4	-70.3%	-54.4%	-37.3%	-20.3%	-9.7%	-4.7%
34	151.3	-74.0%	-58.2%	-40.9%	-22.9%	-10.8%	-4.8%
36	160.2	-77.0%	-61.6%	-44.2%	-25.5%	-12.0%	-4.9%
38	169.1	-79.6%	-64.6%	-47.3%	-28.0%	-13.2%	-5.0%
40	178.0	-81.7%	-67.2%	-50.0%	-30.3%	-14.5%	-5.1%
42	186.9	-83.6%	-69.5%	-52.5%	-32.6%	-15.8%	-5.3%
44	195.8	-85.2%	-71.6%	-54.8%	-34.8%	-17.2%	-5.6%
46	204.7	-86.6%	-73.4%	-56.9%	-36.8%	-18.6%	-5.9%
48	213.6	-87.8%	-75.1%	-58.9%	-38.8%	-19.9%	-6.3%
50	222.5	-88.8%	-76.6%	-60.7%	-40.6%	-21.3%	-6.8%

Table 4.17 Relative change in LEFs between AASHTO LEFs and Irick LEFs for flexible pavements, terminal serviceability of 2.5, and single axles

Axle Load		Structural Number, SN					
Kip	kN	1	2	3	4	5	6
2	8.9	1460.7%	226.3%	72.9%	27.6%	-1.9%	-26.0%
4	17.8	912.1%	153.7%	64.7%	45.5%	29.6%	10.6%
6	26.7	594.2%	106.9%	39.3%	33.0%	28.1%	17.2%
8	35.6	369.9%	83.2%	22.7%	20.0%	20.7%	15.3%
10	44.5	223.7%	65.5%	13.7%	10.6%	13.3%	11.4%
12	53.4	130.3%	48.0%	9.1%	4.6%	7.6%	7.5%
14	62.3	69.5%	30.5%	6.1%	1.5%	3.5%	4.1%
16	71.2	28.5%	14.3%	3.4%	0.2%	1.1%	1.6%
<b>18</b>	<b>80.1</b>	<b>0.0%</b>	<b>0.0%</b>	<b>0.0%</b>	<b>0.0%</b>	<b>0.0%</b>	<b>0.0%</b>
20	89.0	-20.5%	-12.3%	-4.0%	0.3%	0.0%	-0.8%
22	97.9	-35.5%	-22.8%	-8.6%	0.5%	0.8%	-0.8%
24	106.8	-46.9%	-31.7%	-13.4%	0.4%	2.1%	-0.2%
26	115.7	-55.6%	-39.1%	-18.3%	-0.1%	3.7%	1.0%
28	124.6	-62.5%	-45.5%	-23.0%	-1.2%	5.2%	2.7%
30	133.5	-68.0%	-50.9%	-27.6%	-2.7%	6.7%	4.6%
32	142.4	-72.4%	-55.6%	-31.8%	-4.6%	7.9%	6.8%
34	151.3	-76.0%	-59.6%	-35.8%	-6.8%	8.7%	9.0%
36	160.2	-78.9%	-63.1%	-39.5%	-9.1%	9.3%	11.3%
38	169.1	-81.4%	-66.2%	-42.9%	-11.6%	9.4%	13.4%
40	178.0	-83.5%	-68.8%	-46.0%	-14.2%	9.2%	15.4%
42	186.9	-85.3%	-71.2%	-48.9%	-16.7%	8.7%	17.2%
44	195.8	-86.8%	-73.3%	-51.6%	-19.3%	8.0%	18.7%
46	204.7	-88.1%	-75.2%	-54.0%	-21.7%	7.0%	20.0%
48	213.6	-89.2%	-76.9%	-56.3%	-24.2%	5.9%	21.0%
50	222.5	-90.2%	-78.4%	-58.3%	-26.5%	4.6%	21.7%

Table 4.18 Relative change in LEFs between AASHTO LEFs and Irick LEFs for flexible pavements, terminal serviceability of 3.0, and single axles

Axle Load		Structural Number, SN					
Kip	kN	1	2	3	4	5	6
2	8.9	1042.7%	128.1%	45.3%	36.5%	23.8%	1.8%
4	17.8	775.9%	68.2%	24.0%	37.7%	44.3%	34.0%
6	26.7	591.4%	45.9%	1.5%	18.5%	33.0%	32.0%
8	35.6	393.3%	43.6%	-9.1%	4.0%	20.1%	23.8%
10	44.5	242.8%	43.1%	-11.5%	-4.5%	10.0%	15.7%
12	53.4	141.8%	37.2%	-9.2%	-7.9%	3.4%	9.1%
14	62.3	75.3%	26.3%	-5.2%	-7.6%	-0.2%	4.3%
16	71.2	30.7%	13.2%	-1.8%	-4.6%	-1.2%	1.4%
<b>18</b>	<b>80.1</b>	<b>0.0%</b>	<b>0.0%</b>	<b>0.0%</b>	<b>0.0%</b>	<b>0.0%</b>	<b>0.0%</b>
20	89.0	-21.7%	-12.1%	-0.3%	5.3%	3.0%	0.2%
22	97.9	-37.5%	-22.8%	-2.3%	10.6%	7.5%	1.7%
24	106.8	-49.3%	-32.0%	-5.6%	15.1%	13.0%	4.4%
26	115.7	-58.2%	-39.9%	-9.8%	18.6%	19.1%	8.3%
28	124.6	-65.1%	-46.6%	-14.3%	20.8%	25.4%	13.1%
30	133.5	-70.6%	-52.3%	-19.0%	21.7%	31.5%	18.6%
32	142.4	-74.9%	-57.2%	-23.7%	21.6%	37.1%	24.6%
34	151.3	-78.4%	-61.4%	-28.2%	20.6%	42.1%	31.0%
36	160.2	-81.3%	-65.0%	-32.4%	18.8%	46.3%	37.5%
38	169.1	-83.7%	-68.2%	-36.4%	16.5%	49.6%	44.0%
40	178.0	-85.6%	-70.9%	-40.1%	13.8%	52.1%	50.3%
42	186.9	-87.3%	-73.4%	-43.6%	10.8%	53.7%	56.2%
44	195.8	-88.7%	-75.5%	-46.8%	7.7%	54.6%	61.6%
46	204.7	-89.9%	-77.4%	-49.7%	4.5%	54.8%	66.5%
48	213.6	-90.9%	-79.1%	-52.4%	1.2%	54.4%	70.8%
50	222.5	-91.8%	-80.6%	-54.9%	-2.0%	53.6%	74.5%

It can be concluded from Tables 4.16 through 4.18 that:

1. Irick LEFs are very close to AASHTO LEFs for SN=6 and terminal serviceability 2.0.
2. Close results (below 10 percent) were obtained for SN=4, 5, 6 and loads from 62.3 to 98 kN (14 to 22 kip). Outside this range, AASHTO LEFs and Irick LEFs differ significantly.

Table 4.19 Relative change in LEFs between AASHTO LEFs and Irick LEFs for rigid pavements, terminal serviceability of 2.0, and single axles

Axle Load		Slab Thickness, D								
Kip	kN	15 cm	18 cm	20 cm	23 cm	25 cm	28 cm	31 cm	33 cm	36 cm
		(6 in.)	(7 in.)	(8 in.)	(9 in.)	(10 in.)	(11 in.)	(12 in.)	(13 in.)	(14 in.)
2	8.9	756%	1909%	4037%	7483%	12866%	20912%	32515%	48753%	70899%
4	17.8	478%	961%	1666%	2585%	3782%	5306%	7208%	9537%	12349%
6	26.7	287%	514%	802%	1129%	1511%	1953%	2460%	3034%	3678%
8	35.6	177%	293%	429%	566%	715%	875%	1047%	1232%	1430%
10	44.5	111%	172%	240%	304%	367%	433%	500%	568%	639%
12	53.4	68.7%	99.4%	134%	164%	193%	221%	248%	275%	302%
14	62.3	39.4%	53.1%	69.9%	83.3%	95.5%	107%	118%	128%	138%
16	71.2	17.4%	21.9%	28.2%	33.0%	37.1%	40.9%	44.3%	47.5%	50.5%
<b>18</b>	<b>80.1</b>	<b>0.0%</b>	<b>0.0%</b>	<b>0.0%</b>	<b>0.0%</b>	<b>0.0%</b>	<b>0.0%</b>	<b>0.0%</b>	<b>0.0%</b>	<b>0.0%</b>
20	89.0	-14.0%	-16.3%	-19.8%	-22.5%	-24.7%	-26.5%	-28.1%	-29.5%	-30.8%
22	97.9	-25.4%	-28.8%	-34.2%	-38.5%	-41.8%	-44.5%	-46.8%	-48.7%	-50.5%
24	106.8	-11.7%	-18.1%	-26.3%	-32.8%	-37.8%	-41.9%	-45.2%	-48.1%	-50.6%
26	115.7	-42.4%	-47.0%	-53.3%	-58.7%	-62.9%	-66.1%	-68.6%	-70.8%	-72.6%
28	124.6	-48.8%	-53.8%	-59.9%	-65.3%	-69.5%	-72.7%	-75.2%	-77.2%	-78.9%
30	133.5	-54.2%	-59.4%	-65.2%	-70.5%	-74.6%	-77.7%	-80.1%	-81.9%	-83.5%
32	142.4	-58.8%	-64.1%	-69.6%	-74.7%	-78.6%	-81.5%	-83.7%	-85.5%	-86.9%
34	151.3	-62.7%	-68.1%	-73.3%	-78.0%	-81.7%	-84.5%	-86.6%	-88.2%	-89.4%
36	160.2	-66.0%	-71.5%	-76.4%	-80.8%	-84.3%	-86.8%	-88.8%	-90.2%	-91.4%
38	169.1	-68.9%	-74.4%	-79.0%	-83.1%	-86.3%	-88.7%	-90.5%	-91.8%	-92.9%
40	178.0	-71.5%	-76.9%	-81.3%	-85.1%	-88.0%	-90.3%	-91.9%	-93.1%	-94.1%
42	186.9	-73.7%	-79.0%	-83.2%	-86.8%	-89.5%	-91.5%	-93.0%	-94.2%	-95.0%
44	195.8	-75.7%	-80.9%	-84.9%	-88.2%	-90.7%	-92.6%	-94.0%	-95.0%	-95.8%
46	204.7	-77.4%	-82.5%	-86.4%	-89.4%	-91.7%	-93.4%	-94.7%	-95.7%	-96.4%
48	213.6	-79.0%	-84.0%	-87.6%	-90.5%	-92.6%	-94.2%	-95.4%	-96.2%	-96.9%
50	222.5	-80.4%	-85.3%	-88.7%	-91.4%	-93.4%	-94.8%	-95.9%	-96.7%	-97.3%

Table 4.20 Relative change in LEFs between AASHTO LEFs and Irick LEFs for rigid pavements, terminal serviceability of 2.5, single axles

Axle Load		Slab Thickness, D								
Kip	kN	15 cm	18 cm	20 cm	23 cm	25 cm	28 cm	31 cm	33 cm	36 cm
		(6 in.)	(7 in.)	(8 in.)	(9 in.)	(10 in.)	(11 in.)	(12 in.)	(13 in.)	(14 in.)
2	8.9	614%	1741%	3927%	7394%	12795%	20856%	32471%	48717%	70871%
4	17.8	383%	872%	1619%	2553%	3761%	5292%	7198%	9530%	12344%
6	26.7	225%	463%	778%	1115%	1503%	1948%	2456%	3031%	3677%
8	35.6	135%	262%	415%	559%	710%	872%	1046%	1231%	1429%
10	44.5	84.0%	151%	232%	299%	365%	431%	499%	568%	638%
12	53.4	53.0%	86.1%	129%	162%	191%	220%	248%	275%	302%
14	62.3	31.7%	45.3%	66.8%	81.8%	94.8%	107%	118%	128%	138%
16	71.2	14.7%	18.6%	26.8%	32.3%	36.8%	40.7%	44.2%	47.4%	50.4%
<b>18</b>	<b>80.1</b>	<b>0.0%</b>	<b>0.0%</b>	<b>0.0%</b>	<b>0.0%</b>	<b>0.0%</b>	<b>0.0%</b>	<b>0.0%</b>	<b>0.0%</b>	<b>0.0%</b>
20	89.0	-12.7%	-13.8%	-18.6%	-22.0%	-24.5%	-26.4%	-28.1%	-29.5%	-30.8%
22	97.9	-23.5%	-24.9%	-32.0%	-37.4%	-41.3%	-44.3%	-46.7%	-48.7%	-50.5%
24	106.8	-9.4%	-13.1%	-23.5%	-31.5%	-37.2%	-41.6%	-45.1%	-48.0%	-50.5%
26	115.7	-40.4%	-42.0%	-49.6%	-56.8%	-62.0%	-65.6%	-68.4%	-70.6%	-72.5%
28	124.6	-46.9%	-48.8%	-55.8%	-63.1%	-68.4%	-72.2%	-74.9%	-77.1%	-78.8%
30	133.5	-52.4%	-54.6%	-61.0%	-68.0%	-73.4%	-77.1%	-79.8%	-81.8%	-83.4%
32	142.4	-57.1%	-59.6%	-65.4%	-72.0%	-77.2%	-80.8%	-83.4%	-85.3%	-86.8%
34	151.3	-61.1%	-64.0%	-69.1%	-75.3%	-80.2%	-83.7%	-86.2%	-88.0%	-89.3%
36	160.2	-64.6%	-67.7%	-72.4%	-78.1%	-82.7%	-86.0%	-88.4%	-90.0%	-91.3%
38	169.1	-67.6%	-70.9%	-75.3%	-80.5%	-84.7%	-87.9%	-90.1%	-91.6%	-92.8%
40	178.0	-70.2%	-73.7%	-77.8%	-82.6%	-86.5%	-89.4%	-91.4%	-92.9%	-93.9%
42	186.9	-72.6%	-76.1%	-80.0%	-84.4%	-87.9%	-90.6%	-92.6%	-93.9%	-94.9%
44	195.8	-74.6%	-78.2%	-81.9%	-86.0%	-89.2%	-91.7%	-93.5%	-94.7%	-95.6%
46	204.7	-76.4%	-80.1%	-83.6%	-87.3%	-90.3%	-92.6%	-94.2%	-95.4%	-96.2%
48	213.6	-78.1%	-81.7%	-85.1%	-88.6%	-91.3%	-93.3%	-94.9%	-96.0%	-96.7%
50	222.5	-79.5%	-83.2%	-86.4%	-89.7%	-92.1%	-94.0%	-95.4%	-96.4%	-97.1%

Table 4.21 Relative change in LEFs between AASHTO LEFs and Irick LEFs for rigid pavements, terminal serviceability of 3.0, and single axles

Axle Load		Slab Thickness, D								
Kip	kN	15 cm	18 cm	20 cm	23 cm	25 cm	28 cm	31 cm	33 cm	36 cm
		(6 in.)	(7 in.)	(8 in.)	(9 in.)	(10 in.)	(11 in.)	(12 in.)	(13 in.)	(14 in.)
2	8.9	466%	1546%	3790%	7280%	12705%	20785%	32414%	48672%	70833%
4	17.8	283%	769%	1561%	2513%	3734%	5274%	7185%	9521%	12337%
6	26.7	159%	404%	749%	1096%	1491%	1941%	2452%	3028%	3675%
8	35.6	90.8%	224%	398%	549%	705%	869%	1044%	1230%	1428%
10	44.5	54.3%	127%	221%	293%	362%	430%	498%	567%	638%
12	53.4	34.8%	70.3%	123%	158%	190%	219%	247%	274%	302%
14	62.3	22.4%	35.9%	62.9%	79.9%	93.8%	106%	117%	128%	138%
16	71.2	11.3%	14.3%	25.0%	31.5%	36.4%	40.5%	44.1%	47.4%	50.4%
<b>18</b>	<b>80.1</b>	<b>0.0%</b>	<b>0.0%</b>	<b>0.0%</b>	<b>0.0%</b>	<b>0.0%</b>	<b>0.0%</b>	<b>0.0%</b>	<b>0.0%</b>	<b>0.0%</b>
20	89.0	-11.0%	-10.6%	-17.0%	-21.2%	-24.1%	-26.3%	-28.0%	-29.5%	-30.7%
22	97.9	-21.1%	-19.4%	-29.0%	-36.0%	-40.6%	-43.9%	-46.5%	-48.6%	-50.4%
24	106.8	-6.3%	-6.3%	-19.7%	-29.7%	-36.4%	-41.2%	-44.9%	-47.9%	-50.5%
26	115.7	-37.7%	-34.7%	-44.4%	-54.1%	-60.7%	-65.1%	-68.1%	-70.5%	-72.4%
28	124.6	-44.3%	-41.5%	-50.0%	-59.9%	-66.9%	-71.5%	-74.6%	-76.9%	-78.8%
30	133.5	-50.0%	-47.6%	-54.7%	-64.5%	-71.6%	-76.3%	-79.4%	-81.6%	-83.3%
32	142.4	-54.8%	-53.0%	-59.0%	-68.2%	-75.3%	-79.9%	-83.0%	-85.1%	-86.7%
34	151.3	-59.0%	-57.8%	-62.8%	-71.3%	-78.1%	-82.7%	-85.7%	-87.7%	-89.2%
36	160.2	-62.7%	-62.0%	-66.4%	-74.1%	-80.5%	-84.9%	-87.8%	-89.8%	-91.1%
38	169.1	-65.8%	-65.7%	-69.5%	-76.5%	-82.4%	-86.7%	-89.5%	-91.3%	-92.6%
40	178.0	-68.6%	-68.9%	-72.4%	-78.7%	-84.1%	-88.1%	-90.8%	-92.6%	-93.8%
42	186.9	-71.0%	-71.7%	-75.0%	-80.6%	-85.6%	-89.4%	-91.9%	-93.6%	-94.7%
44	195.8	-73.2%	-74.2%	-77.3%	-82.4%	-86.9%	-90.4%	-92.8%	-94.4%	-95.5%
46	204.7	-75.1%	-76.3%	-79.3%	-84.0%	-88.1%	-91.3%	-93.5%	-95.0%	-96.0%
48	213.6	-76.8%	-78.3%	-81.1%	-85.5%	-89.2%	-92.1%	-94.2%	-95.6%	-96.5%
50	222.5	-78.4%	-80.0%	-82.7%	-86.8%	-90.1%	-92.8%	-94.7%	-96.0%	-96.9%

From Tables 4.19 through 4.21, it can be concluded that there is a significant difference between AASHTO LEFs and Irick LEFs. For loads higher than 80 kN (18 kip), the Irick LEFs are 20 percent to 90 percent lower than the AASHTO LEFs. For loads lower than 80 kN (18 kip), Irick's LEFs are significantly higher than the AASHTO LEFs.

## **RECOMMENDATIONS FOR FURTHER STUDIES OF LOAD EQUIVALENCE**

The following are recommended for the further study of LEFs:

1. Include the AASHO test sections with tandem axles.
2. Include strain and deflection histories for all AASHO test sections in the database.
3. Supplement the thickness representation of pavement structures with stress level indicators that are based on each structure's response (deflection, strain, stress) to individual loadings.
4. Re-analyze AASHO Road Test data using other techniques and by grouping test sections via stress level criteria, as opposed to having similar structures in the presented study.
5. Derive empirical equations for LEFs that are dependent on load and structural factors over a selected range of distress types and distress levels.



## CHAPTER 5. EVALUATION OF AASHO AND IRICK MODELS USING RESIDUAL ANALYSIS

### BACKGROUND

Generally, residual analysis can be used (1) to determine if the data fit a model, and (2) to identify what can be done to improve the model when the data do *not* fit. The current LEFs were developed from the AASHO Road Test data using the AASHO model described in Chapter 2. Residual analysis can help to determine if the AASHO model fits the AASHO Road Test data and, in turn, determine if the current LEFs need further improvement. Residual analysis can help determine if Irick's model is adequate for the evaluation of AASHO LEFs.

### MEASURES OF MODEL ADEQUACY

The multiple regression models can be defined as

$$y = \beta_0 + \beta_1 * x_1 + \beta_2 * x_2 + \dots + \beta_k * x_k + \varepsilon \quad (5.1)$$

The model is based on the following five major assumptions (Montgomery 92):

- The relationship between dependent variable  $y$  and independent variable  $x$  is linear, or at least it is well approximated by a straight line.
- The error term  $\varepsilon$  has zero mean.
- The error term  $\varepsilon$  had a constant variance  $\sigma^2$ .
- The errors are uncorrelated.
- The errors are normally distributed.

Gross violations of the assumptions could yield an unstable model in the sense that a different sample could lead to a totally different model with opposite conclusions. Usually, it is impossible to detect departures from underlying assumptions by examining the standard summary statistics, such as the  $t$ - or  $F$ -statistic, or  $R^2$ , because these "global" model properties do not ensure model adequacy. Residual analysis is a useful method for diagnosing violations of the basic regression assumptions. The residuals can be defined as:

$$e_i = y_i - \hat{y}_i, \quad i = 1, 2, \dots, n \quad (5.2)$$

where  $y_i$  is an observation and  $\hat{y}_i$  is the corresponding fitted value. Because a residual is viewed as the deviation between the data and the fit, it is a measure of the variability not explained by the regression model.

Figure 5.1 illustrates a theoretically satisfactory pattern for residual plots. In this figure, residuals are contained in a horizontal band, which indicates that there are no obvious model defects.

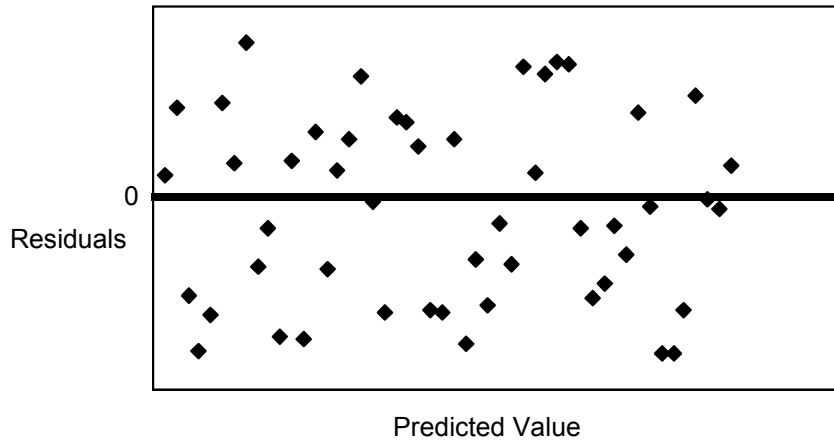


Figure 5.1 Theoretical satisfactory pattern for residual plots

## RESIDUALS FOR LOG APPLICATIONS

In order to examine how good the AASHO and Irick models are with regard to their statistical fitness, plots were performed for each of two models. Figures 5.2 through 5.5 show residual plots for log applications for AASHO and Irick models for flexible and rigid pavements. Equations 5.3 through 5.12 were used to calculate log applications.

### Flexible pavements – AASHO model

$$\log W_t = \log \rho + \frac{G_t}{\beta} \quad (5.3)$$

where:

$$\log \rho = 5.93 + 9.39 * \log_{10}(SN + 1) - 4.79 * \log_{10}(L1 + L2) \quad (5.4)$$

$$G_t = \log_{10} \left( \frac{4.2 - p_t}{4.2 - 1.5} \right) \quad (5.5)$$

$$\beta = 0.40 + \frac{0.081 * (L_1 + L_2)^{3.23}}{(SN + 1)^{5.19} * L_2^{3.23}} \quad (5.6)$$

#### Flexible pavements – Irick model

$$\log W_t = 6.300 - 2.627 * LLOAD + 4.432 * LWSN + 0.690 * LSIL \quad (5.7)$$

where:

- $W_t$  = axle load applications at end of time  $t$ ,
- $LSIL$  = log serviceability index loss for  $SIL = 1.2, 1.7, 2.2, \text{ or } 2.7$ ,
- $LLOAD$  = log LOAD, and
- $LWSN$  = log weighted structural number.

#### Rigid pavements – AASHO model

$$\log W_t = \log \rho + \frac{G_t}{\beta} \quad (5.8)$$

where:

$$\log \rho = 5.85 + 7.35 * \log(D + 1) - 4.62 * \log(L_1 + L_2) \quad (5.9)$$

$$G_t = \log_{10} \left( \frac{4.5 - p_t}{4.5 - 1.5} \right) \quad (5.10)$$

$$\beta = 1.00 + \frac{3.63 * (L_1 + L_2)^{5.2}}{(D + 1)^{8.46} * L_2^{3.52}} \quad (5.11)$$

#### Rigid pavements – Irick model

$$\log W_t = 6.997 - 3.318 * LLOAD + 2.733 * LTHK + 0.082 * LSIL + 0.997 * LLOAD * LTHK \quad (5.12)$$

where:

- $LSIL$  = log serviceability index loss for  $SIL = 1.5, 2.0, 2.5, \text{ or } 3.0$ ,
- $LLOAD$  = log LOAD, and
- $LTHK$  = log PCC thickness.

The residuals for these models were calculated using Equation 5.2.

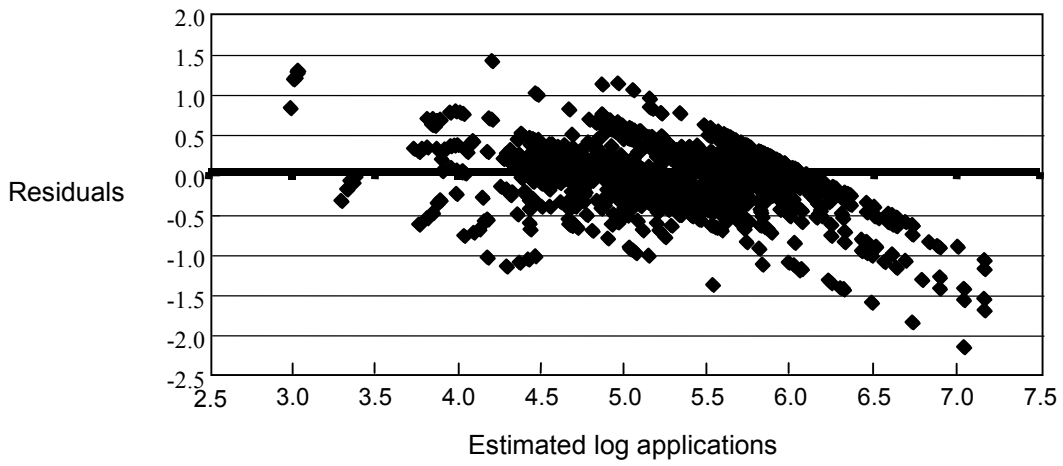


*Figure 5.2 Log application residuals for flexible pavements, AASHO model*

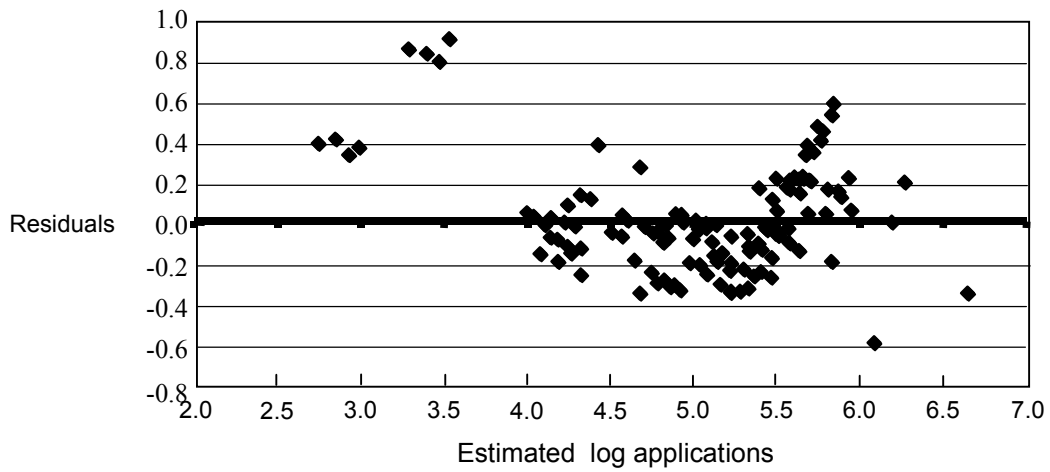


*Figure 5.3 Log application residuals for flexible pavements, Irick model*

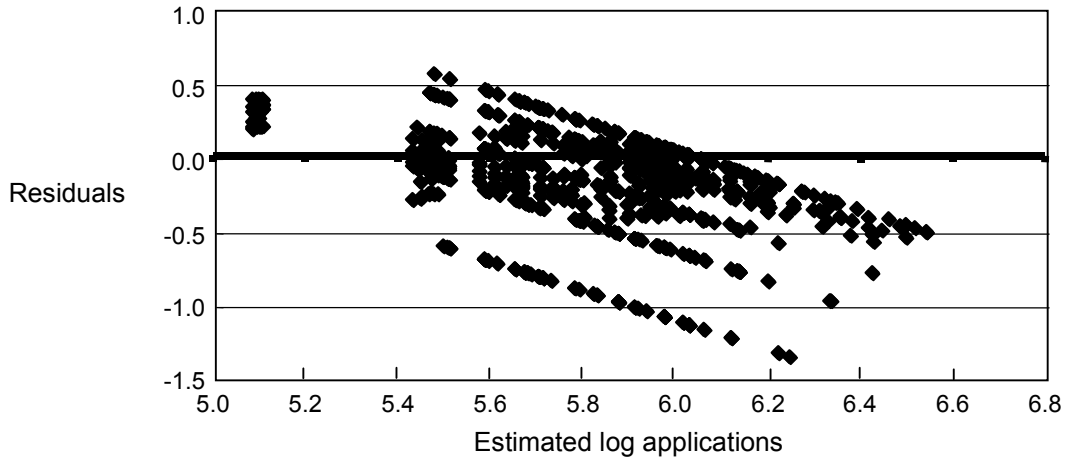


*Figure 5.4 Log application residuals for rigid pavements, AASHO model*

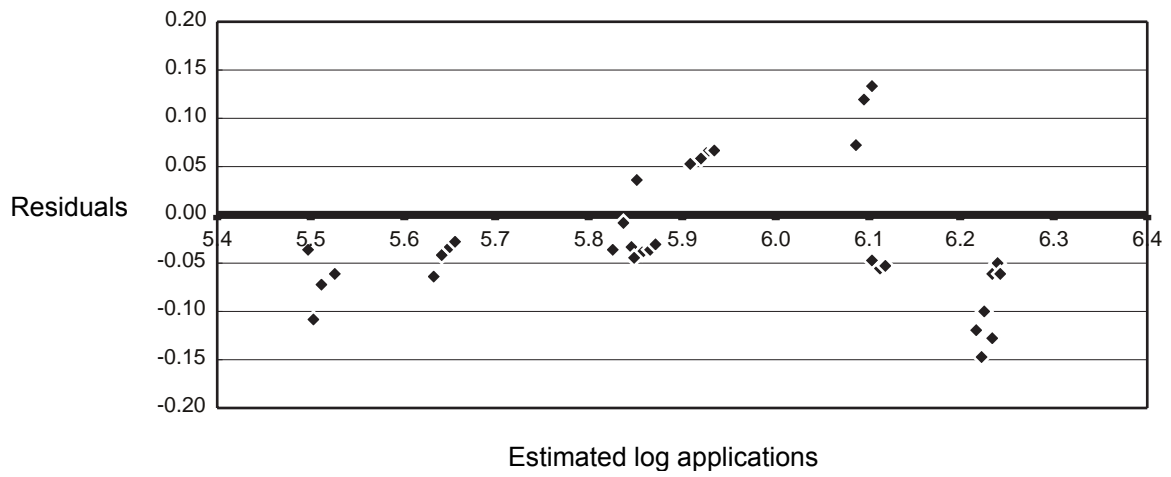


*Figure 5.5 Log application residuals for rigid pavements, Irick model*

## RESIDUALS FOR LOG LER

The LER for two axle loads (L1 and L2), on the same pavement structure and for a given distress level, is the ratio of the number of applications of L1 to the number of applications of L2 when both structures reach the same given distress level. The logarithm of LER is therefore the difference between the logs of the two applications.

Figures 5.6 through 5.9 present residual plots for log LERs for AASHO and Irick models for flexible and rigid pavements for single axles. Using the AASHO Road Test data, calculations were made for the following load equivalency ratios:

a) flexible pavement

$$LER = \frac{W_{t_2}}{W_{t_6}}, \frac{W_{t_2}}{W_{t_{12}}}, \frac{W_{t_2}}{W_{t_{18}}}, \frac{W_{t_6}}{W_{t_{12}}}, \frac{W_{t_6}}{W_{t_{18}}}, \frac{W_{t_6}}{W_{t_{22.4}}}, \frac{W_{t_{12}}}{W_{t_{18}}}, \frac{W_{t_{12}}}{W_{t_{22.4}}}, \frac{W_{t_{12}}}{W_{t_{30}}}, \frac{W_{t_{18}}}{W_{t_{22.4}}}, \frac{W_{t_{18}}}{W_{t_{30}}}, \frac{W_{t_{22.4}}}{W_{t_{30}}}$$

b) rigid pavement

$$LER = \frac{W_{t_{12}}}{W_{t_{18}}}, \frac{W_{t_{18}}}{W_{t_{22.4}}}, \frac{W_{t_{22.4}}}{W_{t_{30}}}$$

Equations 5.13 through 5.16 were used to calculate log LERs.

### Flexible pavements – AASHO model

$$\log_{10}(LER) = \log\left(\frac{W_{tL1}}{W_{tL2}}\right) \quad (5.13)$$

where  $W_{tL1}$  and  $W_{tL2}$  for load L1 and L2 were calculated from Equation 5.3.

### Flexible pavements – Irick model

$$\log_{10}(LER) = LLR * (-2.057 - 2.273 * LWSN - 1.224 * LSIL) \quad (5.14)$$

where:

- LSIL = log serviceability index loss for SIL = 1.2, 1.7, 2.2, or 2.7,
- LLR = log load ratio [ $\log_{10}(L1/L2)$ ], and
- LWSN = log weighted structural number.

**Rigid pavements — AASHO model**

$$\log_{10}(LER) = \log\left(\frac{W_{tL1}}{W_{tL2}}\right) \quad (5.15)$$

where  $W_{tL1}$  and  $W_{tL2}$  for load L1 and L2 were calculated from Equation 5.8.

**Rigid pavements — Irick model**

PSI Loss: SIL = 1.5, 2.0, 2.5, or 3.0

$$\log_{10}(LER) = LLR * (-6.948 + 5.283 * LTHK) \quad (5.16)$$

where:

LSIL = log serviceability index loss for SIL = 1.5, 2.0, 2.5, or 3.0,

LLR = log load ratio [ $\log_{10}(L1/L2)$ ], and

LTHK = log PCC thickness.

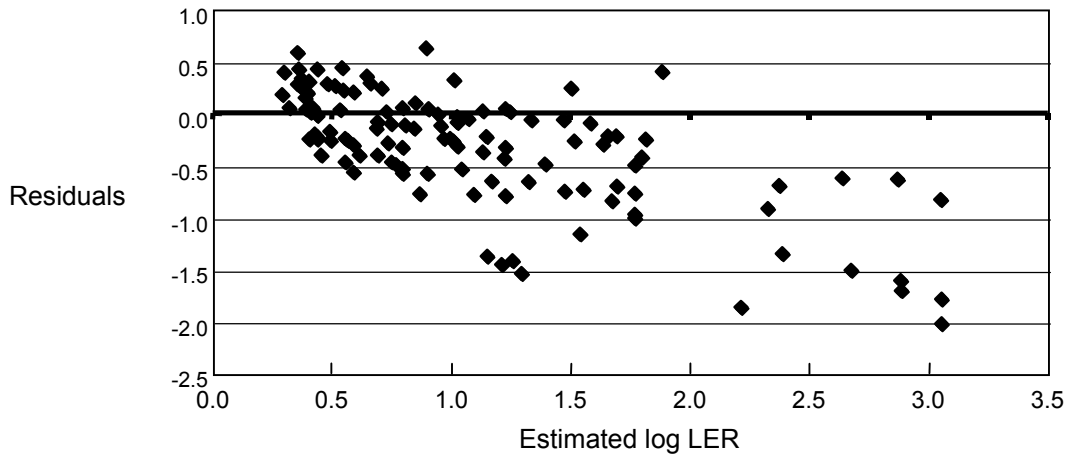


*Figure 5.6 Log LER residuals for flexible pavements, AASHO model*

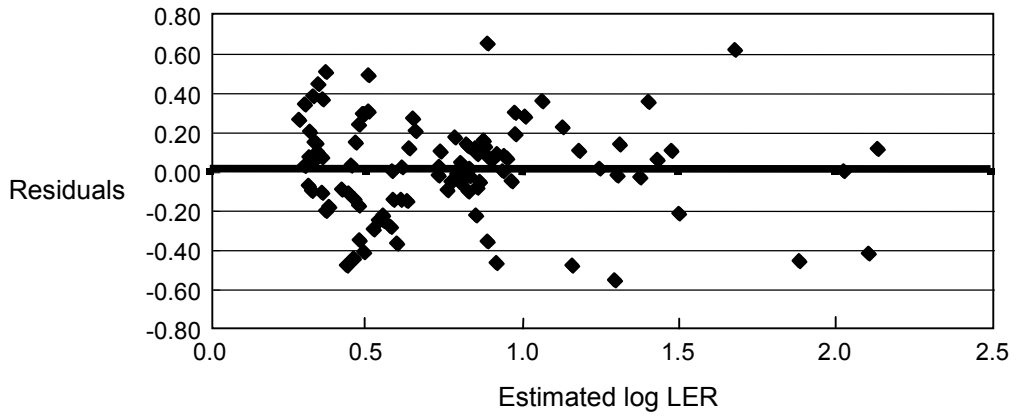


Figure 5.7 Log LER residuals for flexible pavements, Irick model

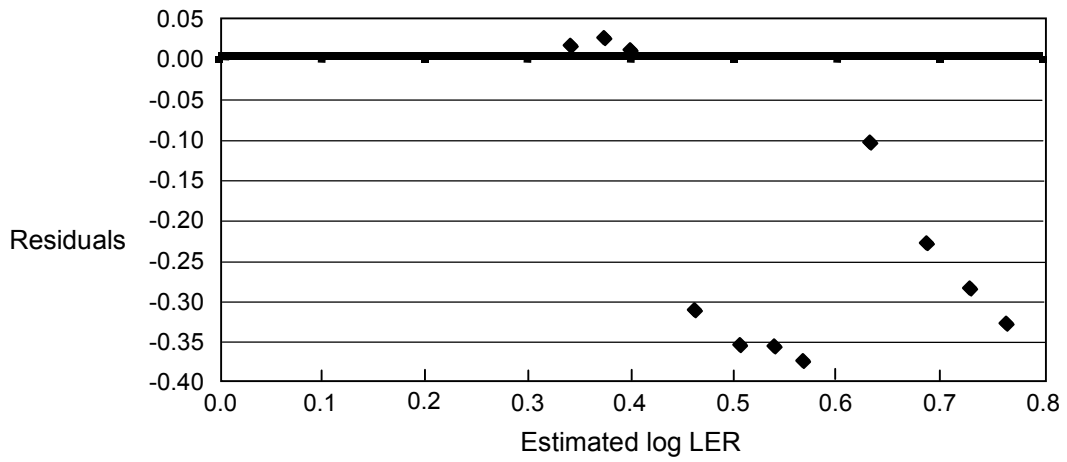


Figure 5.8 Log LER residuals for rigid pavements, AASHTO model

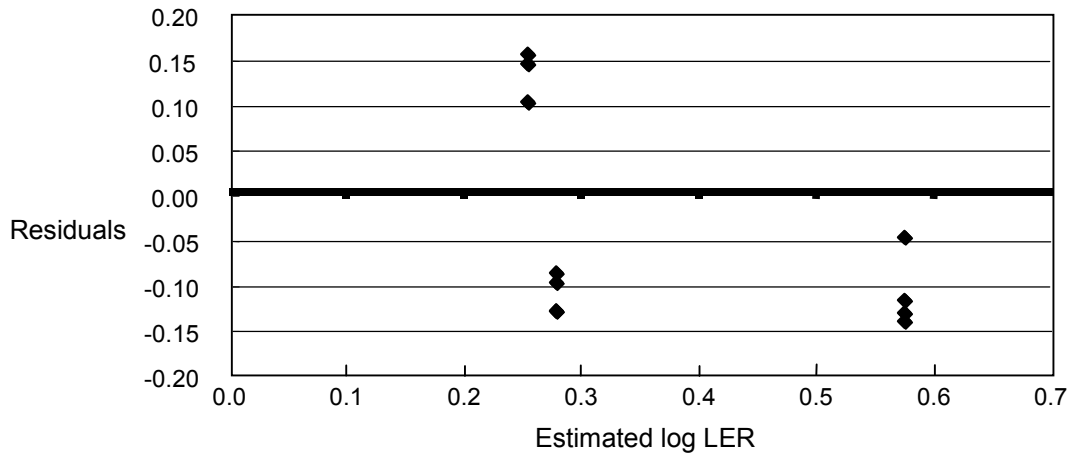


Figure 5.9 Log LER residuals for rigid pavements, Irick model

### CONCLUSIONS ON RESIDUAL ANALYSIS FOR LOG APPLICATIONS

According to the results presented in Figures 5.2 through 5.5, some of the basic regression assumptions are violated in all four cases. Figure 5.2 shows that the AASHO model overpredicts service life of the flexible pavements for the log applications higher than 6.

Figure 5.10 shows the residuals for log applications for the AASHO model of single axles with load higher than or equal to 80 kN (18 kip). A higher variance is in the center of the data.

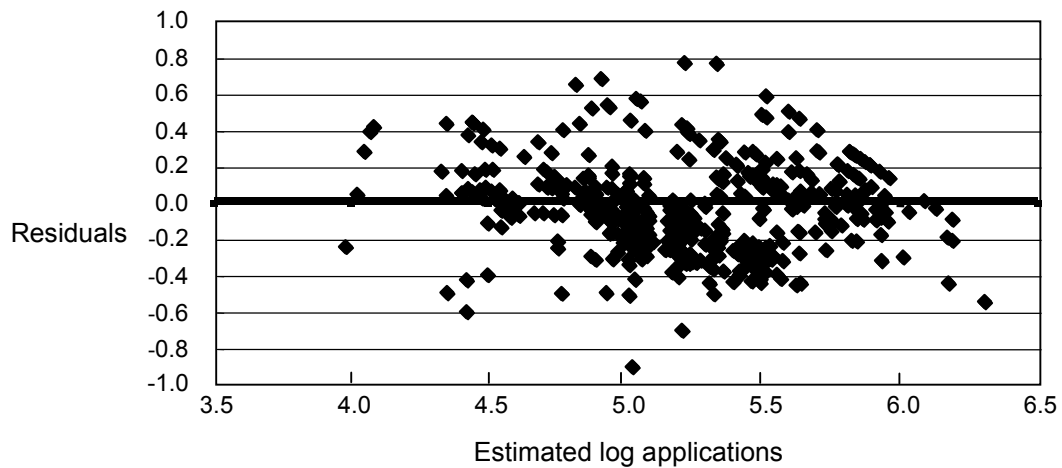
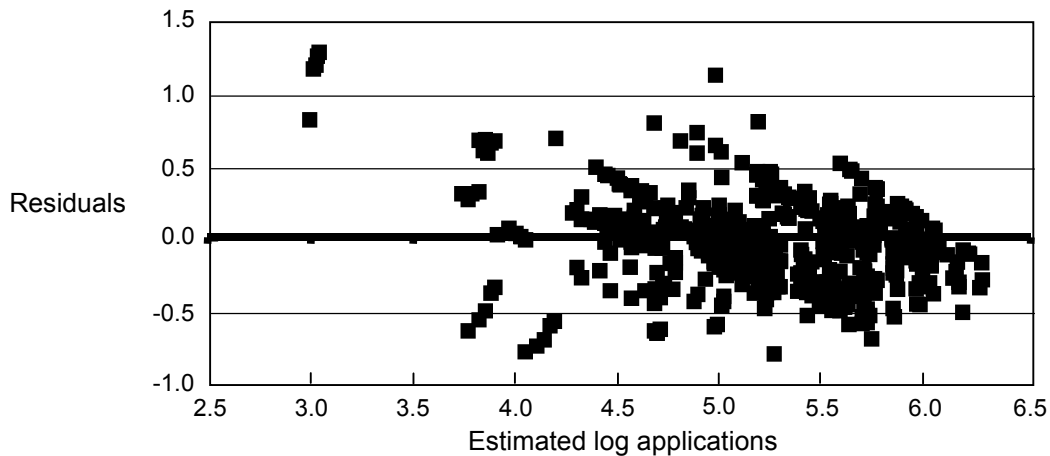


Figure 5.10 Log applications residuals for flexible pavements, AASHO model

Figure 5.11 shows the residuals for log applications of the AASHO model for tandem axles with axle loads higher than or equal to 106.8 kN (24 kip). The AASHO model fits well with these data.



*Figure 5.11 Log applications residuals for flexible pavements, AASHO model*

A curve plot, such as that in Figure 5.3, for the Irick model indicates nonlinearity. This could mean that another regressor variable, for example a squared term, is needed in the model.

A similar pattern is also true for rigid pavements. The AASHO model overpredicts service life for log applications higher than 6.06. Residuals for the Irick model are not contained in a narrow band.

## **CONCLUSIONS ON RESIDUAL ANALYSIS OF LOG LER**

After conducting an analysis of all four cases, the only model that fits the AASHO Road Test data well is Irick's model. The AASHO model for flexible pavements shows a tendency to overpredict log LER when the log LER is higher than 1.5.

Figure 5.12 shows the log LER for heavy loads. The data were drawn for three cases: (1) log (W18/W22.4); (2) log (W18/W30); and (3) log (W22.4/W30). The model does not fit the data well. There is a tendency for the LERs for W18/W22.4 to be underpredicted and the LERs for W18/W30 to be overpredicted.

For rigid pavements both models show a tendency of underpredicting log LERs for low log LERs and overpredicting log LERs for higher LERs.

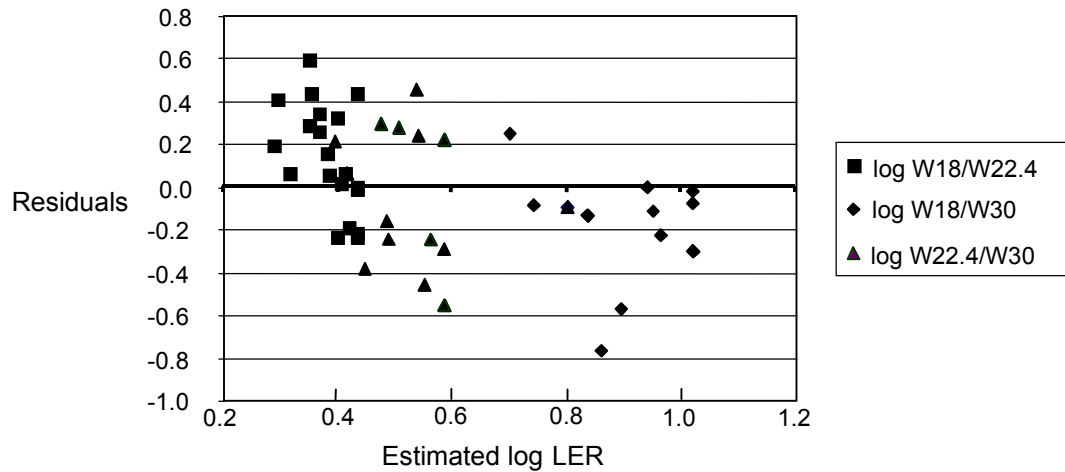


Figure 5.12 Log LER residuals for flexible pavements, AASHO model

## CHAPTER SUMMARY

The model inadequacies discussed in earlier sections could have potentially serious consequences. Gross violations of the assumptions may yield an unstable model in the sense that a different data sample could lead to a totally different model with opposite conclusions.

It was shown that the AASHO model fits a portion of the data related to heavy loads for flexible pavements, but, in general, the model can be unstable. Therefore, any extrapolation of this model outside the data range used at the AASHO Road Test can be very unreliable.

This analysis also shows that the AASHO model does not fit well with the AASHO Road Test data. Therefore, investigations are needed to determine if such incompatibility has any impact on AASHTO LEFs.

**Remedies for the problem.** The violations in basic regression assumptions can be corrected with a suitable transformation to either the regressor or the response variable. Another approach to resolving the problem is to use the weighted-least-squares method. Of course, there is also the option of applying alternative models.



## CHAPTER 6. SUMMARY, CONCLUSIONS, AND RECOMMENDATIONS

### REPORT SUMMARY

**Brief summary of the literature search and important findings.** The AASHO LEFs were developed in the 1960s based on empirical data obtained at the AASHO Road Test, which was the most comprehensive experimental design ever carried out in pavements. The AASHO Road Test had certain limitations (e.g., climatic factors and truck characteristics) that render continued extrapolation of the AASHO Road Test relationships questionable.

The following factors could have significant impact on the calculation of LEFs:

1. Super single tires can cause more damage to the pavement structure. Bonaquist observed that for the same load and tire pressure, fatigue damage of the super single tire 425/65R22.5 is 4 times greater, and layer rutting is 1.0 to 2.4 times deeper than those of the dual tire (Bonaquist 92).
2. There is a general consensus among researchers that increases in tire pressure accelerate pavement deterioration. Most researchers came to this conclusion based on the structural analysis of pavements. The Bonaquist study (Bonaquist 88) showed that doubling the tire pressure from 524.4 to 966 kPa (76 to 140 psi) could increase predicted damage by 20 percent, which is equivalent to an axle load increase of approximately 8.9 kN (2000 lb).
3. The TTI study citation indicates that the subgrade modulus, the AC layer thickness for flexible pavements, and the environmental zone can be important factors in calculating LEFs.
4. According to some researchers, the speed of vehicles could be another factor to consider in calculating LEFs (Hutchinson 87, Papagiannakis 92).

The re-analysis of the AASHO Road Test data by Irick was summarized in Chapter 4. It showed that the Irick re-analysis produced similar LEF values for flexible pavements, but significantly different results for rigid pavements.

Residual analysis was used to evaluate the adequacy of the AASHO and Irick models. It was determined that both models have violated some of the basic regression assumptions. As a result, these models could be unstable — that is, they could yield different results for repeated tests. Therefore, there is an urgent need to further investigate the validity of the LEFs.

## RECOMMENDATIONS

It is recommended that alternative models be used to evaluate the 18-kip equivalency concept. To accomplish this, we suggest the following:

1. Include the AASHO test sections with tandem axles.
2. Include strain and deflection histories for all AASHO test sections in the database.
3. Supplement the thickness representation of pavement structures with stress level indicators that are based on each structure's response (deflection, strain, stress) to individual loadings.
4. Re-analyze AASHO Road Test data using other techniques by grouping of test sections via stress level criteria, as opposed to having similar structures in the presented study.
5. Derivation of empirical equations for LEF that are dependent on load and structural factors over a selected range of distress types and distress levels.

## MOVE TO SECOND PROJECT PHASE

In the second phase of the project, additional analyses will be conducted to further investigate the validity of the current LEFs with respect to environmental conditions, tire pressure, suspensions systems, and other vehicle characteristics.

**Analysis of Vehicular and Traffic Attributes and Their Effect on Pavement Damage.** The AASHO results were empirical. It should be understood that empirical models are valid only within the range of the data used to calibrate them. The following factors should be analyzed to determine if they have any effect on LEFs:

- Higher tire pressures
- New suspension systems
- New tire widths, such as super-single tires
- New axle configurations, such as tridems and double tandems
- Environmental factors

In the AASHO Road Test, tire inflation pressures ranged from 520 to 550 kPa (75 to 80 psi). Today's trucks are normally operated at tire inflation pressures in the range of 600 to 800 kPa (85 to 115 psi); in some cases, tire pressures can go as high as 900 to 1,000 kPa (130 to 145 psi). The literature review shows that higher tire pressures can potentially impose more damage on pavements.

During AASHO Road Test only one type of suspension system was used, namely, steel springs. However, there are additional types of suspensions used in heavy freight vehicles, including:

1. Conventional steel leaf spring
2. Taper leaf spring
3. Air spring

These suspension systems can also potentially impose different types of damage on pavements.

Super-single tires are becoming more popular and are slowly replacing dual tires. Dual tires were used during the AASHO Road Test as the standard single-axle load. Research results (Bonaquist 92) showed that the super-single tires with the same load and tire pressure used with dual tires can impose more damage on pavements. Therefore, there is an urgent need to investigate this factor.

The AASHO Road Test was conducted only in one geographical location — the northern part of the United States. Climatic and environmental conditions are different in Texas. Therefore, LEFs should be validated for Texas climatic and environmental conditions.

There were no tridem axles used during AASHO Road Test. LEFs for tridems were developed by assigning 3 to the axle type variable. So far, researchers cannot reach agreement about how exactly the tridem-axle load is equivalently related to the standard 18-kip single-axle load. Modeling using the finite element method can provide a potential solution to this problem.

Other pavement and vehicular attributes will be modeled using appropriate computer modeling techniques. The impact of changing tire pressure has already been investigated. The finite element method (FEM) computer program ABAQUS was selected to model pavement structures and loading conditions that varied with different tire pressures. The analysis showed that the higher tire pressures can impose more damage on pavements.

The approach used to examine tire pressures worked very well and will be used to evaluate such other factors as super-single tires, tridems, steering axle loads, and new suspension types.



## REFERENCES

- (AASHO 62E) "The AASHO Road Test, Report 5, Pavement Research," Highway Research Board Special Report 61E, National Academy of Science, National Research Council, Publication No. 954. Washington, D.C., 1962.
- (AASHTO 72) "AASHTO Interim Guide for Design of Pavement Structures 1972," American Association of State Highway and Transportation Officials (AASHTO), National Academy of Science, National Research Council, Washington, D.C., 1972.
- (AASHTO 86) "AASHTO Guide for Design of Pavement Structures," Vol. 1, Vol. 2, Vol. 3, AASHTO, 1986.
- (AASHTO 93) "AASHTO Guide for Design of Pavement Structures 1993." AASHTO, Washington, D. C., 1993.
- (Bonaquist 88) Bonaquist, R., C. J. Churilla, and D. M. Freund. "Effect of Load, Tire Pressure, and Tire Type on Flexible Pavement Response," *Transportation Research Record* No. 1207, 1988, pp. 207-216.
- (Bonaquist 92) Bonaquist, R. An Assessment of the Increased Damage Potential of Wide Based Single Tires," Seventh International Conference on Asphalt Pavement, Volume 3, Design and Performance, pp. 1-16.
- (Christison 80) Christison, J. T., and B. P. Shields. "Evaluation of the Relative Damaging Effects of Wide Base Tire Loads on Pavements," RTAC Forum, Vol. 4, No. 1, pp. 65-71, 1980.
- (Christison 86) Christison, J. T. "Vehicle Weights and Dimension Study," Volume 8: Pavement Response to Heavy Vehicle Test Program: Part 1 — Data Summary Report, Road and Transportation Association of Canada, Technical Report, July 1986.
- (Corre 90) Corre, B. J., and T. D. White. "AASHTO Flexible Pavement Design Method: Fact or Fiction?," *Transportation Research Record* No. 1286, pp. 206-216.
- (De Beer 97) De Beer, M., C. Fisher, and F. J. Jooste. Determination of Pneumatic Tyre/Pavement Interface Contact Stresses Under Moving Loads and Some Effects on Pavements with Asphalt Surfacing Layers. Paper prepared for presentation at the Eighth International Conference on Asphalt Pavements, Seattle, Washington, 1997.
- (FHWA 84) Pavement Damage Functions for Cost Allocation, Vol. 1, Damage Functions and Load Equivalency Factors; Vol. 2, Description of Detailed Studies; Vol. 3, Flexible Pavement Damage Functions from AASHO Road Test Data; Rauhut, J. B., Lytton R. L., Darter, M. I.; Brent Rauhut Engineering, Inc.; Federal Highway Admin. Off. Of Eng. & Hwy. Opns.; FHWA/RD 84/019, 84/020; June 1984.

- (Finn 77) Finn, F., C. L. Saraf, R. Kulkarni, K. Nair, W. Smith, and A. Abdullah. "Development of Pavement Structural Subsystems" Vol. 1, Final Report, NCHRP project 1-10B, TRB, National Research Council, Washington, D.C., 1977.
- (Gerrard 70) Gerrard, C. M., and W. J. Harrison. "A Theoretical Comparison of the Effects of Dual-Tandem and Dual-Wheel Assemblies on Pavements," Australian Road Research Board Conference, *Proceedings*, Vol. 5, pp. 112-137, 1970.
- (Hanson 89) Hanson, R. W., C. Bertrand, K. M. Marshek, and W. R. Hudson. "Truck Tire Pavement Contact Distribution Characteristics for Super Single 18-22.5 and Smooth 11R24.5 Tires." Research Report 1190-1. Center for Transportation Research, The University of Texas at Austin, July 1989.
- (Himeno 97) Himeno, K., T. Ikeda, T. Kamijima, and T. Abe. Distribution of Tire Contact Pressure of Vehicles and Its Influence on Pavement Distress. Paper prepared for presentation at the Eighth International Conference on Asphalt Pavements, Seattle, Washington, 1997.
- (Huang 93) Huang, Yang H. *Pavement Design Analysis and Design*, Prentice Hall, Englewood Cliffs, New Jersey, 1993.
- (Hudson 88) Hudson, S. W., and S. B. Seeds. "Evaluation of Increased Pavement Loading and Tire Pressures," *Transportation Research Record* No. 1207, 1988, pp. 197-206.
- (Hudson 91) Hudson, W. R., M. T. McNeerney, and T. Dossey. "Comparison and Reanalysis of AASHO Road Test Rigid Pavement Data," *Transportation Research Record* No. 1307, 1991, pp. 122-128.
- (Hudson 92) Hudson, S. W., V. L. Anderson, P. E. Irick, R. F. Carmichael, and B. F. McCullough. "Impact of Truck Characteristics on Pavements: Truck Load Equivalency Factors," Final Report. 1992/07.9201-9207.
- (Hudson 94) Hudson, W. R., and L. J. Butler. "The Effect of Tridem Axles on Pavement Damage," for the Association of American Railroads, Washington D.C., September 1994.
- (Hutchinson 87) Hutchinson, B. G., R. C. G. Haas, P. Meyer, K. Hadipour, and A. T. Papagiannakis: Equivalencies of Different Axle Load Groups. Proc., 2nd North American Pavement Management Conference, Toronto, Canada, Vol. 3, 1987, pp. 191-202.
- (Irick 89) Irick, P. E. "Characteristics of Load Equivalence Relationships Associated with Pavement Distress and Performance," Austin Research Engineers, September 1989.
- (Jung 74) Jung, F. W., and W. A. Phang. "Elastic Layer Analysis Related to Performance in Flexible Pavement Design" *Transportation Research Record* No. 521, pp. 14-29, 1974.

- (Little 77) Little, R. J., and L. J. McKenzie. "Performance of Pavement Test Sections in the AASHO Test Road," Physical Research Report 76. FHWA-IL-PR-76. Illinois Department of Transportation, FHWA, U.S. Department of Transportation, 1977.
- (Mahoney 95) Mahoney, J. P., B. C. Winters, K. Chatti, T. J. Moran, C. L. Monismith, and S. L. Kramer: Vehicle/Pavement Interaction at the PACCAR Test Site. Research Report WA-RD- 384.1. Washington State Transportation Center (TRAC), University of Washington, Seattle, Washington. November 1995.
- (Montgomery 92) Montgomery, D. C., and E. A. Peck. *Introduction to Linear Regression Analysis*, New York, John Wiley and Sons, Inc., 1992.
- (NCHRP 93) Gillespie, T. D., S. M. Karamihas, M. S. Sayers, M. A. Nasim, W. Hanson, and N. Ehsan. Effects of Heavy-Vehicle Characteristics on Pavement Response and Performance. National Cooperative Highway Research Program (NCHRP), TRB, National Research Council, Washington, D.C. 1993.
- (NCRP 77) The Nordic Cooperative Research Project for the Application of the AASHO Road Test Results. "Failure Models and Pavement Design and Rehabilitation System Developed and Adapted for Conditions Prevailing in the Nordic Countries," Volume I, Proceedings of Fourth International Conference on Structural Design of Asphalt Pavements, 1977, pp. 903-919.
- (Papagiannakis 91) Papagiannakis, T., A. Oancea, N. Ali, J. Chan, and A. T. Bergman. "Application of ASTM E1049-85 in Calculating Load Equivalence Factors from In Situ Strains," *Transportation Research Record* No. 1307, 1991, pp. 82-89.
- (Pezo 89) Pezo, R. F., K. M. Marshek, and W. R. Hudson. "Truck Tire Pavement Contact Pressure Distribution Characteristics for the Bias Goodyear 18-22.5, the Radial Michelin 275/80R/24.5, the Radial Michelin 255/80R/22.5, and the Radial Goodyear 11R24.5 Tires." Research Report 1190-2F, Center for Transportation Research, The University of Texas at Austin, September 1989.
- (Ramsamooj 72) Ramsamooj, D. V, K. Majidzadeh, and E. M. Kauffmann. "The Analysis and Design of the Flexibility of Pavements," *Proceedings*, Third International Conference on the Structural Design of Asphalt Pavements, Vol. 1, pp. 692-704, 1972.
- (Rauhut 82) Rauhut, J. B., R. L. Lytton, and M. I. Darter. "Pavement Damage Functions for Cost Allocation," Vol. 1, Damage Functions and Load Equivalence Factors, U.S. Department of Transportation, 1982.
- (Rilett 88) Rilett, L. R., and B. G. Hutchinson. "LEF, Estimation from Canroad Pavement Load-Deflection Data," *Transportation Research Record* No. 1196, 1988, pp. 170-178.

- (Roberts 87) Roberts, F. L., R. L. Lytton, and Z. Hajeer. "The Development of New Load Equivalency Factors for Flexible Pavement Design in Texas," Research Report 476-1, Texas Transportation Institute, Texas A&M University System, 1987.
- (Scala 70) Scala, A. J., W. J. Cogill, and A. McNeil. "Comparison of the Response of Pavements to Single and Tandem Axle Loads," *Proceedings, Fifth ARRB Conference (5A)*, 1970, pp. 231-252.
- (Small 89) Small, K., C. Winston, and C. A. Evans. *Road Work*, The Brookings Institution, Washington, D.C., 1989.
- (Southgate 84) Southgate, H. F., and R. C. Deen. "Variations of Fatigue Due to Unevenly Loaded Tridem Groups," University of Kentucky Research Report UKTRP-84-11.
- (Southgate 85) Southgate, H. F., and R. C. Deen. "Effects of Load Distributions on Axle and Tire Configurations," Research Report UKTRP-85-13, Kentucky Transportation Research Program, 1985.
- (Tayabji 83) Tayabji, S. D., C. G. Ball, and P. A. Okamoto. "Effects of Tridem Axle Loading on Concrete Pavement Performance," Report No. FHWA/MN/RD-83-07, by Construction Technology Laboratories for Minnesota Department of Transportation, St. Paul Investigation, St. Paul Investigation Number 209, 1983.
- (Tayabji 84) Tayabji, S. D., C. G. Ball, and P. A. Okamoto. "Effect of Frozen Support and Tridem Axle on Concrete Pavement Performance," *Transportation Research Record* No. 954, TRB, National Research Council, Washington, D.C., 1984.
- (Terrel 76) Terrel, R. L., and S. Rimstron. "Pavement Response and Equivalencies for Various Truck Axles and Tire Configurations," *Transportation Research Record* No. 602, 1976, pp. 33-38.
- (Van Til 72) Van Til, C. J., B. A. McCullough, and B. A. Varga. "Evaluation of AASHO Interim Guide for Design of Pavement Structures," NCHRP Report 128, 1972.
- (Von Quintus 78) Von Quintus, H. L. "Equivalency Factor Development," ARE, Inc., Tech Memo FH-4.
- (Yoder 75) Yoder, E. J., and M. W. Witczak. *Principles of Pavement Design (2<sup>nd</sup> ed.)*, New York, John Wiley and Sons, Inc., 1975.